Advanced Delta Hedging using Greeks (DH)

Zhifei Li
CQF Jan 2024

Jul - Aug 2024

Contents

1 Introduction

The Part I of this report utilised the numerical simulations and mathematical derivation to demonstrate the fact that in dynamic hedging setting and suppose the initial option priced at implied volatility is smaller than that price at actual volatility, i.e. $V_a > V_i$, hedging with actual volatility would yield uncertain changes in PnL but certain total PnL which equals $V_a - V_i$, while hedging with implied volatility would yield deterministic $dPnL$ but uncertain total PnL. I have provided proofs both through mathematical derivation and MC simulations, which are based on direct definitive formulas and greeks decomposition of $dPnL$ respectively. The latter has shown better convergence. This section also shows the impacts of Gamma Γ_t onto the daily and cumulative PnL from both mathematical derivation and scatter plots based on the MC simulations. The next section also covers the impacts of the how the difference between realised and actual volatility impact the daily and cumulative PnL. The final section briefly discusses the implications of smaller delta for trading.

The Part II has performed empirical study on the relationship between minimum-variance delta δ_{MV} and the Black-Scholes delta δ_{BS} and how it leads to changes in the trading gains. The methodology is to replicate the approach taken in John & White ([HW17]) with minor modification and upon the wider range of data: Optiondx.com S&P 500 Index Call Options data from 01/01/2010 to 31/12/2023. Several steps of data cleansing, processing and manipulation were made and the 3-Month Treasury yield rate was chosen as the risk free rate for me to obtain theoretical option price. The different option data was then classified into different buckets based on their moneyness (measured by the size of δ_{BS} and the time to maturies (measured by dte provided), which results in 3 monenyness buckets and 7 maturity buckets, leading to 21 different buckets. The approach replicated is to build a quadratic fitting relationship and use the obtained coefficients to calculate the δ_{MV}. After obtaining the initial results of a, b, c for each bucket, further calibration by rolling estimation was conducted and I have innovatively tried to apply both rolling on a daily and monthly frequency to obtain the term structure of a, b, c, then its impacts on the shape of the relationship between δ_{BS} and δ_{MV}, $\mathbb{E}(\Delta\sigma_{imp})$ vs δ_{BS} and vs $\$delta_{MV}$ for each bucket. Finally the gains from taking the δ_{MV} against taking δ_{BS} are analysed for each bucket. We found that most buckets show inverted or non-inverted parabolic shapes between δ_{BS} and δ_{MV}, and after calibration by daily rolling, more become parabolic shapes. The relationship between $\mathbb{E}(\Delta\sigma_{imp})$ vs δ is more complicated and usually shows the shape of ”Single Triangular”, ”Cross” and ”Three-Body”, and after rolling calibration, most visuals remain similar shapes and some visuals have more clusters. Finally, the gains have shown for ATM buckets, high gains can be observed at long maturity buckets, such as ATM 12M (12 months) and ATM 12MM (more than 12 months to expiry). For ITM buckets, the high gains are found around ATM 2 to 3M buckets. In general the gains for ITM buckets are statistically insignificant.

Though aiming to replicate the research produced by Hull & White ([HW17]) with wider range of option data, I have uniquely contributed the rolling estimation of shifting on daily frequency, and made comparison with the monthly frequency.

This report has been developed within limited time and could be developed with more depth in future study. More advanced fitting methods to work with regression, such as Support Vector Machine, Neural Network can be considered as the relationships between different variables are less interpretable with higher dimensions and longer time range of observation. The Monte Carlo methods could be further improved with Brownian Bridge methods, and the Black-Scholes model could be further complicated with Jump-Diffusion models. These areas would be taken greater attention for future study.

The complete scripts I have created for completing Part I and Part II are also uploaded to my personal GitHub repository: `https://github.com/L-Zhifei/CQF-Advanced-Delta-Hedging-2024-Jan/tree/main`.

2 Part I: The Volatility Arbitrage with Improved GBM and MC (Antithetic Varaite and Sobol Sequence)

2.1 Model Settings

2.1.1 Improvement on GBM

I have incorporated the *Euler-Maruyana* discretisation scheme to improve the modeling of GBM asset evolution in Monte Carlo simulation. The process of the discretisation is to transform the SDE from the continous form:

$$dS_t = rS_t dt + \sigma S_t dW_t$$

into

$$S_{t+\delta t} = S_t(1 + r\delta t + \sigma\sqrt{\delta t} w_t)$$

where:

- δt is the time step defined before simulation
- w_t is usually the random variable that follows a certain distribution, such as normal distribution (most commonly used)

I have adopted the *low discrepency sequence* of *Sobol sequence* in the place of w_t where normal random variable is mostly used, which can reduce the number of simulations to reach convergence. This would be introduced in the following session:

2.1.2 Improvement on Monte Carlo

The simplest Monte Carlo simulation uses the normal distributed variate which is easy to compute. With large enough number of simulations, one can use central limit theorem as justification to constructing the confidence intervals for Monte Carlo estimates. But it causes more than necessary number of simulations which reaches convergence slower than optimal. To solve this issue, I have incorporated the antithetic variate and Sobol Sequence instead of the normally distributed variate.

Based on the theory and practices provided by [Jae02], first, The antithetic variate is when generating random variables $X_1, X_2, ...X_n$, we also generate a series of negatively correlated variables to these $X_1, X_2, X_3...X_n$. This would reduce the variance of the estimator and result in a smaller confidence interval. Suppose for the generated Sobol sequence X, their negatively related "copies" (i.e. linear transformation) are created as $X_1, X_2...$, suppose for any positive integer $m \geq 1$, let $n = 2m$ which is even, the mean estimator of these paired variable $X_1, X_2, ...$ are

$$\bar{X}(n) = \frac{1}{2m}\sum_{j=1}^{2m} X_j = \frac{1}{m}\sum_{j=1}^{m} Y_j = \bar{Y}(m)$$

where

$$\begin{aligned} Y_1 &= \frac{X_1 + X_2}{2} \\ Y_2 &= \frac{X_3 + X_4}{2} \\ &... \\ Y_m &= \frac{X_{n-1} + X_n}{2} \end{aligned}$$

This means that $\bar{Y}(m)$ and $\bar{X}(n)$ are identical for estimating the mean of original series X.

The use of $Y_i = \frac{X_i + X_{i+1}}{2}$ can transform the estimation of the mean of this randomly generated sequence $\mu = \mathbb{E}(X) = \mathbb{E}(Y)$, moreover the variance of this variable Y is

$$\begin{aligned} Var(Y) =& \frac{1}{4}[Var(X_{n-1}) + Var(X_n) + 2Cov(X_{n-1}, X_n)] \\ =& \frac{1}{2}[\sigma^2 + Cov(X_{n-1}, X_n)] \end{aligned}$$

And if every X_{n-1} and X_n are selected negatively related, the variance should be smaller than $\frac{1}{2}\sigma^2$, a desired outcome that can help to reduce the number of simulations.

In my simulation codes, I have chosen the simplest linearly negative relationship of each w_t as $1 - X_i$. This also requires me to take the number of simulation to be the power of 2 i.e. 2^N

Second, before applying the *antithtetic variables*, I have replaced the w_t random variable with low discrepancy sequence of *Sobol sequence*. The detailed construction steps are technically challenging, a brief intuition is given. In each dimension of the sequence, the i^{th} number in Sobol Sequence is

$$x_i = \oplus_{j=1}^{\infty} b_j(i) v_j$$

where the first term $b_j(i)$ is the *binary expansion* of an integer i, and the second term v_j is the j^{th} *direction number*. The $\oplus$ is the binary (bitwise) XOR operation. Since the $b_j(i)$ is the binary bit which only takes 0 or 1, the integer i has a binary expansion:

$$i = \sum_{j=1}^{\infty} b_j(i) 2^{j-1}$$

And the direction numbers v_j are binary fractions $v_j \in (0, 1)$ which results the Sobol number being a binary fraction $x_j \in (0, 1)$, the direction number can be represented as:

$$v_j = \frac{m_j}{2^j} = \frac{1}{2^j} \left(\oplus_{k=1}^{d} 2^k a_k m_{j-k} \right) \oplus_{j-d}$$

where m_j takes integer values and ranges between $(1, 2^j)$, the initial values $m_1.m_2..., m_d$ are odd integers and numbers $a_0, a_1, ..., a_d$ are the coefficients of the primitive polynomial of degree d in $\mathbb{Z}$, the $p_i(x)$, which is written as:

$$p_i(x) = \sum_{k=0}^{d} a_k x^{d-k}$$

In my simulation codes, I have resorted to the package *qmc* (*Quasi Monte Carlo*) which processes a preset Sobol Sequence generator.

2.2 Hedging with Actual Volatility based δ_{actual} and Implied Volatility based $\delta_{implied}$

2.2.1 Actual Volatility δ_{actual}

Under the conditions of $V_a > V_i$, we can confirm that by hedging with actual volatility based delta δ_{actual} the cumulative PnL would be certain at the level of $V_a - V_i$, while the component PnL at each time step dt is uncertain.

Assume the asset price follows the Geometric Brownian Motion (GBM) as:

$$dS_t = \mu_t S_t dt + \sigma_{imp} S_t dW_t$$

To hedge with actual volatility, the actual volatility value is measured and used to derive a delta δ_a. The portfolio is constructed by longing 1 unit of the option V_i (with i at subscript to indicate the *implied volatility* is used to price the option), and shorting the underlying asset priced at S_t with δ_a (with a at subscript to indicate the *actual volatility* is used to derive the delta).

Though the values of the portfolio is :

$$V_i - \delta_a S$$

And this gives us the cash values of $-V_i$ (from longing/buying the option priced with implied volatility) and $+\delta_a S$ (derived with actual volatility)

$$-V_i + \delta_a S$$

The total value of the portfolio and the cash is thus 0:

$$(V_i - \delta_a S) + (-V_i + \delta_a S) = 0$$

This value of 0 meets the condition of *"...out of nothing"* in the arbitrage of *"earning out of nothing"*.

Next, when the underlying asset's price moves by dS during the time from t to $t+dt$, the option value changes by an amount which can be labeled dV_i, which has no necessity to expand to its actual form. This makes the value of long option position at time $t + dt$ equals

$$V_i + dV_i$$

The underlying assets which is in short position is affected by the amount of price change dS timing the value of delta position δ_a as $\delta_a dS$. This makes the value of short underlying position at time $t + dt$ equals

$$-\delta_a S - \delta_a dS$$

The cash, on the other hand, is not affected directly by the changes in underlying asset's price dS, because it is regarded as risk-free. The only change is the additional risk-free interest rdt, the additional cash occurred is $(-V_i + \delta_a S)rdt$. This makes the value of cash position at time $t + dt$ equals:

$$(-V_i + \delta_a S)(1 + rdt)$$

Totaling up the values of portfolio and cash arrives at:

$$\begin{aligned} &[V_i + dV_i] + [-\delta_a S - \delta_a dS] + [(-V_i + \delta_a S)(1 + rdt)] \\ =&dV_i - \delta_a dS + (-V_i + \delta_a S)rdt \end{aligned}$$

Then applying a trick that knowing that if the option price is valued using its actual volatility σ_{actual}, rather than the implied volatility $\sigma_{implied}$, which is what the market perceives, the portfolio + cash should still be zero (i.e. no additional value added from the change of S_t within the timestep dt, since by the *no arbitrage condition in risk-free measure*, the correctly priced options and underlying assets should have no arbitrage opportunity, the return from options and underlying assets should be the risk-free return r, which means

$$dV_a = rV_a dt$$
$$dS = rSdt$$

This give a sum of zero equation:

$$dV_a - \delta_a dS - r(V_a - \delta_a S)dt = 0$$

Then to have this term minused by the previous term, and rearranging:

$$
\begin{aligned}
&dV_i - \delta_a dS + (-V_i + \delta_a S) r dt && (1)\\
=&dV_i - \delta_a dS + (-V_i + \delta_a S) r dt - dV_a + \delta_a dS + r(V_a - \delta_a S)dt && (2)\\
=&dV_i - dV_a + r(V_a - \delta_a S)dt - r(V_i - \delta_a S)dt && (3)\\
=&dV_i - dV_a - r(V_i - V_a)dt && (4)\\
=&e^{rt} d(e^{-rt}(V_i - V_a)) && (5)
\end{aligned}
$$

This is the values of the portfolio and cash values at $t + dt$, and since at t the value of such is 0, this is also the increment value of one time step dt. Essentially, this is the *"Mark-to-market"* profit over one time step dt. Rewritting as:

$$d(PnL_t) = e^{rt} d(e^{-rt}(V_i - V_a))$$

The $d(PnL_t)$ is a stochastic term since

$$d(e^{rt}(V_i - V_a)) = -re^{-rt}dt(V_i - V_a) + e^{-rt}[dV_i - dV_a]$$

and dV_i and dV_a are stochastic terms as they involve the Brownian motion term dW_t. By applying Ito's lemma directly, the differential of the option value $V(S_t, t)$ can be decomposed as:

$$
\begin{aligned}
dV(S_t, t) &= \frac{\partial V}{\partial t}dt + \frac{\partial V}{\partial S}dS_t + \frac{1}{2}\frac{\partial^2 V}{\partial S^2}dS_t dS_t + O((dS_t)^3) + ... && (6)\\
&= (\frac{\partial V}{\partial t} + \underbrace{\frac{1}{2}\frac{\partial^2 V}{\partial S^2}\sigma_a S_t^2}_{\text{since the } \sigma_{imp} \text{ is just an exogenous factor not determined by the model}})dt + \frac{\partial V}{\partial S}dS_t && (7)\\
&= (\frac{\partial V}{\partial t} + \frac{1}{2}\frac{\partial^2 V}{\partial S^2}\sigma_a^2 S_t^2 + \mu S_t \frac{\partial V}{\partial S})dt + \frac{\partial V}{\partial S}\sigma_a S_t dW_t && (8)
\end{aligned}
$$

To investigate further, plug the above $dV(S_t, t)$ into the *Mark-to-market* profit over timestep dt.

$$
\begin{aligned}
&dV_i - \delta_a dS + (-V_i + \delta_a S)rdt - dV_a - \delta_a dS - r(V_a - \delta_a S)dt\\
=&dV_i - \delta_a dS + (-V_i + \delta_a S)rdt\\
=&(\underbrace{\frac{\partial V}{\partial t}}_{\Theta_i} + \frac{1}{2}\underbrace{\frac{\partial^2 V}{\partial S^2}}_{\Gamma_i}\sigma_a^2 S^2)dt + \underbrace{\frac{\partial V}{\partial S}}_{\delta_i}\underbrace{dS_t}_{dS_t = \mu S dt + \sigma_a S dW_t}\\
&- \delta_a dS + (-V_i + \delta_a S)rdt\\
=&(\Theta_i + \frac{1}{2}\Gamma_i \sigma_a^2 S^2)dt + \delta_i dS - \delta_a dS + (-V_i + \delta_a S)rdt\\
=&(\Theta_i - rV_i)dt + \frac{1}{2}\sigma_a^2 S^2 \Gamma_i dt + (\delta_i - \delta_a)S(\mu dt + \sigma_a dW_t) + r\delta_a S dt
\end{aligned}
$$

Now recall the Black-Scholes PDE that $\frac{\partial V}{\partial t} + \frac{1}{2}\sigma^2 S^2 \frac{\partial^2 V}{\partial S^2} = rV - rS\frac{\partial V}{\partial S}$, rearranging can make $\Theta_i - rV_i$ on the LHS

$$
\begin{aligned}
&\Theta - rV\\
=&\frac{\partial V}{\partial t} - rV\\
=&-rS\frac{\partial V}{\partial S} - \frac{1}{2}\sigma^2 S^2 \frac{\partial^2 V}{\partial S^2}\\
=&-rS\sigma - \frac{1}{2}\sigma^2 S^2 \Gamma
\end{aligned}
$$

And if pricing the option with implied volatility σ_{imp} the subscript can be added

$$\Theta_i - rV_i = -rS\sigma_i - \frac{1}{2}\sigma_i^2 S^2 \Gamma_i$$

Plug this into the $d(PnL)$

$$\begin{aligned}
=&\sigma_i rSdt - \frac{1}{2}\sigma_i^2 S^2 \Gamma_i dt + \frac{1}{2}\sigma_a^2 S^2 \Gamma_i dt + (\sigma_i - \sigma_a)S(\mu dt + \sigma_a dW_t) \\
=&\frac{1}{2}(\sigma_a^2 - \sigma_i^2)S^2\Gamma_i dt + (\delta_i - \delta_a)S(\mu dt + \sigma_a dW_t) + (\delta_a - \delta_i)rSdt \\
=&\frac{1}{2}(\sigma_a^2 - \sigma_i^2)S^2\Gamma_i dt + (\delta_i - \delta_a)S[(\mu - r)dt + \sigma_a dW_t]
\end{aligned}$$

With under risk-neutral measure $\mu = r$, the unit change of PnL converts to

$$d(PnL) = \frac{1}{2}(\sigma_a^2 - \sigma_i^2)S^2\Gamma_i dt + (\delta_i - \delta_a)S\sigma_a dW_t \tag{9}$$

which shows that the stochastic term dW_t cannot be eradicated, which causes the randomness of $d(PnL)$. Next we will look at how integration of such term leads to certain payoff.

However, if integrating the $d(PnL_t)$ we can get the total PnL. Suppose the starting time point is t_0, this requires us to discount the $e^{rt}d(e^{-rt}(V_i - V_a))$ to t_0 as

$$\begin{aligned}
&e^{-rt_0}e^{rt}d(e^{-rt}(V_i - V_a)) \\
=&e^{-r(t-t_0)}e^{rt}d(e^{-rt}(V_i - V_a)) \\
=&e^{rt_0}d(e^{-rt}(V_i - V_a))
\end{aligned}$$

This gives rise to the present value (PV) of the changes of PnL at dt, to integrate from the initial time to the expiry time T:

$$\begin{aligned}
\int_{t_0}^{T} d(PnL_t) &= \int_{t_0}^{T} e^{rt_0}d(e^{-rt}(V_i(t) - V_a(t))) \\
&= e^{rt_0}\int_{t_0}^{T} d(e^{-rt}(V_i(t) - V_a(t))) \\
&= e^{rt_0}[e^{-rT}(V_i(T) - V_a(T)) - e^{-rt_0}(V_i(t_0) - V_a(t_0))] \\
&= e^{-rt_0+rt_0}(V_a(t_0) - V_i(t_0)) \text{ , since } V_i(T) = V_a(T) = 0 \\
&= V_i - V_a
\end{aligned}$$

The term $V_i - V_a$ is deterministic at time t_0. This mathematical derivation shows the total profit and loss is deterministic while the change in each timestep dt is uncertain.

And in Monte Carlo simulation, we can verify this fact by observing the convergence properties of the simulated cumulative PnL paths from the start to the end of the period. We can find that the paths converge to a smaller range, eventually become certain values with more simulations.

The following simulation is made by taking strike $K = 100$, initial asset price $S_0 = 100$, risk free interest rate $r = 5\%$. For the choices of actual and implied, I have separately tested two scenarios (1) $\sigma_a > \sigma i$: $\sigma_a = 35\%, \sigma_i = 20\%$ and (2) $\sigma_a < \sigma_i 20\% : \sigma_a = 20\%, \sigma_i = 35\%$, the total number of timesteps is 514 and the total expiry length as 1. I took the number of simulations to be 2, 128 and 256.

By the Black-Scholes equation, the theoretical value of V_a is 11.659417163090303, while the V_i is 16.128428881575886, the resulting theoretical gain at expiry should be 4.469011718485582.

For scenario (1) $\sigma_a > \sigma_i$: $\sigma_a = 35\%, \sigma_i = 20\%$, the Monte Carlo simulation convergence speed is slow and the convergence to a certain value of around 4.47 should require much larger number of convergence (Figure 1). However, expanding the difference between the higher σ_a and the lower σ_i can improves the convergence to some extent (Figure 2). This shows that the 35% - 25% selection would eventually converge with larger number of simulations, which is computationally costly.

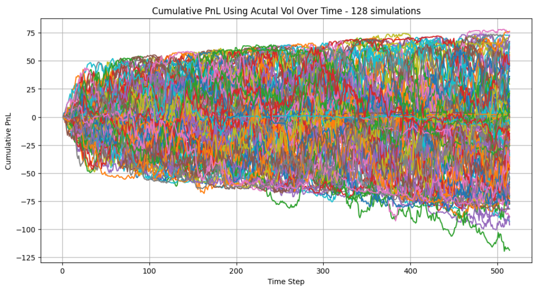

Figure 1: The PnL Paths of MC Simulations with Actual Volatility converges quickly - 128 simulations of 35% and 25%

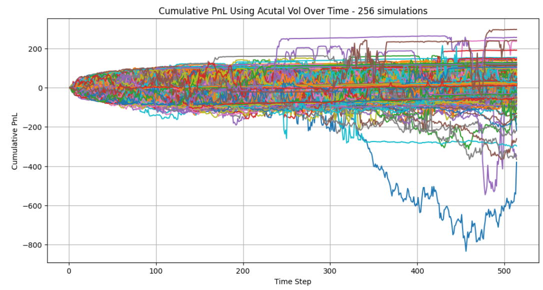

Figure 2: The PnL Paths of MC Simulations with Actual Volatility converges quickly - 256 simulations of 95% and 15%

Figure 3: Scenario 1 Simulation

For scenario (2) $\sigma_a < \sigma_i$: $\sigma_a = 20\%, \sigma_i = 35\%$, the convergence speed is faster and can be better reflected from observing the narrowing range of terminal values. By increasing the number of simulations from 128 (Figure 4) to 256 (Figure 5), the convergence becomes more obvious. Though having the reverse relationship with desired setting $\sigma_a > \sigma_i$, this finishes the proof with Monte Carlo simulation in essence.

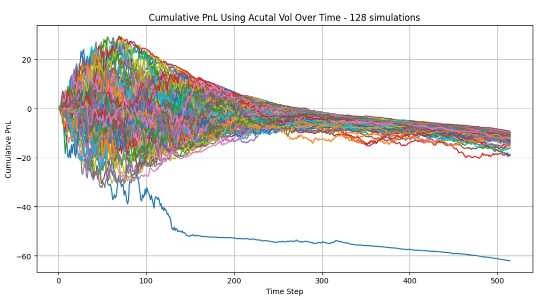

Figure 4: The PnL Paths of MC Simulations with Actual Volatility converges quickly - 128 simulations

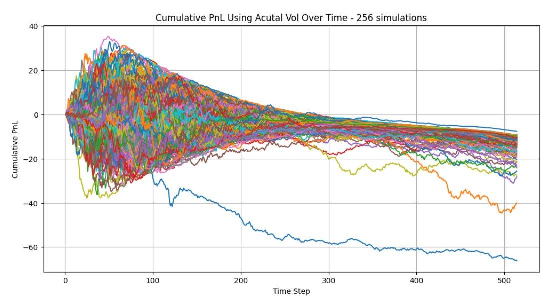

Figure 5: The PnL Paths of MC Simulations with Actual Volatility converges quickly - 256 simulations

Figure 6: Scenario 2 Simulation

2.2.2 Pros and Cons of Hedging with Actual Volatility δ_{actual}

Pros: The main advantage of hedging with actual volatility is the final income at the option's expiry is certain.

Cons: The fluctuation of the time-step-wise income is uncertain, i.e. while it is appealing in global the local return can look unpredicted and volatile so from the risk management perspective, posing huge pressure from the necessary regular reporting of trading books which focuses more on short-term time frame. Also, it highly depends on the credibility of volatility estimation for σ_a. One has to be very accurate on the σ_a they worked out.

2.2.3 Implied Volatiltiy $\delta_{implied}$

If hedging based on the implied volatility δ_{imp}, the PnL at each time step would be certain but the total PnL would be uncertain. By replacing the δ_a with δ_i from the $dV_i - \delta_a dS + (-V_i + \delta_a S)rdt$, we can get

$$dV_i - \delta_i dS + (-V_i + \delta_i S)rdt \tag{10}$$

$$= \underbrace{(\Theta_i + \frac{1}{2}\Gamma_i \sigma_a^2 S^2)dt}_{\text{use } \sigma_a \text{ since it came from the Ito lemma application on } dV(S,t)} - \underbrace{[\sigma_i - \sigma_i]dS}_{=0} + (-V_i + \delta_i S)rdt \tag{11}$$

$$= \frac{1}{2}\Gamma_i \sigma_a^2 S^2 dt + \underbrace{\Theta_i dt + (-V_i + \delta_i S)rdt}_{\text{since } \Theta_i dt = rV_i dt - r\delta_i S dt - \frac{1}{2}\sigma_i^2 S^2 \Gamma_i dt} \tag{12}$$

$$= \frac{1}{2}\Gamma_i \sigma_a^2 S^2 dt - \frac{1}{2}\sigma_i^2 S^2 \Gamma_i dt \tag{13}$$

$$= \frac{1}{2}\Gamma_i S^2 (\sigma_a^2 - \sigma_i^2)dt \tag{14}$$

The intuition behind the finding is the gain from curvature $\frac{1}{2}\sigma_a^2 S^2 \Gamma_i dt$ can be offsetted be time decay from $\frac{1}{2}\sigma_i^2 S^2 \Gamma_i dt$, based on the simplified Black Scholed PDE $\frac{\partial V}{\partial t} + \frac{1}{2}\sigma^2 S^2 \frac{\partial^2 V}{\partial S^2} = rV - rS\frac{\partial V}{\partial S} = 0 \Rightarrow \Theta_i = -\frac{1}{2}\sigma_i^2 S^2 \Gamma_i$ if taking $\sigma = \sigma_i$.

The *Mark-to-market* profit over time step dt when hedging with implied volatility σ_{imp} is certain since each $S = S_t$ at earlier time t is deterministic at the observation time $t + dt$, and the other terms are all deterministic as well.

Now to get the total PnL by integrating the above term,

$$\int_{t=t_0}^{T} \frac{1}{2}\Gamma_i S^2 (\sigma_a^2 - \sigma_i^2)dt$$
$$= \frac{1}{2}(\sigma_a^2 - \sigma_i^2)\int_{t=t_0}^{T} e^{-rt} S^2 \Gamma_i dt$$

This would be a stochastic term since at observation time point $\forall t < T$ the paths are usually unknown (i.e. path-dependent). These mathematical derivation shows the total profit and loss is uncertain while the change in each time step dt is certain.

Upon the Monte Carlo simulation, by taking the parameters like in hedging with σ_a and introduce two scenarios:(1) $\sigma_a > \sigma i$: $\sigma_a = 35\%, \sigma_i = 20\%$ and (2) $\sigma_a < \sigma_i 20\% : \sigma_a = 20\%, \sigma_i = 35\%$.

For both scenarios, by setting the number of simulation to be 128, the resulting simulation paths does not show good convergence [See Fig.7, 10], and still poor convergence with the number of simulations rising to 256 [See Fig.8, 10]. Relative to hedging with σ_a, the range of terminal total PnL at Scenario 1 has a larger interval which indicates its higher uncertainty. The Scenario 2, though look relatively alike hedging with σ_a, has also a larger interval between [-100, 75+], while the former's interval is between [-100, 50+]. This somehow shows the relative certainty of the total PnL of hedging with σ_a relative to with σ_i.

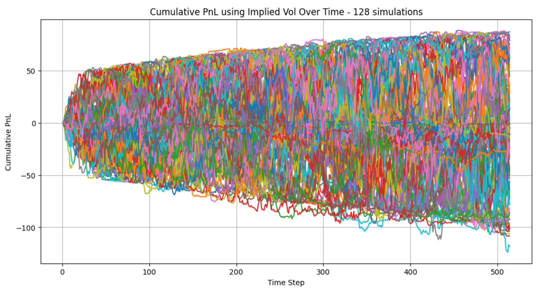

Figure 7: The PnL Paths of MC Simulations with Implied Volatility - 128 simulations

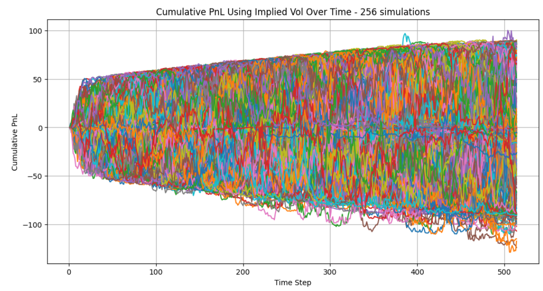

Figure 8: The PnL Paths of MC Simulations with Implied Volatility - 256 simulations

Figure 9: Scenario 1 Simulation

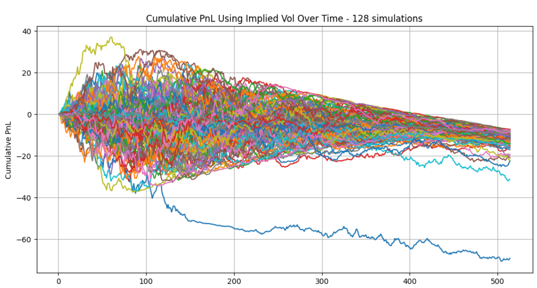

Figure 10: The PnL Paths of MC Simulations with Implied Volatility - 128 simulations

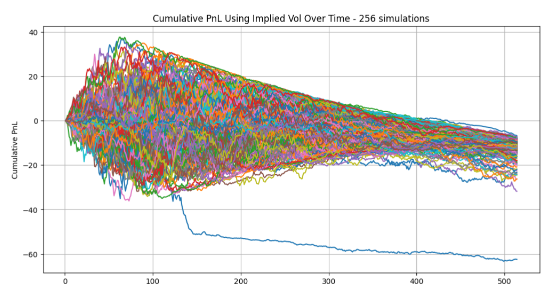

Figure 11: The PnL Paths of MC Simulations with Implied Volatility - 256 simulations

Figure 12: Scenario 2 Simulation

The MC simulations for this model is based on the following script where key variables are defined and served as base for choosing parameter values and generating plots.

```python
class MCOptionPricing:

    def __init__(self, S0:float, strike:float, rate:float, sigma_actual:float, sigma_implied:float, dte:int, nsim:int, timesteps:int=514) -> float: #514
        self.S0 = S0
        self.K = strike
        self.r = rate
        self.sigma_actual = sigma_actual
        self.sigma_implied = sigma_implied
        self.T = dte
        self.N = nsim # has to be the power of 2 like 64
        self.ts = timesteps

    @property
    def rvgenerator(self):
        # Generate Sobol sequences with antithetics without Brownian Bridge
        sobol = Sobol(d = self.ts) # the dimension of each point/timesteps
        sobol_sequences = sobol.random_base2(m=int(np.log2(self.N))) # the number of points/simulations
        antithetic_sobol_sequences = 1.0 - sobol_sequences
        # combine the original and antithetic sequences
        # full_sequences = np.vstack((sobol_sequences, antithetic_sobol_sequences))
        return sobol_sequences, antithetic_sobol_sequences

    @property
    def simulate_path(self):
        np.random.seed(2024)
        ''' asset price simulation using actual vol'''
        #define dt
        dt = self.T/self.ts

        #simulate paths
        S = np.zeros((self.N, self.ts))
        S_antithetic = np.zeros((self.N, self.ts))
        S_new = np.zeros((self.N, self.ts))
        S[:,0] = self.S0
        S_antithetic[:,0] = self.S0

        sobol_sequences, antithetic_sobol_sequences = self.rvgenerator

        for i in range(0, self.ts-1):
            z = norm.ppf(sobol_sequences[:,i])
            z_antithetic = norm.ppf(antithetic_sobol_sequences[:,i])
            S[:,i+1] = S[:,i] * np.exp((self.r - (1/2) * self.sigma_actual ** 2) * dt + self.sigma_actual * np.sqrt(dt) * z)
            S_antithetic[:,i+1] = S_antithetic[:,i] * np.exp((self.r - (1/2) * self.sigma_actual ** 2) * dt + self.sigma_actual * np.sqrt(dt) * z_antithetic)
        S_new = (S + S_antithetic) / 2

        return S_new


    # cannot put @property because we need it as a function
    def asset_delta(self, use_implied_vol = False):
        S = self.simulate_path
        dt = self.T / self.ts
        # chose the appropriate sigma
        sigma = self.sigma_implied if (use_implied_vol) else self.sigma_actual

        # Debugging prints
        print(f"S: {S}")
        print(f"S.shape: {S.shape}")
        print(f"K: {self.K}")
        print(f"r: {self.r}")
        print(f"sigma: {sigma}")
        print(f"T: {self.T}")
        for t in range(self.ts):
            T_t = self.T - (t * dt)  # Time to maturity
```

```
            if T_t <= 0:
                continue

        d1 = (np.log(S / self.K) + (self.r + 0.5 * sigma ** 2) * (T_t)) / (sigma * np.sqrt(T_t))
        # More debugging
        print(f"d1: {d1}")

        delta = norm.cdf(d1)  # Delta for a European Call Option

        # Final check before returning
        print(f"delta: {delta}")
        return delta

    @property
    def optionprice(self): # using implied sigma
        S = self.simulate_path
        dt = self.T / self.ts
        option_price = np.zeros(self.ts)

        # Use actual volatility for pricing
        sigma = self.sigma_implied

        for t in range(self.ts):
            T_t = self.T - (t * dt)  # Time to maturity
            if T_t <= 0:
                continue

            # Calculate d1 and d2 for BSM formula
            d1 = (np.log(S[:, t] / self.K) + (self.r + 0.5 * sigma ** 2) * T_t) / (sigma * np.sqrt(T_t))
            d2 = d1 - sigma * np.sqrt(T_t)

            # BSM formula for European call option
            call_prices = S[:, t] * norm.cdf(d1) - self.K * np.exp(-self.r * T_t) * norm.cdf(d2)

            # Average call prices over all simulations for the current time step
            option_price[t] = np.mean(call_prices)

        return option_price

    def portfolio_value(self, use_implied_vol = False):
        S = self.simulate_path
        option_price = self.optionprice
        #option_price = option_price.reshape(1,-1)
        delta = self.asset_delta(use_implied_vol = use_implied_vol) # necessary so that the portfolio value can use either implied or actual vol

        option_price_broadcasted = np.tile(option_price, (S.shape[0], 1))

        portfolio = option_price_broadcasted - delta * S

        return portfolio


    def cashflow_replication(self, use_implied_vol = False):
        # necessary because we assume dynmaic hedging meaning that the delta position can change in different time steps, depending on the asset price's changes
        # this is not shown in the mathematical derivation
        S = self.simulate_path
        delta = self.asset_delta(use_implied_vol = use_implied_vol)
        cashflow_replication = np.zeros_like(S)

        for i in range (1, S.shape[0]):
            for j in range(S.shape[1]):
                cashflow_replication[i,j] = S[i,j] * (delta[i,j] - delta[i,j-1])
        return cashflow_replication


    def cash_account(self,use_implied_vol = False):
```

```
        S = self.simulate_path
        portfolio = self.portfolio_value(use_implied_vol = use_implied_vol) # necessary so taht the cash_account follows the binary choice of portfolio value
        cash_account = np.zeros_like(S)
        cashflow_replication = self.cashflow_replication(use_implied_vol = use_implied_vol)
        dt = self.T/self.ts

        cash_account[:,0] = - portfolio[:,0]

        # discounted sum of cash account
        for i in range(cash_account.shape[0]):
            for j in range(1, cash_account.shape[1]):
                cash_account[i,j] = cashflow_replication[i,j] + np.exp(self.r * dt) * cash_account[i,j-1]
        return cash_account


    def pnl_cum(self, use_implied_vol = False):
        cash_ac = self.cash_account(use_implied_vol = use_implied_vol)
        portfolio = self.portfolio_value(use_implied_vol = use_implied_vol)
        pnl = cash_ac + portfolio
        return pnl

    # Asset return
    @property
    def asset_return(self):
        S = self.simulate_path
        asset_return = np.zeros_like(S)
        asset_return[:,1:] = (self.simulate_path[:,1:] - self.simulate_path[:,:-1]) / self.simulate_path[:,:-1]
        return asset_return

    @property
    #the return^2 - implied_vol^2  * timestep_t
    def ret_vol_diff(self):
        ret = self.asset_return
        dt = self.T/self.ts
        result = ret ** 2 - self.sigma_implied * dt
        return result

    @property
    #the return^2 - implied_vol^2  * timestep_t
    def ret_vol2_diff(self):
        ret = self.asset_return
        dt = self.T/self.ts
        result = ret ** 2 - self.sigma_implied ** 2 * dt
        return result
```

Listing 1: Python Script for MC on Delta Hedging

2.3 Monte Carlo Simulation based on the Gamma-decomposed $d(PnL)$

Another Monte Carlo Simulation based on the Gamma decomposition of $d(PnL)$ based on the Equations 9 and 14 can better illustrate the convergence property. Taking the same parameters and setting $\sigma_a = 35\%$ and $\sigma_i = 20\%$, the cumulative discounted sum of PnL which hedges with actual volatility σ_a is converging at the expiry (Figure 13), which indicates high degree of certainty of total PnL at expiry T, while the cumulative sum of PnL which hedges with implied volatility σ_i is not converging (Figure 14), meaning the uncertainty of the total PnL at expiry T. Please refer to the Figure 15.

```python
class MCOptionPricing:

    def __init__(self, S0:float, strike:float, rate:float, sigma_actual:float, sigma_implied:float, dte:int, nsim:int, timesteps:int=514) -> float: #514
        self.S0 = S0
        self.K = strike
        self.r = rate
        self.sigma_actual = sigma_actual
        self.sigma_implied = sigma_implied
        self.T = dte
        self.N = nsim # has to be the power of 2 like 64
        self.ts = timesteps

    # Gamma based on either implied or actual vol
    def gamma(self, use_implied_vol = False):
        S = self.simulate_path
        dt = self.T / self.ts
        TTE = np.linspace(self.T, (S.shape[0],1)) # create a 128 * 514 matrix for T, each row is the time to expiry array
        TTE_matrix = np.tile(TTE, (S.shape[0],1))
        # chose the appropriate sigma
        sigma = self.sigma_implied if (use_implied_vol) else self.sigma_actual

        # Debugging prints
        print(f"S: {S}")
        print(f"S.shape: {S.shape}")
        print(f"K: {self.K}")
        print(f"r: {self.r}")
        print(f"sigma: {sigma}")
        print(f"T: {self.T}")
        for t in range(self.ts):
            T_t = self.T - (t * dt)  # Time to maturity
            if T_t <= 0:
                continue

        d1 = (np.log(S / self.K) + (self.r + 0.5 * sigma ** 2) * (T_t)) / (sigma * np.sqrt(T_t))

        phi_d1 = norm.pdf(d1) # get the standard normal pdf of d1
        # More debugging
        print(f"d1: {d1}")

        gamma = phi_d1/ (S * sigma * np.sqrt(T_t))  # Gamma for a European Call Option

        # Final check before returning
        print(f"delta: {gamma}")
        return gamma

        #the discounted total PnL
    def pnl_gamma_discounted(self,use_implied_vol=False):
        S = self.simulate_path
        time_steps_gone = np.arange(S.shape[1])
        dt = self.T/self.ts
        gamma_discount = self.pnl_gamma(use_implied_vol = use_implied_vol)
        discount_factor = np.exp(-self.r * time_steps_gone * dt)
        pnl_discounted = gamma_discount * discount_factor
        # Initialize an array to store the cumulative discounted PnL
        cumulative_pnl_discounted = np.zeros_like(pnl_discounted)
```

```python

    # Iterate through each simulation path (i) and each time point (j) to calculate the cumulative discounted PnL
    for i in range(pnl_discounted.shape[0]):  # Iterate over simulations
        for j in range(pnl_discounted.shape[1]):  # Iterate over time steps
            if j == 0:
                cumulative_pnl_discounted[i, j] = pnl_discounted[i, j]
            else:
                cumulative_pnl_discounted[i, j] = cumulative_pnl_discounted[i, j-1] + pnl_discounted[i, j]
    return cumulative_pnl_discounted
```

Listing 2: Python Script for MC on Gamma-decomposed PnL

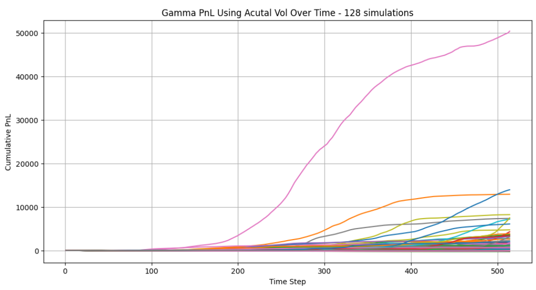

Figure 13: The Gamma-decomposed Cumulative PnL Paths of MC Simulations with Actual Volatility - 128 simulations

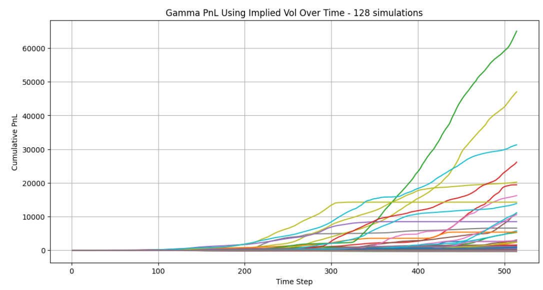

Figure 14: The Gamma-decomposed Cumulative PnL Paths of MC Simulations with Implied Volatility - 128 simulations

Figure 15: Gamma-decomposed Cumulative PnL of 128 simulations

2.3.1 Pros and Cons of Hedging with Implied Volatility $\delta_{implied}$

Pros: The main advantage is the certainty of the PnL at each time step, and since $\Gamma_i > 0$ for all European calls, the positive return is guaranteed (as long as $\sigma_a > \sigma_i$). This would make trading book risk management smooth. The second advantage is the convenience of making the trade. One simply needs to long the option and short δ_i amounts of its underlying asset when $\sigma_a > \sigma_i$, and commit the reverse action (short the option and long δ_i positions of the underlying asset) when $\sigma_a < \sigma_i$. And this does not cost traders to work out the actual volatility by themselves, at the risk of wrong decision-making, but simply observe the implied volatility data from VIX or the likes.

Cons: The disadvantage is the total profit and loss at the end of the contract is unknown, albeit being positive as long as $\sigma_a > \sigma_i$.

2.4 Analytics on MC Convergence

I have performed two MC simulations based on two interpretations of the hedging portfolio (1) Follow directly the definitions of "portfolio value" + "cashflow" (which equals the negative value of portfolio and the cash generated from adjusting the replicating delta every time the underlying price changes)(2) Further decompose the $d(PnL)$ into Gamma Γ and Theta Θ according to Equation 9. I have observed that the MC (1) gives poor convergence properties while (2) has relatively more apparent convergence. The reasons behind the discrepancy can be:

- The explicit form of MC (1) is more complex than MC (2), which involves more numerical differences and issues in accuracy as the values transmits through different formulas. The MC (2) is much simpler and the short transmission chain between formulas makes it more accurate.

- The hedging frequency chosen here is 1/514 which is the annualised version of once per 0.71 days. In reality the rebalancing frequency can be much more or less frequent than this, which causes the errors in the cashflow generated from delta. The frequency can be further increased.

- The paths for multiple different values: option price, portfolio value, cashflow replication, cash account and pnl cum, make the final value more path-dependent. It may require more paths to simulate, or taking improved random number generator like Sobol with Brownian Bridge which works well with jumps ([Gur11]).

2.5 Greeks Decomposition and the Impacts of Gamma Γ_t

The PnL per time step dt can be decomposed to Greeks as has been shown above,

For hedging with σ_a in Equation 9

$$d(PnL) = \frac{1}{2}(\sigma_a^2 - \sigma_i^2)S^2\Gamma_i dt + (\delta_i - \delta_a)S\sigma_a dW_t$$

For hedging with σ_i in Equation 14

$$d(PnL) = \frac{1}{2}\Gamma_i S^2(\sigma_a^2 - \sigma_i^2)dt$$

This shows that the local PnL (from t to $t+\Delta t$) depends on the time-dependent Γ_t via the term $\frac{1}{2}\Gamma_i S^2(\sigma_a^2 - \sigma_i^2)dt$ in both scenarios.

Plotting the Γ_t and cumulative PnL of 128 simulations would yield the following visuals. From the Figures 16 and 17, the Γ_t at both ends (i.e close to 0 or highest level of more than 0.25 in my simulation) are usually mapped to high levels of daily PnL. Such trend is less obvious for the implied volatility σ_i visuals in Figures 19 and 20. This could indicate that when the option is either extremely sensitive or insensitive to the changes in slope of option price wrt underlying asset price, the changes in PnL would be large. Practically...

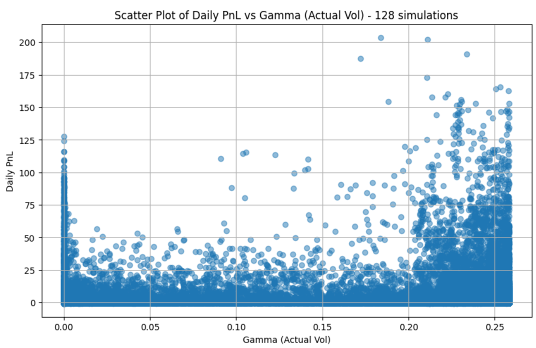

Figure 16: The Gamma-decomposed Daily PnL vs Gamma Scatter Plot with Actual Volatility - 128 simulations

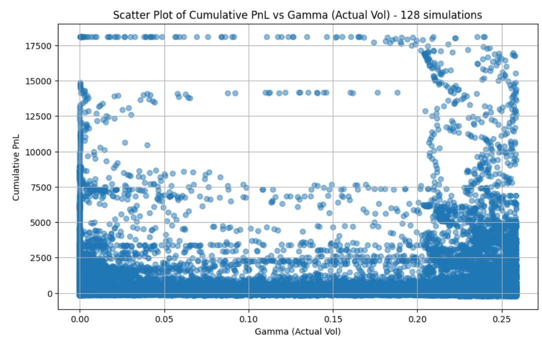

Figure 17: The Gamma-decomposed Cumulative PnL vs Gamma Scatter Plot with Actual Volatility - 128 simulations

Figure 18: Gamma-decomposed PnL of 128 simulations

Also reflecting on the theory, the delta-hedging is aiming to hedge the risk from the stock price. Recall the direct application of Ito lemma on dV from Equation 15

$$dV = (\underbrace{\frac{\partial V}{\partial t}}_{\Theta} + \frac{1}{2}\underbrace{\frac{\partial^2 V}{\partial S^2}}_{\Gamma}\sigma^2 S^2)dt + \underbrace{\frac{\partial V}{\partial S}}_{\delta}dS$$

Since delta hedging has taken place, the δ term should be taken to the LHS. Also take from continuous to discrete form, from t to $t+\Delta t$, this converts to

$$dV - \delta dS = (\Theta + \frac{1}{2}\sigma^2 S^2\Gamma)dt \quad (15)$$

$$\Rightarrow d(V - \delta S) = (\Theta + \frac{1}{2}\sigma^2 S^2\Gamma)dt \quad (16)$$

$$\Rightarrow d(PnL) = (\Theta + \frac{1}{2}\sigma^2 S^2\Gamma)dt \quad (17)$$

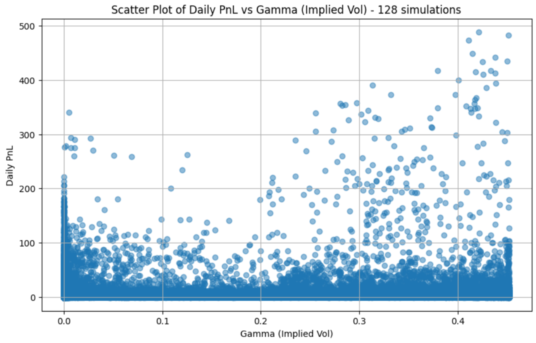

Figure 19: The Gamma-decomposed Daily PnL vs Gamma Scatter Plot with Implied Volatility - 128 simulations

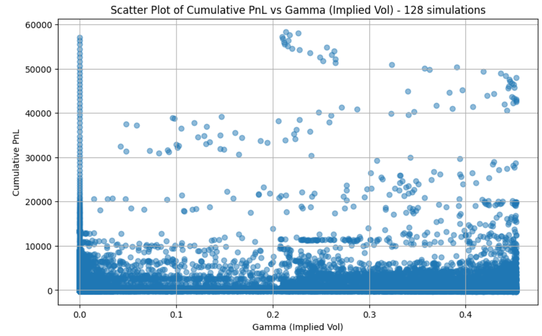

Figure 20: The Gamma-decomposed Cumulative PnL vs Gamma Scatter Plot with Implied Volatility - 128 simulations

Figure 21: Gamma-decomposed PnL of 128 simulations

This formula shows the convex payoff relationship, as the gains are obtained from Gamma $\frac{1}{2}\sigma^2 S^2 \Gamma$ and decay from Theta Θ.

This also fits thee intuition that when the delta-risk is hedged, the option trade can face the risks from other Greeks: Gamma Γ_t (wrt δ), Theta Θ_t (wrt t), Vega ν (wrt σ_{imp}), which converts to

$$d(PnL) = \frac{1}{2}\Gamma(\Delta S)^2 + \Theta(\Delta t) + \nu(\Delta\sigma_{imp}) + ...$$

where ΔS is the change in the underlying asset price, Δt is the fraction of time passed by (typically annualised as 1/256 or 1/365), and $\Delta\sigma_{imp}$ is the change in implied volatility.

Returning to the changes in PnL from Equation 17, and the simplified Black Scholes has given $\Theta_i = -\frac{1}{2}\sigma_i^2 S^2 \Gamma_i$, we can get the changes in $d(PnL)$:

$$d(PnL) = P\&L_{\Delta t,\Delta S} = (\Theta + \frac{1}{2}\sigma^2 S^2 \Gamma)dt \tag{18}$$

$$= \frac{1}{2}\Gamma \underbrace{(\Delta S)^2}_{\text{Recall Ito's Lemma } dSdS=\sigma^2 S^2 dt} - \frac{1}{2}\Gamma_i S^2 \sigma_i^2 (\Delta t) \tag{19}$$

$$= \frac{1}{2}\Gamma S^2 [\underbrace{(\frac{\Delta S}{S})^2}_{\text{realise volatility over } \Delta t \text{ equals } r_t^2=\sigma^2\Delta t} - \sigma_i^2 \Delta t] \tag{20}$$

$$= \frac{1}{2}\Gamma S^2 [(r^2 - \sigma_i^2)\Delta t] \tag{21}$$

The term $\frac{\Delta S}{S}$ is the percentage change in the asset price or the daily asset return, also can be reinterpreted as the realised one-day volatility. The second term $\sigma_i^2 \Delta t$ is the daily implied volatility (over a time step of Δt, i.e. one day here). And the $\Gamma_t \S_t^2$ is the Dollar Gamma, the adjusted approximated measure of second-order sensitivity of the option's price to a change in asset's price. In essence, the formula 21 shows the change in PnL or daily PnL depends on the difference between realised and implied volatility multiplying the Dollar Gamma.

It is worth noting that the integral form of the formula 21 is given by

$$PnL = \sum_{t=0}^{n} \frac{1}{2}\Gamma S^2 [(r^2 - \sigma_i^2)\Delta t]$$

This is close to the payoff of a variance swap:

$$N_{var} * (\sigma^2_{realised} - \sigma_{strike})$$

where the N_{var} is the variance notional, $\sigma^2_{realised}$ is the realised variance and σ_{strike} is the variance strike. The variance notion term has been replace by the various Dollar Gamma terms, which works like a weighted sum, whose weights are determined by the Gamma Γ_t over time. This makes the daily PnL path-dependent, making the total PnL path-dependent as well.

2.6 Impacts of $r^2 - \sigma^2_{imp}\delta t$

There are not clear relationship between these two, but generally the higher the difference between realised and implied volatility over time step Δt, the lower the changes in PnL as well as cumulative PnL. When the difference between the two volatility measures is large, meaning the realised difference is much larger than what the market perceives, then the lower our changes in PnL generally is.

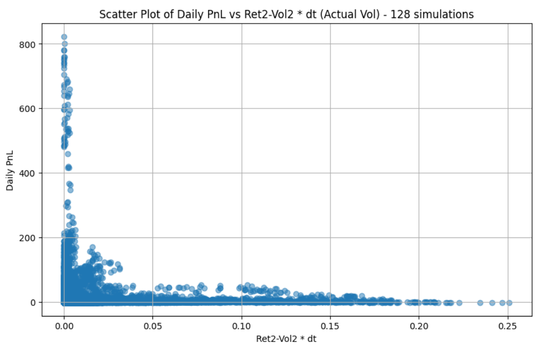

Figure 22: The Gamma-decomposed Daily PnL vs $r^2 - \sigma^2_{imp}\delta t$ Scatter Plot with Actual Volatility - 128 simulations

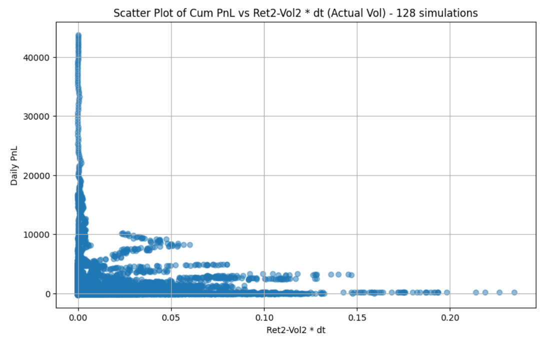

Figure 23: The Gamma-decomposed Cumulative PnL vs $r^2 - \sigma^2_{imp}\delta t$ Scatter Plot with Actual Volatility - 128 simulations

Figure 24: Gamma-decomposed PnL vs $r^2 - \sigma^2_{imp}\delta t$ (Implied Vol) of 128 simulations

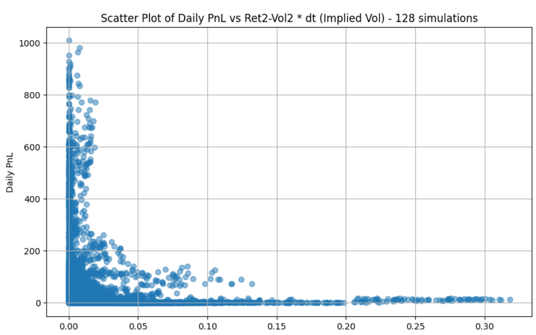

Figure 25: The Gamma-decomposed Daily PnL vs $r^2 - \sigma^2_{imp}\delta t$ Scatter Plot with Implied Volatility - 128 simulations

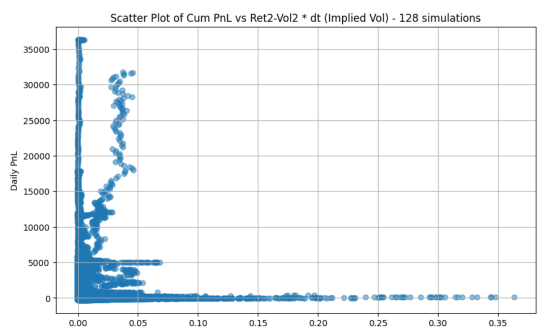

Figure 26: The Gamma-decomposed Cumulative PnL vs $r^2 - \sigma^2_{imp}\delta t$ Scatter Plot with Implied Volatility - 128 simulations

Figure 27: Gamma-decomposed PnL vs $r^2 - \sigma^2_{imp}\delta t$ (Implied Vol) of 128 simulations

2.7 Implications of Smaller Delta

In general, a smaller delta means less short positions to hold against the underlying asset when performing the delta hedge. This means the Black Scholes deltas are usually overhedged, ie excessive money is spent unnecessarily on managing the delta risks and less for other types of risks, such as gamma risks.

3 Part II: Minimum Variance Delta

3.1 Data Manipulation and the Term Structure of Implied Volatility

Like John and Hull ([HW17]), the option data was downloaded from OptionDx.com and the SPX (S&P 500 Index) Option (only call) between 2010 to 2023 daily price data was selected. This period covered is longer than the length of John and Hull's which starts from 02/01/2004 to 31/08/2015, thus different results or effectiveness of its methodology are expected to be different. The dataset for each type of option contains mostly consecutive daily underlying asset's price, expiry date, the date to maturity (dte), implied volatility, option bid, ask and last price of the day. Practioner's *delta*, *vega*, *gamma*, *rho* and *theta* are also provided. The total line items of 2010 - 2023 amounts to 15,556,477. I have further processed the data by the following steps:

- Divide the dte by 256 since the dte is expressed in days, and the τ to be used in pricing formula is expressed in year. 256 is selected as the number of trading days each year.
- Divide the *vega* by 100 since the presented data has it magnified by 100.
- Several dates' implied volatility data are missing (due to holidays, weekends or data issues), thus I have removed these data points by only selecting data. I have also tried to use *df.fillna(method = "ffill")* method to populate the missing implied volatility by its nearest last data record, but it was later verified to lead to bad results.

I have also imported the daily three-month Federal Reserve's treasury bill secondary market rate (discount basis) from 2010 to 2023 as the risk-free interest rates. As expected due to holidays and weekends or other data issues, there are missing rates data on several dates, and I have populated these missing values by *df.fillna(method = "ffill")*.

I have sorted out the data to merge the implied volatility data of different maturities 1M, 3M, 6M, 9M and 12M. The term structures of the Implied Volatility of different maturities are illustrated in Fig.28. We can observe that the long-term IV term structure has relatively smooth term structure wile the short-terms IV such as 1M and 3M can have volatile term structure, which is as expected.

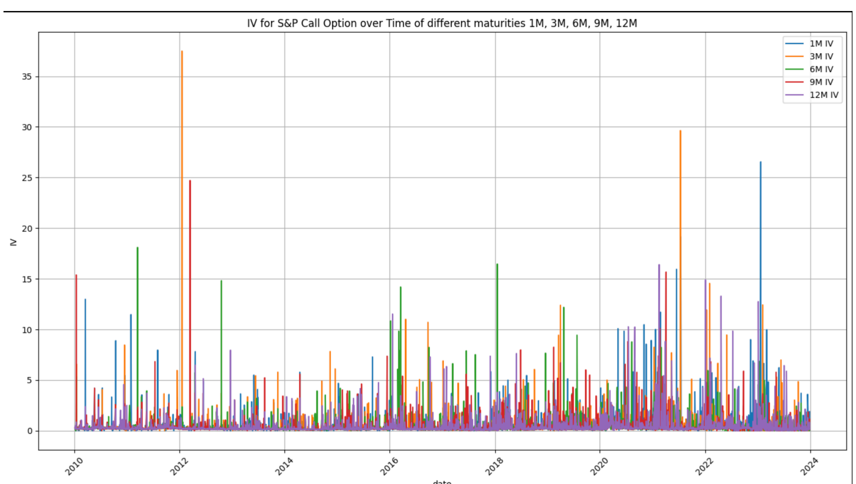

Figure 28: The Term Structure of IV of SPX from 2010 to 2023

In the later stage, I have worked out the Black Scholes option price by applying the Black-Scholes pricing equation $C(S_t, t, \sigma_{imp}) = S_t N(d_1) - e^{-r\tau} K N(d_2)$. The motivation for doing this is the option quotes are: bid, ask and last price on the trading day, and after attempting with the average of the ask and bid, and directly using the last price, they were proved to be not representative and therefore, not fit for quadratic regression. By merging with the interest rate table (The Fed three-month treasury yield rate) based on dates, and used the implied volatility data σ_{imp}, the obtained BS option price proves to be reasonable (close to bid, call and last price traded and in reasonable magnitude).

3.2 Bucketing

The motivation for bucketing rather than apply on the whole dataset is because the delta positions to hold vary from the moneyness and maturities. John and Hull ([HW17]) has used nine different moneyness buckets by rounding δ_{BS} and seven different option maturity buckets (14-30 days, 31-60 days, 61-91days, 92-122 days, 123-182 days, 183-365days and more than 365 days).

For simplicity, the bucketing I chose is based on just three different *moneyness* and the same number of *maturities*:

The moneyness buckets:

- ATM: $0.45 \leq \delta_{BS} \leq 0.55$
- ITM: $0 \leq \delta_{BS} \leq 0.40$
- OTM: $0.60 \leq \delta_{BS} \leq 1.00$

The maturity buckets:

- 1M: $0 \leq$ dte ≤ 30
- 2M: $31 \leq$ dte ≤ 60
- 3M: $61 \leq$ dte ≤ 91
- 4M: $92 \leq$ dte ≤ 122
- 6M: $123 \leq$ dte ≤ 182
- 12M: $183 \leq$ dte ≤ 365
- 12MM: dte ≥ 366, which means more than 12 months

3.3 The Minimum Variance Delta δ_{MV}

According to John and Hull ([HW17]), the minimum variance delta δ_{MV} is targeting to reduce the variance of $\Delta f - \sigma_{MV}\Delta S$, the change of the delta-hedging portfolio. This in application aims to reduce the delta-risk exposure and improves the stability of the portfolio values. The following shows how the analytical form of δ_{MV} can be derive.

We define the value of an option (assuming European call) is a function of underlying price S_t and the implied volatility σ_{imp} as $f(S_t, \sigma_{imp})$. This is for certain as we have already in the standpoint of knowing Black Scholes Option price as:

$$C(S_t, t, \sigma_{imp}) = S_t N(d_1) - e^{-r\tau} K N(d_2)$$

where

$$\begin{aligned}
\tau &= T - t \\
d_1 &= \frac{\log \frac{S_t}{K} + (r + \sigma_{imp}^2)\tau}{\sigma_{imp}\sqrt{\tau}} \\
d_2 &= d_1 - \sigma_{imp}\tau
\end{aligned}$$

By Taylor's equation, we can expand the above function $f(S_t, \sigma_{imp})$ as:

$$df(S, \sigma_{imp}) = \frac{\partial f}{\partial S} dS + \frac{\partial f}{\partial \sigma_{imp}} d\sigma_{imp} + O((dS)^2) + ...$$

and since by definitions of Greeks, $\frac{\partial f}{\partial S} = \delta_{BS}, \frac{\partial f}{\partial \sigma_{imp}} = \nu_{BS}$, and rewrite df as Δf, dS as ΔS and $d\sigma_{imp}$ as $\Delta\sigma_{imp}$ the above approximation can be written as:

$$\Delta f = \delta_{BS}\Delta S + \nu_{BS}\Delta\sigma_{imp} \tag{22}$$
$$\tag{23}$$

And by minusing the the $\delta_{MV}\Delta S$, the value of the short position of underlying asset using the δ_{MV}

$$\Delta f - \delta_{MV}\Delta S = (\delta_{BS} - \delta_{MV})\Delta S + \nu_{BS}(\Delta\sigma_{imp})$$

To minimise the variance of $\Delta f - \delta_{MV}\Delta S$, essentially it is to minimise the changes of the portfolio values conditional on the changes of underlying asset price ΔS, i.e. $\mathbb{E}(d\Pi|\Delta S) = 0$ thus we can apply:

$$\mathbb{E}[\Delta f - \delta_{MV}\Delta S|\Delta S] = 0$$

This gives rise to:

$$\Leftrightarrow \mathbb{E}[(\delta_{BS} - \delta_{MV})\Delta S + \nu_{BS}(\sigma_{imp})|\Delta S] = 0$$

and we can observe that:

$$\begin{aligned}
\mathbb{E}(\delta_{BS} - \delta_{MV}\Delta S|\Delta S) &= (\delta_{BS} - \delta_{MV})\Delta S \\
\mathbb{E}(\nu_{BS}\Delta\delta_{imp}|\Delta S) &= \nu_{BS}\mathbb{E}[\Delta\sigma_{imp}|\Delta S] \\
\Rightarrow \delta_{MV} &= \delta_{BS} + \nu_{BS}\frac{\mathbb{E}[\Delta\sigma_{imp}]}{\Delta S} \\
&= \frac{\partial f_{BS}}{\partial S} + \frac{\partial f_{BS}}{\partial\sigma_{imp}}\frac{\partial\mathbb{E}(\sigma_{imp})}{\partial S}
\end{aligned}$$

This is the logic from Hull & White ([HW17]) and we have an explicit form of the minimum variance delta. We would use this to calculate the new delta positions for each observation in each bucket.

3.4 Quadratic OLS Fitting

3.4.1 The Methodology

The fitting is based on John & Hull ([HW17]) paper and enlighten by the Tutorial Lecture on DH (CQF) where the expected changes in the implied volatility σ_{imp} is modelled by quadratic fitting of moneyness metric δ_{BS} and scaled with change in asset price:

$$\mathbb{E}[\Delta\sigma_{imp}] = (\frac{a + b\sigma_{BS} + c\sigma_{BS}^2}{\sqrt{\tau}})\frac{\Delta S}{S} \tag{24}$$

And to plug this into Equation. 23, after taking expectation and getting $\Delta f - \sigma_{BS}\Delta S = \nu_{BS}\mathbb{E}(\Delta\sigma_{imp})$, which yields:

$$\Delta f - \sigma_{BS}\Delta S = \mu_{BS}(\frac{a + b\sigma_{BS} + c\sigma_{BS}^2}{\sqrt{\tau}})\frac{\Delta S}{S} + \epsilon_t$$

To construct variables used for this regression, the tutorial and extra materials have given a precise form of as:

$$y = (\frac{\Delta V}{\Delta S} - \delta_{BS}) \times \frac{S\sqrt{\tau}}{\nu_{BS}}$$

where:

- ΔV: the difference of today's option price with its previous price record
- ΔS: the difference of today's underlying asset price with its previous price record
- δ_{BS}: the Black-Scholes delta
- S: the underlying asset's price for today
- τ: the time to maturity/time to expiry (dte), which is calculated by dividing the days-to-maturity over 256 for annualisation
- ν_{BS}: the Black-Scholes vega

Then the regression below can be performed on each bucket:

$$y = a + b\delta_{BS} + c\delta_{BS}^2 + \epsilon$$

I have followed this approach to calculate the dependent variable y. I have also used the option's practical delta from OptionDx datasets to construct the independent variable δ_{BS} and its square term δ_{BS}^2 in two different columns. Then I performed the quadratic fitting using the statsmodels.api.

3.4.2 The Results by Buckets

I have obtained the initial results for each bucket by applying the quadratic regression based on OLS methods. As has been explained by Hull & White ([HW17]), the regression may not be statistically significant, which is observed from each bucket's regression report's R^2 and p-values. However, it is worth noting that the regression results have returned results for correlations between these variables and with the values of a, b, c, I am able to derive the values of δ_{MV} based on:

$$\begin{aligned} \delta_{MV} &= \frac{\partial V_{BS}}{\partial S} + \frac{\partial V_{BS}}{\partial \sigma_{imp}} \frac{\partial E(\sigma_{imp})}{\partial S} \\ &= \delta_{BS} + \nu_{BS} \frac{\partial E(\sigma_{imp})}{\partial S} \end{aligned}$$

where we can observe the expected changes in implied volatility σ_{imp}

$$\mathbb{E}[\Delta\sigma_{imp}] = (\frac{a + b\sigma_{BS} + c\sigma_{BS}^2}{\sqrt{\tau}}) \frac{\Delta S}{S}$$

Combining these, we should be able to approximate the values of Minimum Variance Delta of each time step t, $\delta_{MV,t}$ by the following:

$$\widehat{\delta_{MV,t}} = \delta_{BS,t} + \frac{\nu_{BS,t}}{S_t\sqrt{\tau}}(\hat{a} + \hat{b}\delta_{BS,t} + \hat{c}\delta_{BS,t}^2)$$

The resulting coefficients a, b, c for different buckets are listed in Table.1. The regression results for ATM and OTM buckets were generally good and the magnitudes were reasonable: most resulting δ_{MV} is between 0 to 1 with a few smaller than 0. The results for ITM buckets of all maturities are generally not ideal, with many δ_{MV} being larger than 1.

maturity	moneyness	a	b	c
1M	ATM	-1445.7163	6341.8393	-6845.4224
2M	ATM	-198.0232	1294.0424	-1801.1699
3M	ATM	-103.2144	870.4088	-1369.2492
4M	ATM	466.3182	-1419.7700	942.7533
6M	ATM	357.3970	-1079.1668	672.4402
12M	ATM	546.1064	-1900.7705	1548.6653
12MM	ATM	-165.1337	807.6225	-1008.1340
1M	OTM	8.9843	5.8265	-158.2308
2M	OTM	12.4918	-57.7769	-7.8205
3M	OTM	4.5254	-5.0387	-127.9948
4M	OTM	31.6746	-278.2971	509.7345
6M	OTM	31.9810	-298.5904	511.3667
12M	OTM	46.6491	-472.6796	898.6944
12MM	OTM	79.5800	-711.8466	1364.1130
1M	ITM	338100	-865700	544300
2M	ITM	71290	-184900	117900
3M	ITM	6945000	-1806000	11550000
4M	ITM	359600	-940600	605300
6M	ITM	80840	-213300	138600
12M	ITM	28070	-74300	48350
12MM	ITM	-83280	222900	-147100

Table 1: Fitting Results of Different Buckets

3.5 Calibration: Rolling Estimation of $a(t;T), b(t;T), c(t;T)$

I have applied the same rolling window estimation in John and Hull ([HW17]) where the window size of 36M is used. And different from the one-month rolling frequency, I shifted the start day by 1 Day each time of rolling, and assign the obtained a, b, c to the very first day after the 36M rolling window, so on and so fourth, to generate the term structure of the a, b and c. This would result in a different set of values of a, b, c for each observation date of each type of option (of different maturities and strikes), while the first 36M time length data has to be discarded.

After obtaining unique a, b, c for each 36M window, Hull & White ([HW17]) applied a constant set of a, b, c obtained from a day in the month to each observation day in the month the a, b, c was chosen from. Since the detailed selection criteria of such day has not been revealed in the paper, I have decided to test both my daily frequency rolling estimation and [HW17]'s monthly frequency rolling, and a:

- the a, b, c obtained from every 36M windows to the next day after the window (i.e a rolling frequency of 1 day)
- the a, b, c obtained from every 36M windows to the next month period after the window (i.e a rolling frequency of 30 day)

The rolling daily is based on the following script:

```
def rolling_quadratic_regression(df1, window_size_days=1095):  # ~3 years (365 * 3)
    min_date = df1['date'].min()
    max_date = df1['date'].max()
    window_size = pd.Timedelta(days=window_size_days)

    results = []

    # Start rolling from the first date after the initial 3 years
    start_date = min_date + window_size
    while start_date <= max_date:
        end_date = start_date
```

```
        window_start_date = start_date - window_size

        # Select data within the 3-year window
        window_data = df1[(df1['date'] > window_start_date) & (df1['date'] <= end_date)]

        if len(window_data) > 1:  # At least two data points needed for regression
            y = window_data['LHS']
            X = window_data[['RHS1', 'RHS2']]
            X = sm.add_constant(X)

            # Fit the quadratic regression model
            model = sm.OLS(y, X).fit()

            # Store the coefficients for the current date
            results.append({
                'date': end_date,
                'a': model.params['const'],
                'b': model.params['RHS1'],
                'c': model.params['RHS2']
            })

        # Move forward by one day
        start_date = start_date + pd.DateOffset(days=1)

    return pd.DataFrame(results)

df1M_ATM_calibrating = df1M_ATM_regression_noinf
df1M_ATM_calibrating = df1M_ATM_calibrating.rename(columns = {'date_x':'date'})

df1M_ATM_calibrating.head()

df1M_ATM_calibrated = rolling_quadratic_regression(df1M_ATM_calibrating)
```

Listing 3: Python Script for Rolling Daily

and the rolling monthly is based on this:

```
from pandas.tseries.offsets import MonthEnd

def rolling_quadratic_regression_monthly(df1, window_size_days=1095):  # ~3 years (365 * 3)
    min_date = df1['date'].min()
    max_date = df1['date'].max()
    window_size = pd.Timedelta(days=window_size_days)

    results = []

    # Start rolling from the first date after the initial 3 years
    start_date = min_date + window_size
    while start_date <= max_date:
        end_date = start_date
        window_start_date = start_date - window_size

        # Select data within the 3-year window
        window_data = df1[(df1['date'] > window_start_date) & (df1['date'] <= end_date)]

        if len(window_data) > 1:  # At least two data points needed for regression
            y = window_data['LHS']
            X = window_data[['RHS1', 'RHS2']]
            X = sm.add_constant(X)

            # Fit the quadratic regression model
            model = sm.OLS(y, X).fit()

            # Apply the coefficient to the next month
            next_month_start = end_date + pd.DateOffset(days=1)
            next_month_end = next_month_start + MonthEnd(1)

            days_in_next_month = pd.date_range(next_month_start, next_month_end)

            # Store the coefficients for the current date
            results.append({
```

```python
                'date': end_date,
                'a': model.params['const'],
                'b': model.params['RHS1'],
                'c': model.params['RHS2']
            })

        # Move forward by one day
        start_date = start_date + pd.DateOffset(months=1)

    return pd.DataFrame(results)
```

Listing 4: Python Script for Rolling Monthly

The detailed term structure of a, b, c have been given in Appendix 1. Throughout the buckets, the b ad c are mostly symmetric to each other over the x-axis. In the ATM buckets, the 1M (Figure 31), 4M (Figure 40) and 6M (Figure 43) buckets are relatively less volatile comparing with others. The Bucket 12MM has the highest volatility, indicating the longest dates to maturity would yield higher degree of uncertainty, while shorter time-to-maturity options would yield relatively lower levels of uncertainty. The OTM buckets in general has less volatility comparing to ATM, indicating that OTM options are less traded due to no intrinsic values and would drop to zero value at expiry. The ITM buckets has the longest range of constant values of a, b, c close to 0, comparing to the other buckets, indicating that its posessing of intrinsic values makes its delta-risk relatively stable. However, most of them have undergone a large jump in values from post-2016 (1M, Figure 73), post-2018 (2M, Figure 76), and post-2023 (3M, Figure 79 to 12MM, Figure 91). The economic reasons behind are worth further studying.

3.6 Model Validation: $\delta_{MV} - \delta_{BS}$ and $\mathbb{E}(\Delta\sigma_{imp})$ vs δ_{BS} and vs δ_{MV}

The following section presents the four charts of each bucket which illustrates the relationships of minimum variance delta and Black-Scholes delta $\delta_{MV} - \delta_{BS}$), its fitting curve, the expected changes in implied volatility $\mathbb{E}(\Delta\sigma_{imp})$ w.r.t. δ_{BS} and w.r.t. δ_{MV}.

The values of a, b, c determines the shape of the $\delta_{MV} - \delta_{BS}$ from a quadratic function point of view. If $c > 0$ the shape should be parabolic and inverted parabolic if $c < 0$.

The relationship between $\mathbb{E}(\Delta\sigma_{imp})$ vs δ is expected to be specific to bucket, depending on Equation. 24. If the $c\Delta S$ >0, there should be positive correlation, and vice versa.

3.6.1 No Rolling Results

We can observe that the shape of $\delta_{MV} - \delta_{BS}$ are parabolic shapes/inverted parabolic shape. For the results generated from non-rolling regression, the inverted parabolic shapes are observed at:

- ATM-1M (Fig.92), since the $c = -6845$
- ATM-2M(Fig.99), since the $c = -1801$
- ATM-3M(Fig.106), since the $c = -1369$
- ATM-12MM (Fig.134), since the $c = -1008$
- OTM-1M (Fig.141), however the $c = 158$
- OTM-2M (Fig.148), however the $c = -8$
- OTM-3M (Fig.155), however the $c = -128$

The parabolic shapes are observed at:

- AMT-4M (Fig.113), since the $c = 943$
- ATM-6M (Fig.120), since the $c = 672$
- ATM-12M (Fig.127), since the $c = 1549$

Other types of shapes are observed. For example some are sine function like, for example in the bucket OTM-4M (Fig.162), OTM-6M (Fig.169).

And some show almost a horizontal line, like:

- OTM-12M (Fig.176), with $c = 899$
- OTM-12MM (Fig.183), with $c = 1364$
- All ITM buckets (Fig.190 to Fig.232)

For the fitting lines, we have also observed inverted parabolic shapes for the quadratic regression fitting curves between $\delta_{MV} - \delta_{BS}$. The inverted parabolic fitting curves are seen at:

- ATM-1M(Fig.93)
- ATM-2M (Fig.100)
- ATM-3M (Fig.107)
- ATM-12MM (Fig.135
- OTM-1M (Fig.142)
- OTM-3M (Fig.156)

The parabolic fitting curves are seen at:

- ATM-4M (Fig.114)
- ATM-6M (Fig.121)
- ATM-12M (Fig.128)
- OTM-4M (Fig.163)
- OTM-6M (Fig.170)
- OTM-12M (Fig.177)
- OTM-12MM (Fig.184)

For ITM buckets, most $\delta_{MV} - \delta_{BS}$ relationships are horizontal lines which indicates the Black-Scholes deltas do not have significant effects on the minimum variance deltas, which was unexpected. Their regression fitting curve is also almost horizontal, indicating the similar relation.

The relationships between $\mathbb{E}(\Delta\sigma_{imp})$ vs δ in general are classified into three types: The "Cross X" (or a triangle with an inverted triangle on its top), the single triangle and "Three-Body" (three triangles connecting). The "Cross X" indicates that most changes in implied volatility σ_{imp} is matched to values closing to the upper and lower bounds of the delta chosen (either σ_{BS} or σ_{MV}), and very few of them are distributed in the midpoint of all the values of the chosen delta. The relative size of these two triangles reflects the relative size of those closer to the upper bound relative to the lower bound. So the higher the "intersection" point, the larger the triangle relative to the inverted triangle meaning more $\mathbb{E}(\Delta\sigma_{imp})$ are mapped to values away from the upper bound of the chosen delta.

The "Cross X" has:

- ATM 1M Figure.96
- ATM 2M Figure.103
- ATM 3M Figure.110
- ATM 4M Figure.117
- ATM 6M Figure.124
- ATM 12M Figure.131
- OTM 1M δ_{BS} Figure.143
- OTM 2M δ_{BS} Figure.150
- OTM 3M δ_{BS} Figure.157
- OTM 4M δ_{BS} Figure.164
- OTM 6M δ_{BS} Figure.171
- OTM 12M δ_{BS} Figure.178
- OTM 12MM δ_{BS} Figure.185

The Single Triangle:

- ATM 12MM Figure.138
- OTM 1M δ_{MV} Figure.144
- OTM 2M δ_{MV} Figure.151
- OTM 3M δ_{MV} Figure.158

- OTM 4M δ_{MV} Figure.165
- OTM 6M δ_{MV} Figure.172
- OTM 12M δ_{MV} Figure.179, however it is cluster around level of 0 of MV delta δ_{MV}
- OTM 12MM δ_{MV} Figure.186, however it is cluster around level of 0 of MV delta δ_{MV}
- ITM 1M δ_{MV} Figure.193, however it is cluster around level of 0 of MV delta δ_{MV}
- ITM 2M δ_{MV} Figure.200, however it is cluster around level of 0 of MV delta δ_{MV}
- ITM 3M δ_{MV} Figure.207, however it is cluster around level of 0 of MV delta δ_{MV}
- ITM 4M δ_{MV} Figure.214, however it is cluster around level of 0 of MV delta δ_{MV}
- ITM 6M Figure.222
- ITM 12M δ_{MV} Figure.228, however it is cluster around level of 0 of MV delta δ_{MV}
- ITM 12MM δ_{MV} Figure.235, however it is cluster around level of 0 of MV delta δ_{MV}

The ”Three-Body”:

- ITM 1M Figure.192
- ITM 2M Figure.199
- ITM 3M δ_{BS} Figure.206
- ITM 4M δ_{BS} Figure.213
- ITM 12M δ_{BS} Figure.227
- ITM 12MM Figure.234

3.6.2 Rolling Daily Results

For the results based on daily rolling estimation, the inverted parabolic shapes can be observed at:

- ATM-1M (Fig.97), with mostly $c < 0$, but comparing with its counterpart in Fig.92, it has more layers of such inverted parabolic shapes
- ATM-2M (Fig.104), with mostly $c < 0$, and similarly more layers of such shapes than its counterpart
- ATM-3M (Fig.111), with mostly $c < 0$ and similarly more layers

The parabolic shapes can be observed at:

- ATM-4M (Fig.118), with mostly $c > 0$
- ATM-6M (Fig.125), with mostly $c > 0$
- ATM-12M (Fig.132), with mostly $c > 0$
- OTM-4M (Fig.167), with most $c > 0$ during 2018-2022 and $c < 0$ for the rest
- OTM-6M (Fig.174), with most $c > 0$
- OTM-12M (Fig.181), with most $c > 0$
- OTM-12MM (Fig.188), with most $c > 0$
- ITM-1M (Fig.195) with also large part being inverted parabolic, but the parabolic part looks ”higher”, and with most c around 0 and a significant jump around 2018

- ITM-12MM (Fig.237), with most c around 0, a mild increase around 2018 and a significant jump around 2022

Also there are some buckets showing mixed types: that contain similar amount of inverted and proper parabolic shapes:

- ATM-12MM (Fig.139, with almost half $c < 0$ and half $c > 0$
- OTM-1M (Fig.146), with $c > 0$ during 2016-2020 and $c < 0$ for the rest
- OTM-2M (Fig.153), with $c > 0$ during 2016-2022 and $c < 0$ for the rest
- OTM-3M (Fig.160), with $c > 0$ during 2018-2022 and $c < 0$ for the rest
- ITM-2M (Fig.202), with most c around 0 and a significant jump around 2018
- ITM-3M (Fig.209), with most c around 0 and a significant jump around 2022
- ITM-4M (Fig.216), with most c around 0 and a significant jump around 2022
- ITM-6M (Fig.223), with most c around 0 and a significant jump around 2022
- ITM-12M (Fig.230), with most c around 0 and a significant jump around 2022

The relationships between $\mathbb{E}(\Delta\sigma_{imp})$ vs δ generally follows the findings from last part (No Rolling), with a few exceptions:

- ATM 1M to 12M: δ_{MV} changes from the "Cross" to "Three-Body"
- OTM 1M: δ_{MV} changes from the "Single Triangle" to "Three-Body"
- OTM 2M - 3M: δ_{MV} changes from the "Single Triangle" to "Cross"
- OTM 4M - 12MM: δ_{MV} "Single Triangle" has "inverted" (turned upside down), though the 12M and 12MM has more drastic transformation from almost horizontal line to an inverted triangle.
- ITM 1M - 12MM: δ_{MV} from "Single Triangle" (horizontal line) to inverted one

3.6.3 Rolling Monthly Results

Comparing the monthly rolling results with their daily rolling counterparts, each pair has almost identical shape of $\delta_{MV} - \delta_{BS}$ between the two only that the monthly results is a "thinner" version of the daily result, i.e. there are more layers of curves in the monthly result. This is expected as the daily rolling produces different results of a, b, c on each trading day between 2013 to 2023, while the monthly rolling produces constant results of a, b, c, thus more likely to make similar values of δ_{MV}, therefore less data points. Since for each bucket, these two regressions are identical in fitting methods except in rolling frequency, the general trend should be the same while the density of scatters are higher for daily rolling than monthly rolling.

3.6.4 The Analysis of Model Validation

The naive approach of quadratic fitting is taken to analyse the relationship between δ_{BS} and δ_{MV}. The regression results are subject to rolling estimation as part of model validation. This step is necessary since at each time point, one trader could only judge based on history and forecast, thus the whole population regression for each bucket is unreliable and the rolling estimation is more realistic. The daily or monthly frequency selection is subject to the assumption to dynamic hedging. With daily and monthly calibration, the distribution of data points become more widely distributed in general, like an invertd parabolic shape becomes such of multiple layers, with more layers for daily rolling comparing to monthly rolling. If the liquidity of the asset is good and the hedging cost is low everytime a trader adjusts the positions, then the daily rolling should be a feasible choice and ensures more effective hedging.

The use of more advanced data analytics tools such as deep learning can be used to extend the study of model validation.

3.7 $\mathbb{E}(\Delta\sigma_{imp})$ and Hedging Gain

3.7.1 Positivity of $\mathbb{E}(\Delta_{imp})$

The expected changes in implied volatility $\mathbb{E}(\Delta\sigma_{imp})$ is not always negative. My result shows if applying the constant a, b, c obtained from regression over the entire bucket regardless (no rolling window), the results show in Table 2. For ATM and OTM buckets, all of them have more positive $\mathbb{E}(\Delta\sigma_{imp})$ than negative ones, and the opposite is true for ITM bucket.

maturity	moneyness	$\mathbb{E}(\Delta\sigma_{imp}) \geq 0$	$\mathbb{E}(\Delta\sigma_{imp}) < 0$
1M	ATM	25,972	12,234
2M	ATM	26,221	11,739
3M	ATM	18,807	10,015
4M	ATM	17,312	9,199
6M	ATM	26,641	17,212
12M	ATM	27,532	20,912
12MM	ATM	27,458	23,674
1M	OTM	651,803	611,243
2M	OTM	264,351	246,514
3M	OTM	148,100	136,476
4M	OTM	100,398	96,949
6M	OTM	117,860	110,950
12M	OTM	165,532	163,589
12MM	OTM	117,794	122,818
1M	ITM	701,564	764,863
2M	ITM	379,634	397,978
3M	ITM	220,707	229,399
4M	ITM	167,990	173,437
6M	ITM	200,255	236,693
12M	ITM	247,205	248,975
12MM	ITM	168,395	169,389

Table 2: $\mathbb{E}(\Delta\sigma_{imp})$ positivity of Different Buckets

The hedging gains are calculated by considering the gains being calculated by below:

$$\epsilon_{t,MV} = \Delta V - \widehat{\delta_{MV,t}}\Delta S$$
$$\epsilon_{t,BS} = \Delta V - \widehat{\delta_{BS,t}}\Delta S$$

where the $\widehat{\delta_{MV,t}}$ can be calculated by the formulae given above.

Hull & While has further calculated the Gains for each bucket in by

$$Gain = 1 - \frac{SSE(\epsilon_{MV})}{SSE(\epsilon_{BS})} = 1 - \frac{\sum_t \epsilon_{MV,t}}{\sum_t \epsilon_{BS,t}}$$

Though with an explicit formulae to calculate the gains and sum of squared errors $SSE(.)$, the calculation of $\delta_{MV,t}$ involves the selection of a, b, c. So far I have managed to derive the bucket-specific values of a, b, c which are listed in the Table.1. The calibrated values based on the 66-Day rolling window at a frequency of 1 Day has also provided me with date-specific values of a, b, c. Hull & White (2017) has adopted monthly constant a, b, c when generating the values of minimum-variance deltas δ_{MV}. However, the specific calculation of the a, b, c to apply as constants for each month is not explained in the literature, where quoted *"The residual for all options and then considering only the residuals from options in a particular delta bucket."* Thus, I take three different approaches to select a, b, c and take the *Gain* of each bucket. I have firstly applied the bucket specific a, b, c based on my results in Table 1, then I have applied the values of a, b, c from the first day of each month, assuming the delta positions are made on the first day of the month and fixed for the rest of the month.

3.7.2 Hedging Gains

The hedging gains from the minimum-variance delta δ_{MV} relative to the Black-Scholes delta δ_{BS} is calculated by constructing a hedging ratio Gain. Hull & White (2017) has firstly defined the residual terms from the two delta hedging actions. The residuals from hedging using the mean-variance delta and Black-Scholes delta and the Gains from hedging are already defined above. By these equations, I have computed the Gains for each bucket and listed them below in Table.3.

maturity	moneyness	Gains (%) - No Rolling	Gains (%) - Daily Rolling	Gains (%) - Monthly Rolling
1M	ATM	23.33	-28.76	-29.13
2M	ATM	49.47	13.45	13.14
3M	ATM	63.78	41.59	39.17
4M	ATM	52.50	37.12	33.78
6M	ATM	59.35	53.74	52.45
12M	ATM	56.21	48.29	47.26
12MM	ATM	36.24	18.98	16.62
1M	OTM	18.33	-52.68	-63.97
2M	OTM	20.80	-68.43	-80.03
3M	OTM	31.82	-38.52	-48.96
4M	OTM	4.40	-114	-130.72
6M	OTM	19.83	-17.76	-25.05
12M	OTM	5.83	-38.05	-46.67
12MM	OTM	-3.14	-41.94	-46.31
1M	ITM	-64,433,712.75	-69,343,823.85	-98,486,116.61
2M	ITM	-36,134,500	-66,430,508.20	-85,281,546.73
3M	ITM	-47,556,924,600	-57,878,278,147.96	-10,155,712,089.37
4M	ITM	-34,707,500	-23,072,089.12	-24,981,953.18
6M	ITM	-153,908,214,100	-3,668,024.52	-3187,300.60
12M	ITM	-1,080,200	-11,382,438.66	-12,497,546.45
12MM	ITM	-5,288,454	-740,696.12	-808,971.94

Table 3: Hedging Gains by Constant a, b, c for each Different Buckets

For the non-calibrated groups, all the ATM buckets (regardless of maturities) have a Hedging Gain larger than 20% (minimum is 23.33%), which all passes above the threshold of 15% asked in Task 5. Almost all the OTM buckets have reached 15% and above except the buckets of maturities of 4M, 12M, and 12MM (which has negative gains which is a loss). All the ITM buckets show insignificant results with smaller than -100% Gain values. This corresponds to the abnormal results of a, b, c observed when doing the quadratic regression fitting.

With rolling daily calibration, all the buckets' gain has decreased. The only few buckets whose gains are over 15% is ATM 3M, ATM 4M, ATM6M, ATM 12M. The ATM 1M is having negative gain, indicating the nature of ATM call with only less than one month to expiry. The closer to expiry, the more volatile the price of options which made positive earnings more difficult.

With rolling monthly calibration, all the buckets' gains have further decreased. This indicates that a less dynamic hedging has decreased the return in general, as the hedging position is not sensitive to the changes in the practical delta.

It is also worth noting that the rolling by both daily or monthly have all yielded δ_{MV} larger than 1, which is unrealistic from theory. This might indicate that with a different and longer range of date points, the quadratic fitting approach may not be the best tool to get the δ_{MV}. It is worth further study to implement more advanced fitting tools using Machine Learning, such as support vector machines.

4 Conclusion

5 Appendix 1: The Term Structures of Quadratic Regression Coefficients a, b, c over 2014 - 2023 by Rolling Estimation of Daily and Monthly Basis

5.1 ATM Buckets

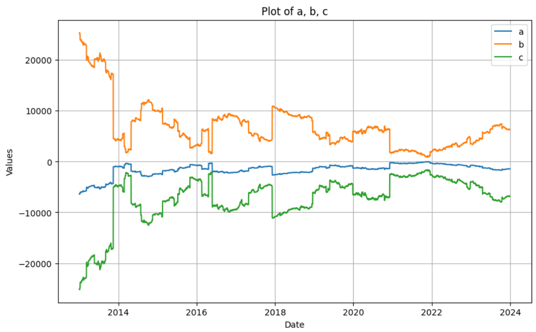

Figure 29: The Term Structure of a, b, c for Rolling on Daily Frequency

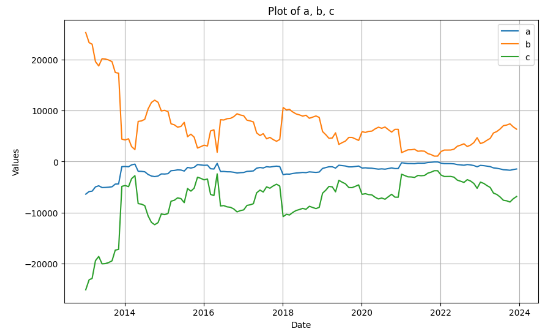

Figure 30: The Term Structure of a, b, c for Rolling on Monthly Frequency

Figure 31: The Term Structure of a, b, c for Rolling of Bucket ATM1M

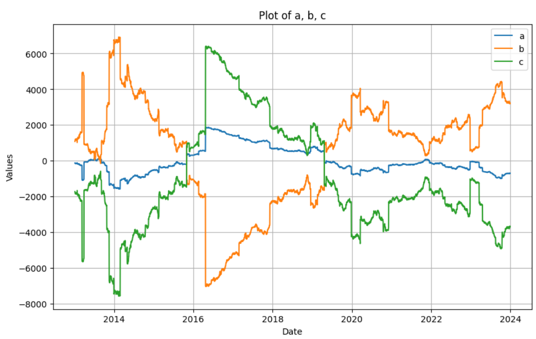

Figure 32: The Term Structure of a, b, c for Rolling on Daily Frequency

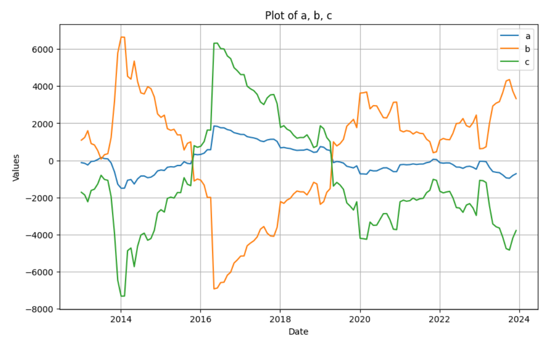

Figure 33: The Term Structure of a, b, c for Rolling on Monthly Frequency

Figure 34: The Term Structure of a, b, c for Rolling of Bucket ATM2M

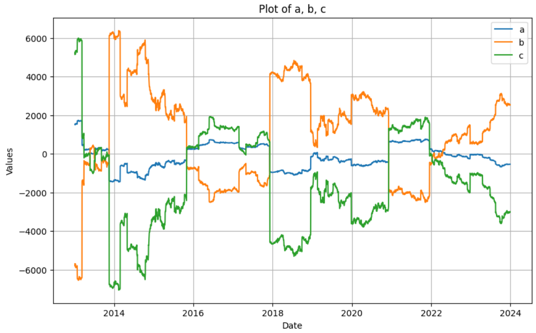

Figure 35: The Term Structure of a, b, c for Rolling on Daily Frequency

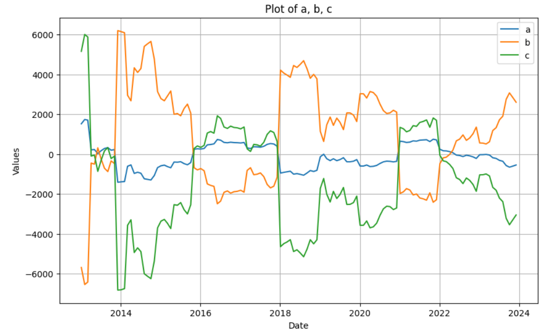

Figure 36: The Term Structure of a, b, c for Rolling on Monthly Frequency

Figure 37: The Term Structure of a, b, c for Rolling of Bucket ATM3M

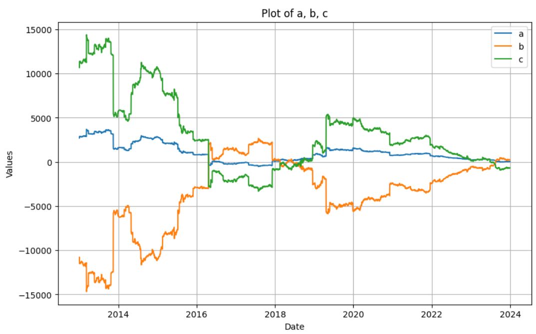

Figure 38: The Term Structure of a, b, c for Rolling on Daily Frequency

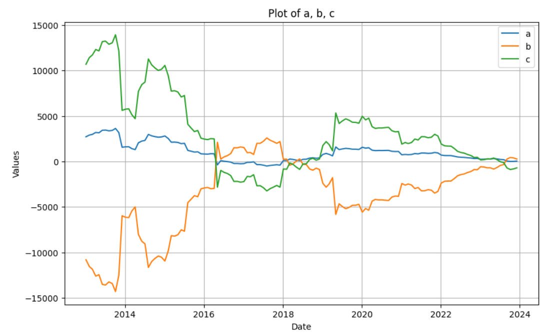

Figure 39: The Term Structure of a, b, c for Rolling on Monthly Frequency

Figure 40: The Term Structure of a, b, c for Rolling of Bucket ATM4M

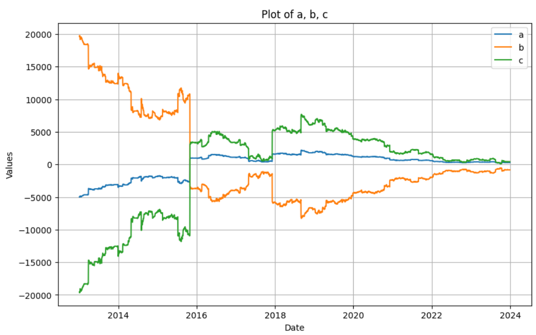

Figure 41: The Term Structure of a, b, c for Rolling on Daily Frequency

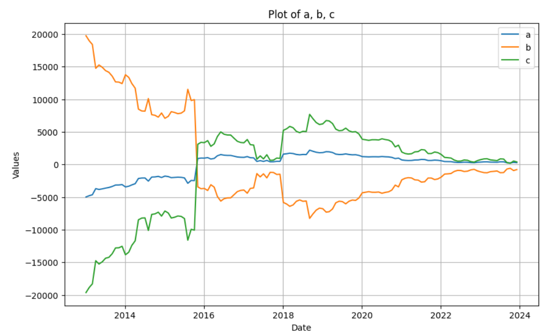

Figure 42: The Term Structure of a, b, c for Rolling on Monthly Frequency

Figure 43: The Term Structure of a, b, c for Rolling of Bucket ATM6M

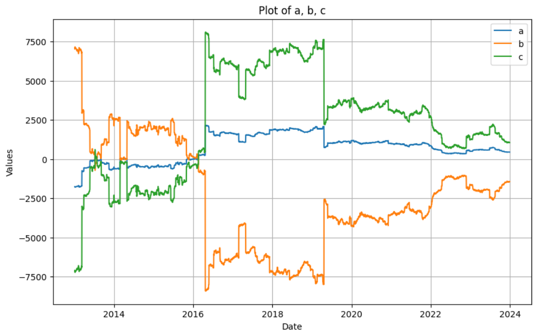

Figure 44: The Term Structure of a, b, c for Rolling on Daily Frequency

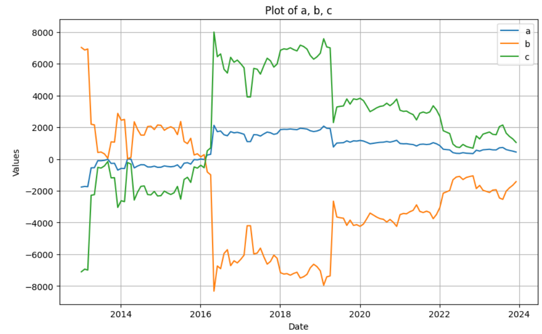

Figure 45: The Term Structure of a, b, c for Rolling on Monthly Frequency

Figure 46: The Term Structure of a, b, c for Rolling of Bucket ATM12M

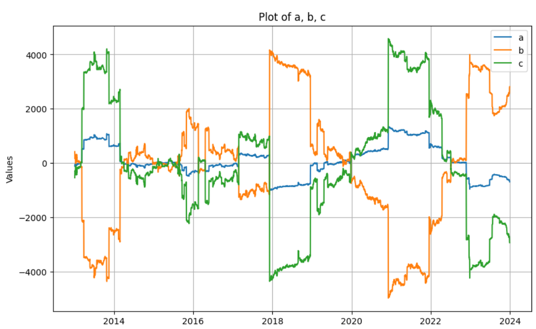

Figure 47: The Term Structure of a, b, c for Rolling on Daily Frequency

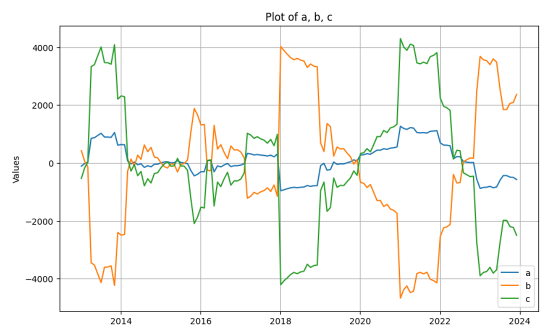

Figure 48: The Term Structure of a, b, c for Rolling on Monthly Frequency

Figure 49: The Term Structure of a, b, c for Rolling of Bucket ATM12MM

5.2 OTM Buckets

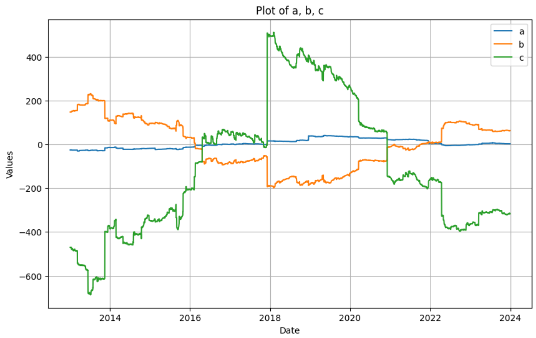

Figure 50: The Term Structure of a, b, c for Rolling on Daily Frequency

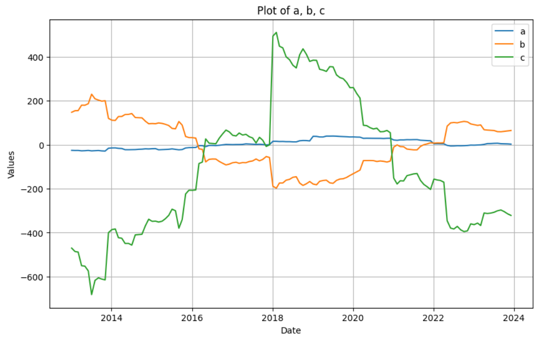

Figure 51: The Term Structure of a, b, c for Rolling on Monthly Frequency

Figure 52: The Term Structure of a, b, c for Rolling of Bucket OTM1M

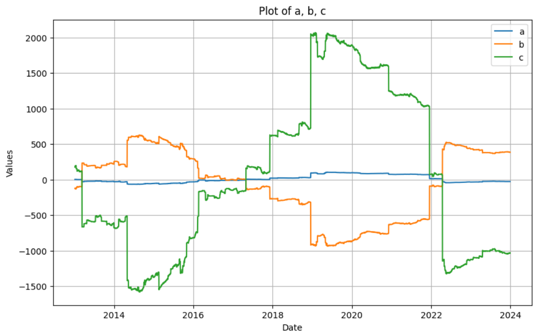

Figure 53: The Term Structure of a, b, c for Rolling on Daily Frequency

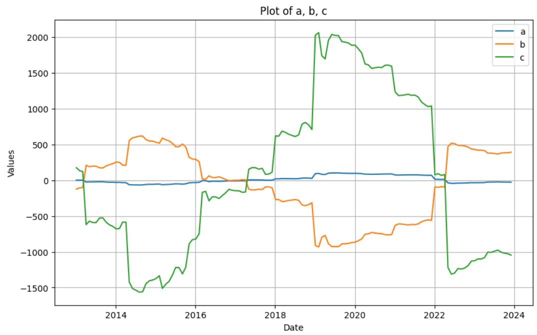

Figure 54: The Term Structure of a, b, c for Rolling on Monthly Frequency

Figure 55: The Term Structure of a, b, c for Rolling of Bucket OTM2M

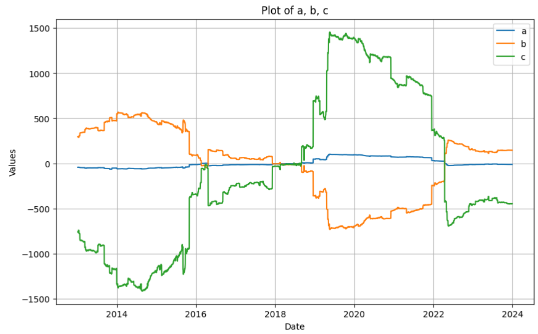

Figure 56: The Term Structure of a, b, c for Rolling on Daily Frequency

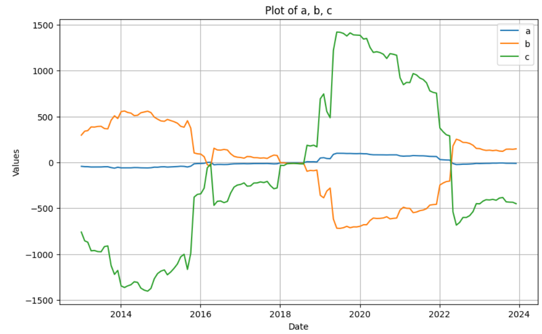

Figure 57: The Term Structure of a, b, c for Rolling on Monthly Frequency

Figure 58: The Term Structure of a, b, c for Rolling of Bucket OTM3M

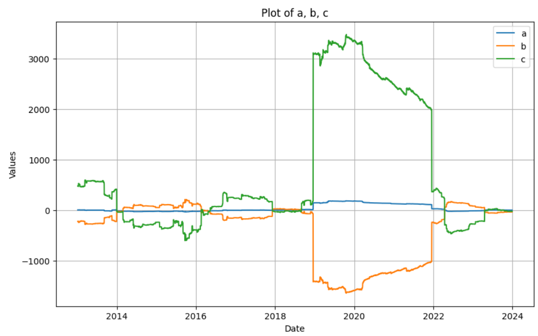

Figure 59: The Term Structure of a, b, c for Rolling on Daily Frequency

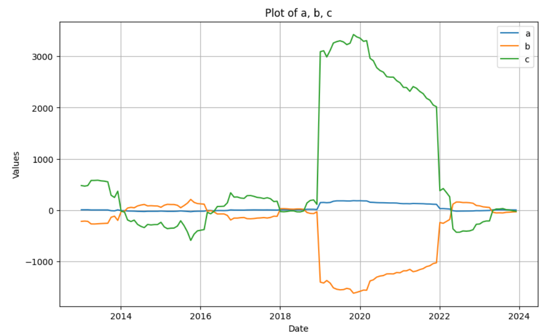

Figure 60: The Term Structure of a, b, c for Rolling on Monthly Frequency

Figure 61: The Term Structure of a, b, c for Rolling of Bucket OTM4M

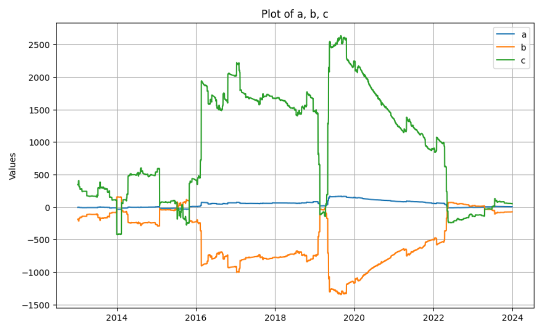

Figure 62: The Term Structure of a, b, c for Rolling on Daily Frequency

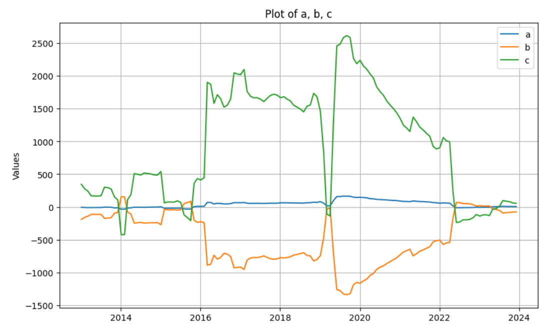

Figure 63: The Term Structure of a, b, c for Rolling on Monthly Frequency

Figure 64: The Term Structure of a, b, c for Rolling of Bucket OTM6M

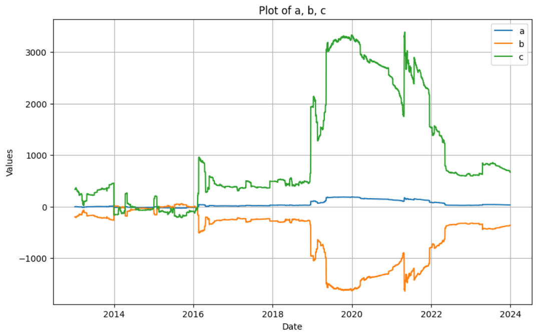

Figure 65: The Term Structure of a, b, c for Rolling on Daily Frequency

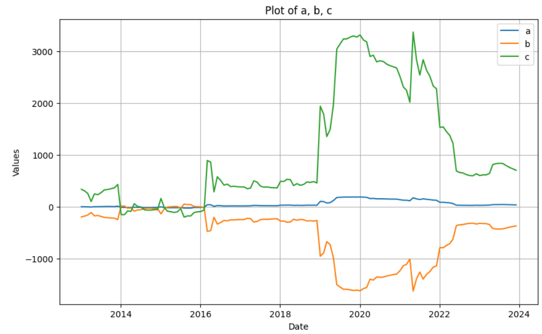

Figure 66: The Term Structure of a, b, c for Rolling on Monthly Frequency

Figure 67: The Term Structure of a, b, c for Rolling of Bucket OTM12M

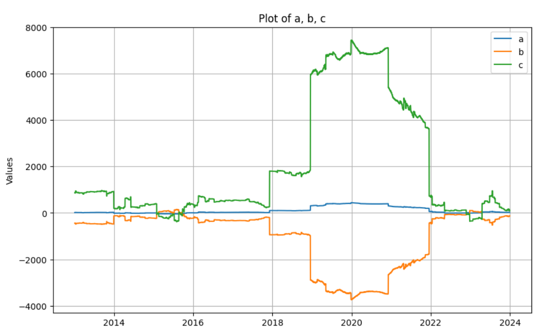

Figure 68: The Term Structure of a, b, c for Rolling on Daily Frequency

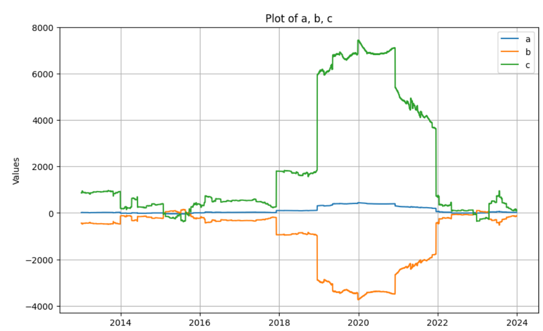

Figure 69: The Term Structure of a, b, c for Rolling on Monthly Frequency

Figure 70: The Term Structure of a, b, c for Rolling of Bucket OTM12MM

5.3 ITM Buckets

Figure 71: The Term Structure of a, b, c for Rolling on Daily Frequency

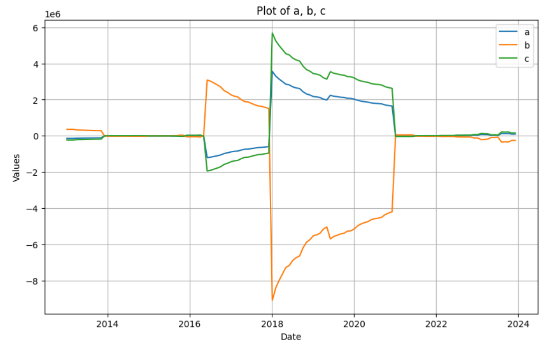

Figure 72: The Term Structure of a, b, c for Rolling on Monthly Frequency

Figure 73: The Term Structure of a, b, c for Rolling of Bucket ITM1M

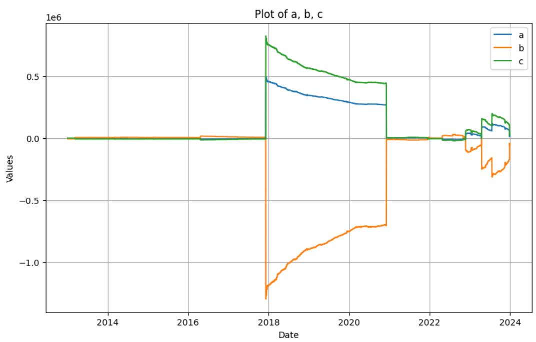

Figure 74: The Term Structure of a, b, c for Rolling on Daily Frequency

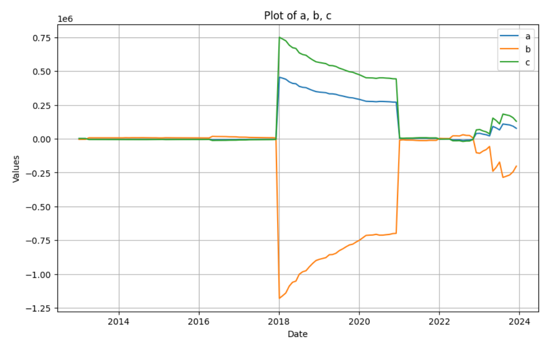

Figure 75: The Term Structure of a, b, c for Rolling on Monthly Frequency

Figure 76: The Term Structure of a, b, c for Rolling of Bucket ITM2M

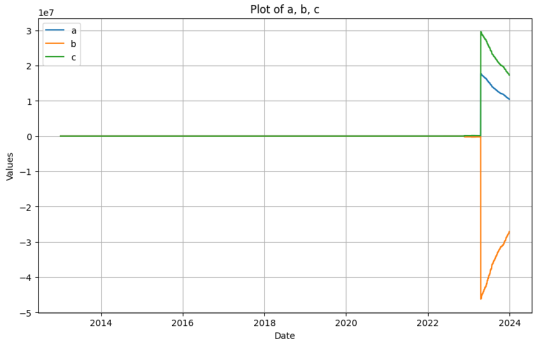

Figure 77: The Term Structure of a, b, c for Rolling on Daily Frequency

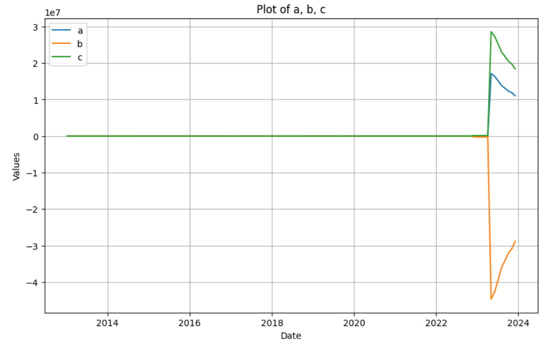

Figure 78: The Term Structure of a, b, c for Rolling on Monthly Frequency

Figure 79: The Term Structure of a, b, c for Rolling of Bucket ITM3M

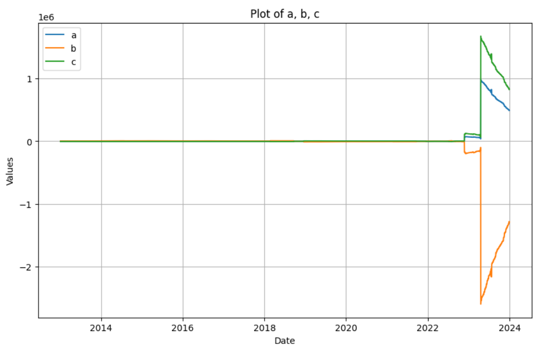

Figure 80: The Term Structure of a, b, c for Rolling on Daily Frequency

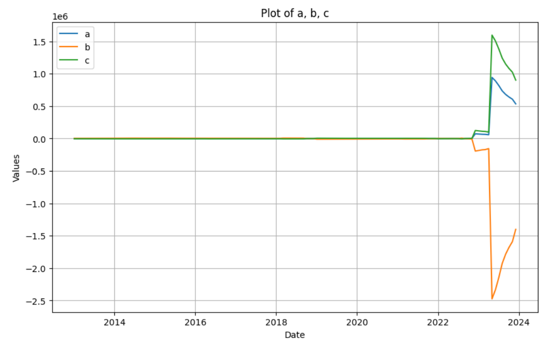

Figure 81: The Term Structure of a, b, c for Rolling on Monthly Frequency

Figure 82: The Term Structure of a, b, c for Rolling of Bucket ITM4M

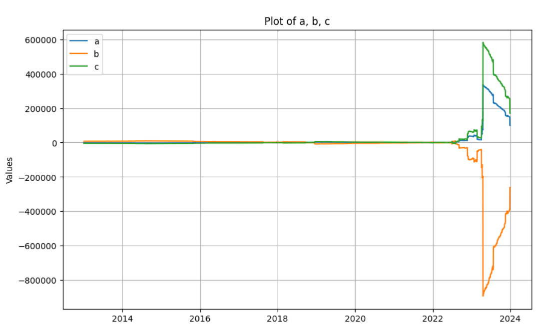

Figure 83: The Term Structure of a, b, c for Rolling on Daily Frequency

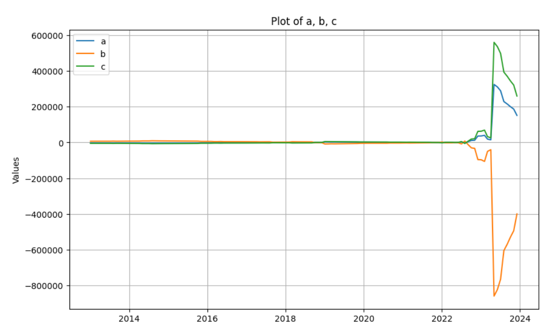

Figure 84: The Term Structure of a, b, c for Rolling on Monthly Frequency

Figure 85: The Term Structure of a, b, c for Rolling of Bucket ITM6M

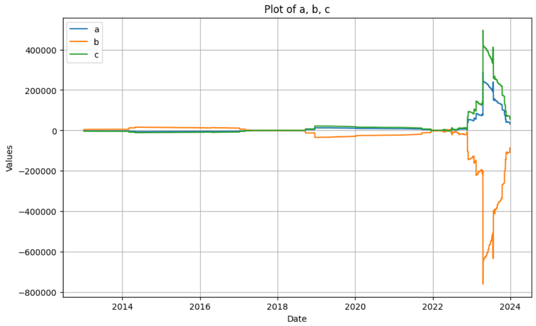

Figure 86: The Term Structure of a, b, c for Rolling on Daily Frequency

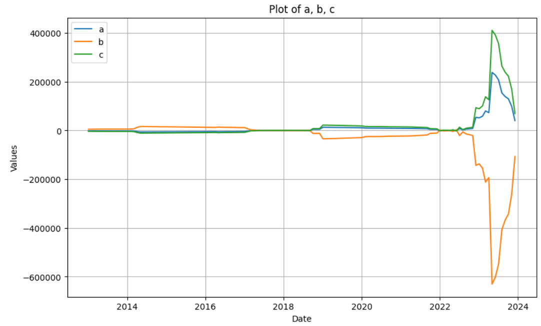

Figure 87: The Term Structure of a, b, c for Rolling on Monthly Frequency

Figure 88: The Term Structure of a, b, c for Rolling of Bucket ITM12M

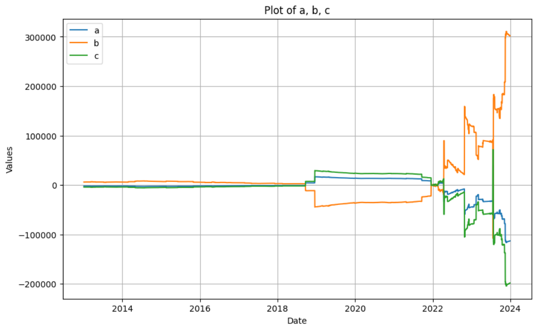

Figure 89: The Term Structure of a, b, c for Rolling on Daily Frequency

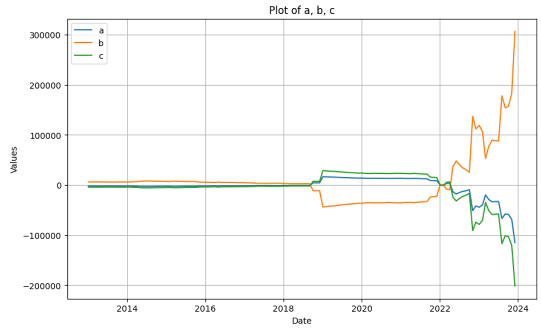

Figure 90: The Term Structure of a, b, c for Rolling on Monthly Frequency

Figure 91: The Term Structure of a, b, c for Rolling of Bucket ITM12MM

6 Appendix 2: The $\delta_{MV} - \delta_{BS}$ and $\mathbb{E}(\Delta\sigma_{imp})$ vs δ_{BS} and vs δ_{MV} for Each Bucket

6.1 ATM Buckets

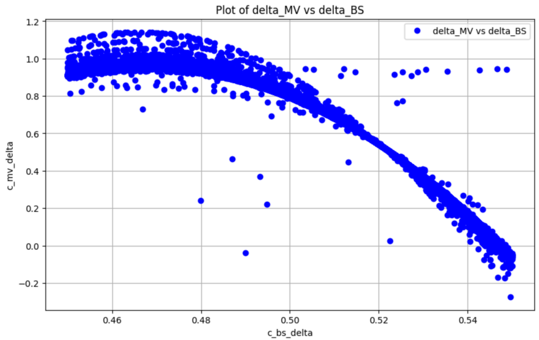

Figure 92: δ_{MV} vs δ_{BS}

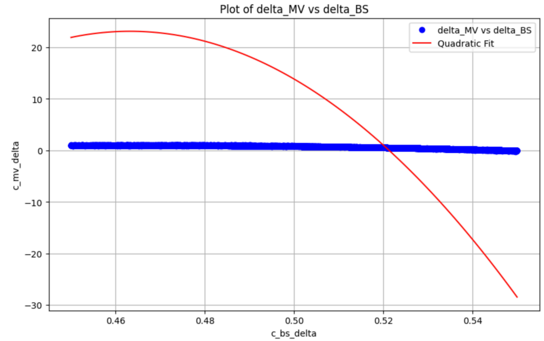

Figure 93: δ_{MV} vs δ_{BS} and the Fitting Line

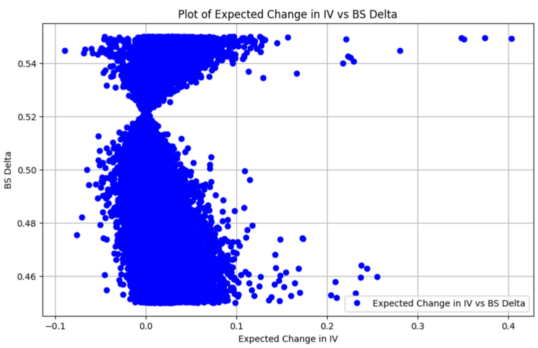

Figure 94: $\mathbb{E}(\Delta\sigma_{imp})$ vs δ_{BS}

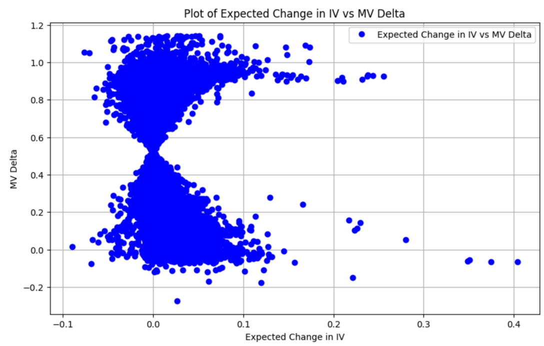

Figure 95: $\mathbb{E}(\Delta\sigma_{imp})$ vs δ_{MV}

Figure 96: The $\delta_{MV} - \delta_{BS}$ and $\mathbb{E}(\Delta\sigma_{imp})$ vs δ_{BS} and vs δ_{MV} for ATM 1M Bucket

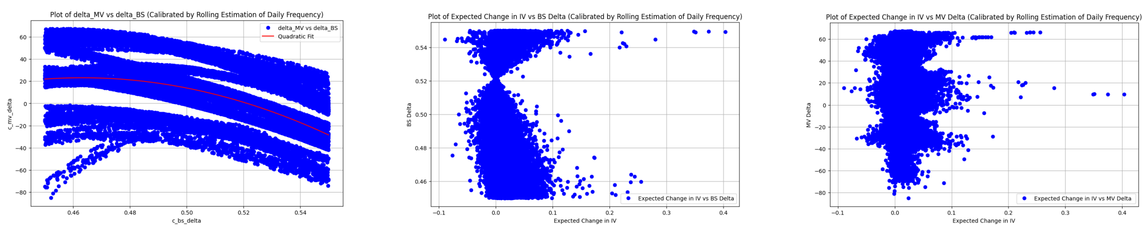

Figure 97: The $\delta_{MV} - \delta_{BS}$ and $\mathbb{E}(\Delta\sigma_{imp})$ vs δ_{BS} and vs δ_{MV} for ATM 1M Bucket - Rolling Daily

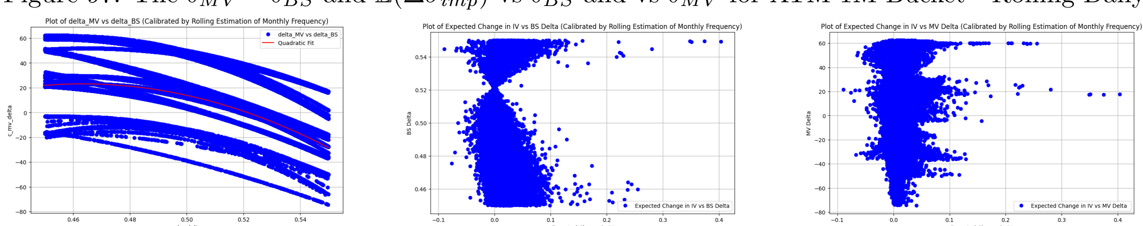

Figure 98: The $\delta_{MV} - \delta_{BS}$ and $\mathbb{E}(\Delta\sigma_{imp})$ vs δ_{BS} and vs δ_{MV} for ATM 1M Bucket - Rolling Monthly

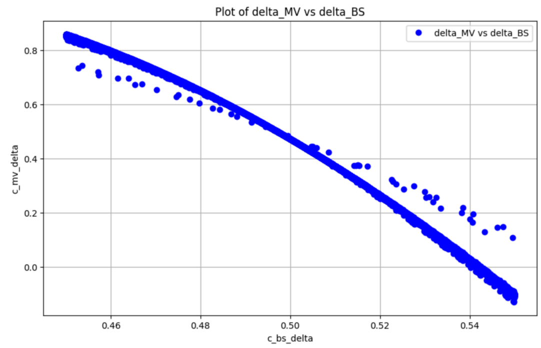

Figure 99: δ_{MV} vs δ_{BS}

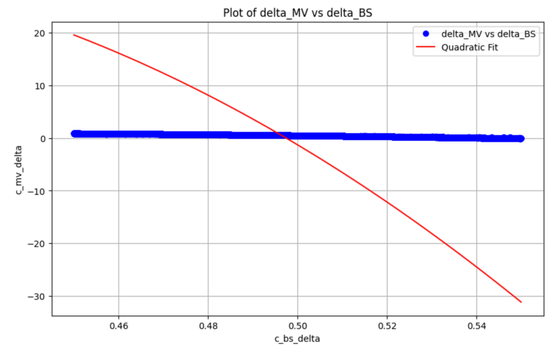

Figure 100: δ_{MV} vs δ_{BS} and the Fitting Line

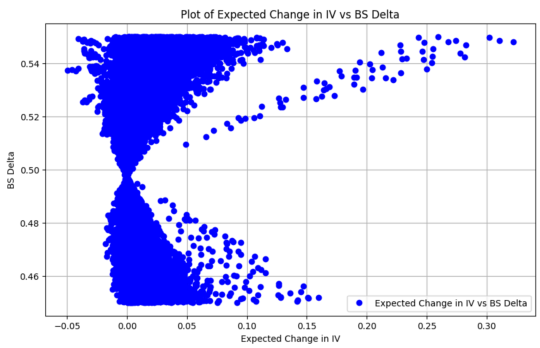

Figure 101: $\mathbb{E}(\Delta\sigma_{imp})$ vs δ_{BS}

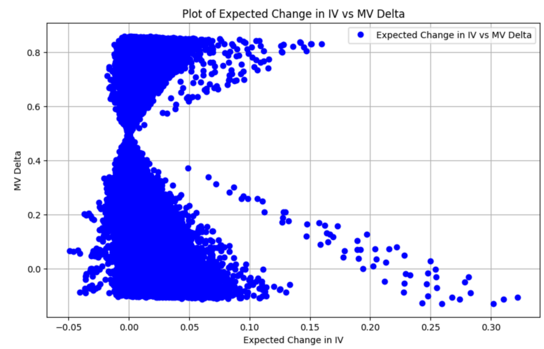

Figure 102: $\mathbb{E}(\Delta\sigma_{imp})$ vs δ_{MV}

Figure 103: The $\delta_{MV} - \delta_{BS}$ and $\mathbb{E}(\Delta\sigma_{imp})$ vs δ_{BS} and vs δ_{MV} for ATM 2M Bucket

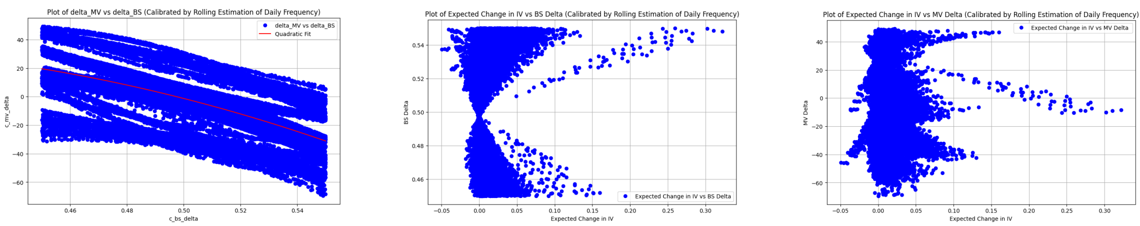

Figure 104: The $\delta_{MV} - \delta_{BS}$ and $\mathbb{E}(\Delta\sigma_{imp})$ vs δ_{BS} and vs δ_{MV} for ATM 2M Bucket - Rolling Daily

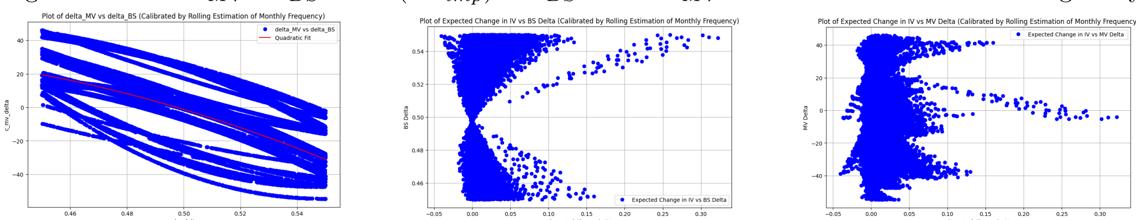

Figure 105: The $\delta_{MV} - \delta_{BS}$ and $\mathbb{E}(\Delta\sigma_{imp})$ vs δ_{BS} and vs δ_{MV} for ATM 2M Bucket - Rolling Monthly

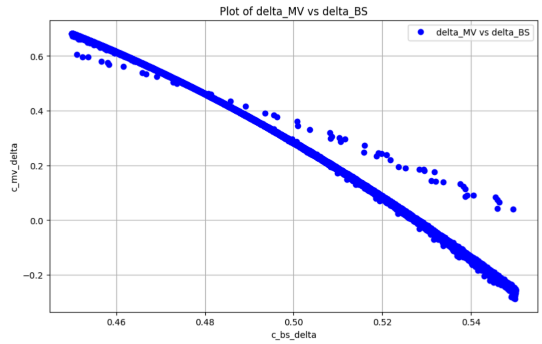

Figure 106: δ_{MV} vs δ_{BS}

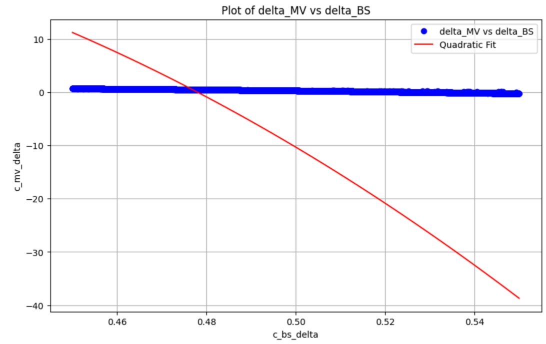

Figure 107: δ_{MV} vs δ_{BS} and the Fitting Line

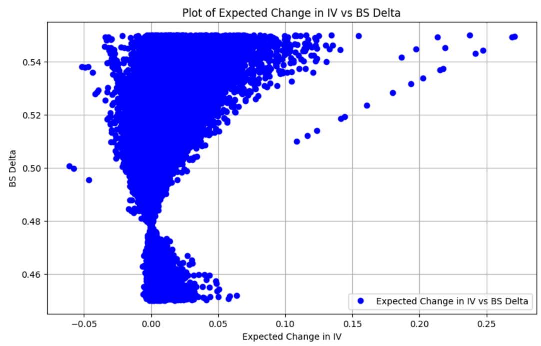

Figure 108: $\mathbb{E}(\Delta\sigma_{imp})$ vs δ_{BS}

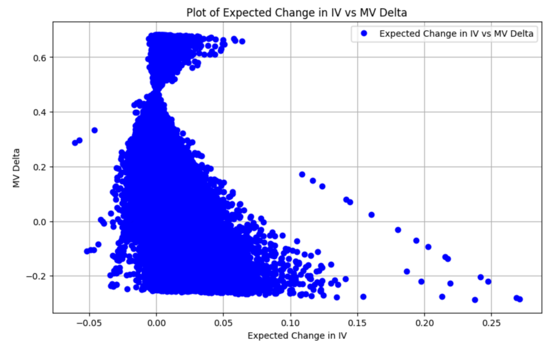

Figure 109: $\mathbb{E}(\Delta\sigma_{imp})$ vs δ_{MV}

Figure 110: The $\delta_{MV} - \delta_{BS}$ and $\mathbb{E}(\Delta\sigma_{imp})$ vs δ_{BS} and vs δ_{MV} for ATM 3M Bucket

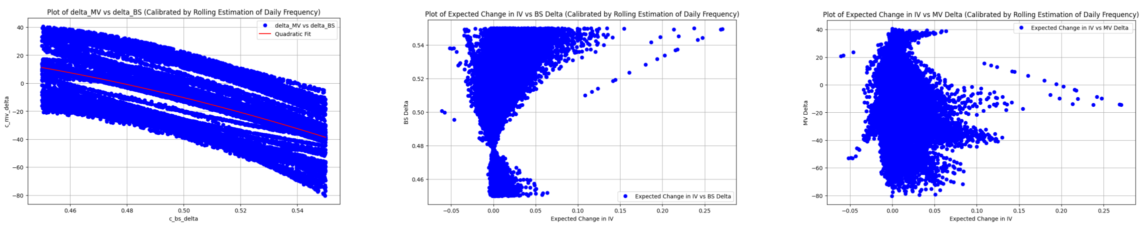

Figure 111: The $\delta_{MV} - \delta_{BS}$ and $\mathbb{E}(\Delta\sigma_{imp})$ vs δ_{BS} and vs δ_{MV} for ATM 3M Bucket - Rolling Daily

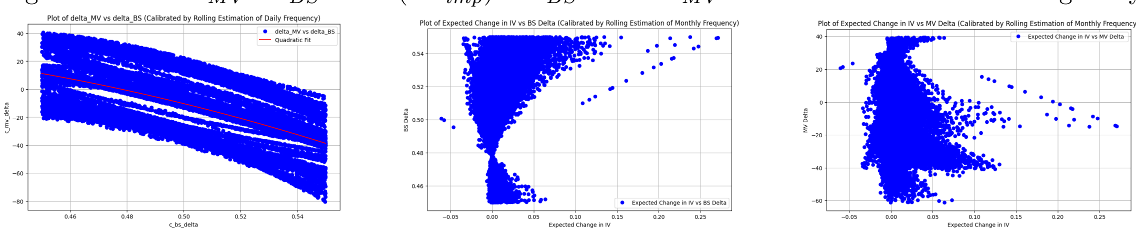

Figure 112: The $\delta_{MV} - \delta_{BS}$ and $\mathbb{E}(\Delta\sigma_{imp})$ vs δ_{BS} and vs δ_{MV} for ATM 3M Bucket - Rolling Monthly

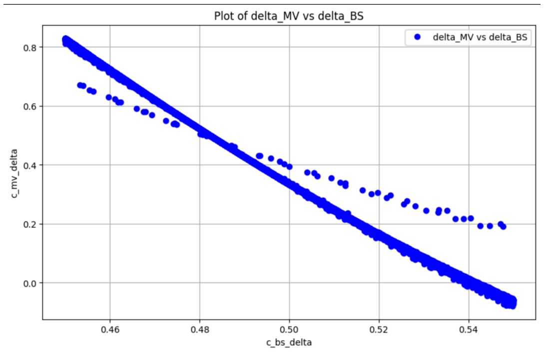

Figure 113: δ_{MV} vs δ_{BS}

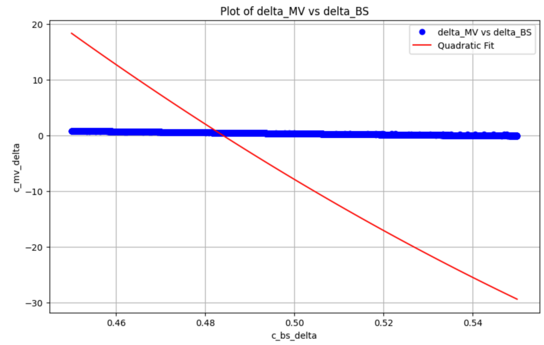

Figure 114: δ_{MV} vs δ_{BS} and the Fitting Line

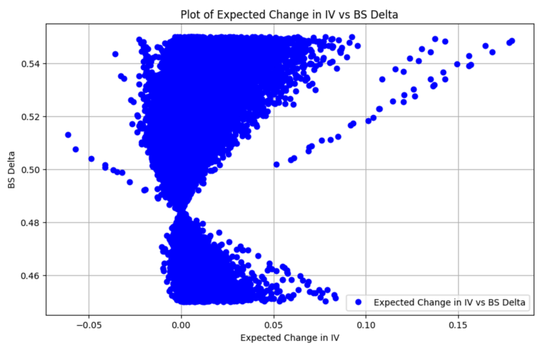

Figure 115: $\mathbb{E}(\Delta\sigma_{imp})$ vs δ_{BS}

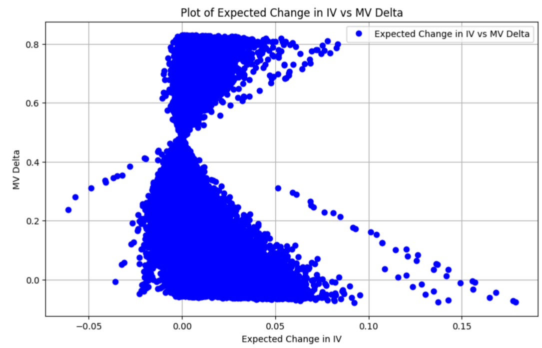

Figure 116: $\mathbb{E}(\Delta\sigma_{imp})$ vs δ_{MV}

Figure 117: The $\delta_{MV} - \delta_{BS}$ and $\mathbb{E}(\Delta\sigma_{imp})$ vs δ_{BS} and vs δ_{MV} for ATM 4M Bucket

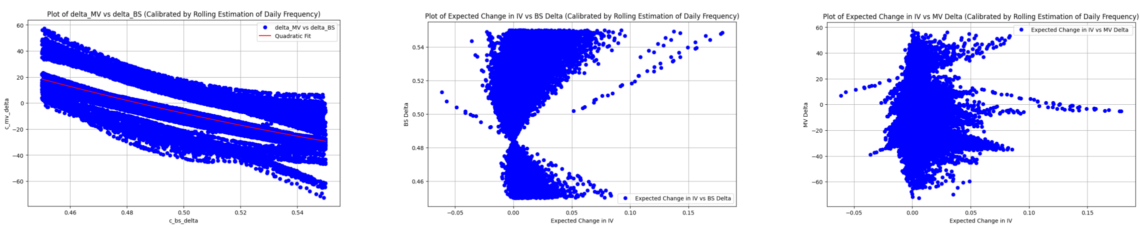

Figure 118: The $\delta_{MV} - \delta_{BS}$ and $\mathbb{E}(\Delta\sigma_{imp})$ vs δ_{BS} and vs δ_{MV} for ATM 4M Bucket - Rolling Daily

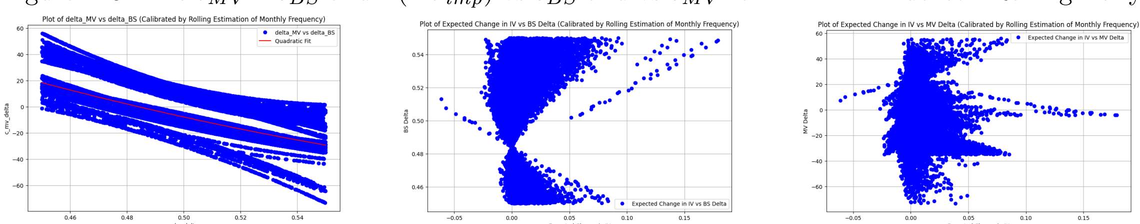

Figure 119: The $\delta_{MV} - \delta_{BS}$ and $\mathbb{E}(\Delta\sigma_{imp})$ vs δ_{BS} and vs δ_{MV} for ATM 4M Bucket - Rolling Monthly

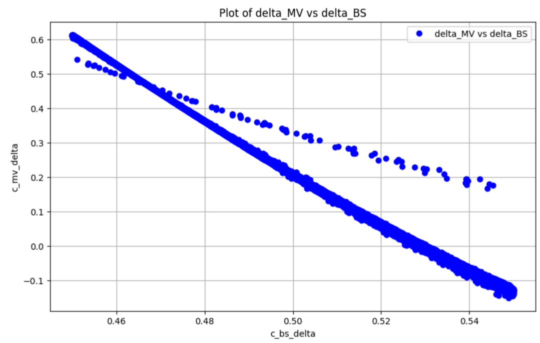

Figure 120: δ_{MV} vs δ_{BS}

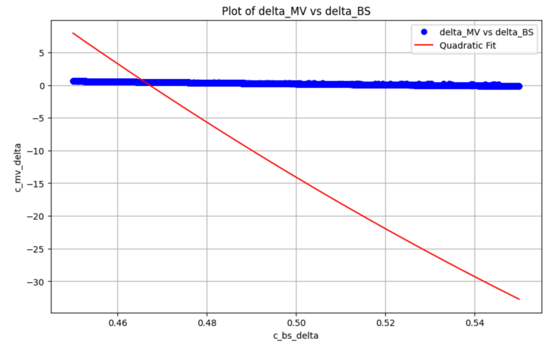

Figure 121: δ_{MV} vs δ_{BS} and the Fitting Line

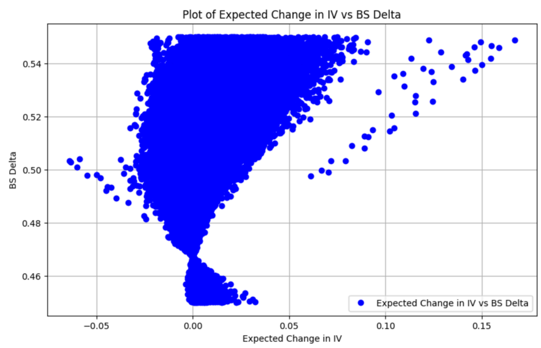

Figure 122: $\mathbb{E}(\Delta\sigma_{imp})$ vs δ_{BS}

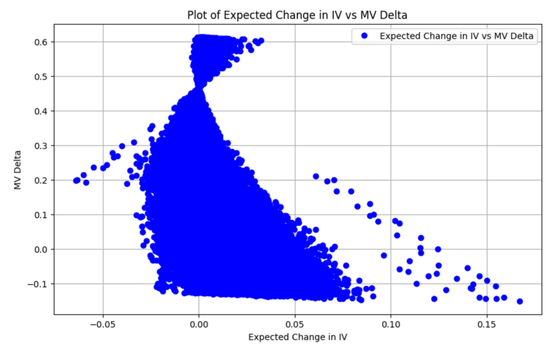

Figure 123: $\mathbb{E}(\Delta\sigma_{imp})$ vs δ_{MV}

Figure 124: The $\delta_{MV} - \delta_{BS}$ and $\mathbb{E}(\Delta\sigma_{imp})$ vs δ_{BS} and vs δ_{MV} for ATM 6M Bucket

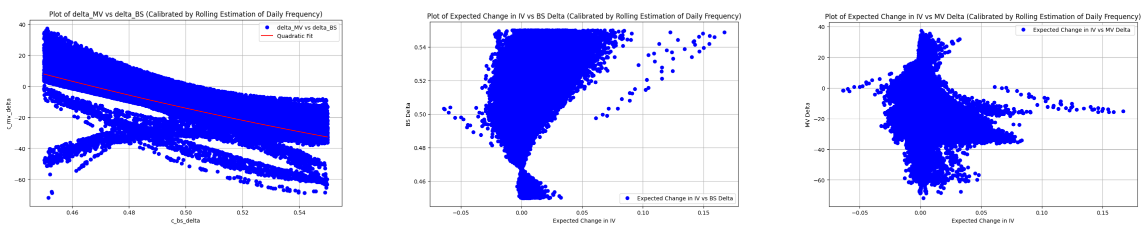

Figure 125: The $\delta_{MV} - \delta_{BS}$ and $\mathbb{E}(\Delta\sigma_{imp})$ vs δ_{BS} and vs δ_{MV} for ATM 6M Bucket - Rolling Daily

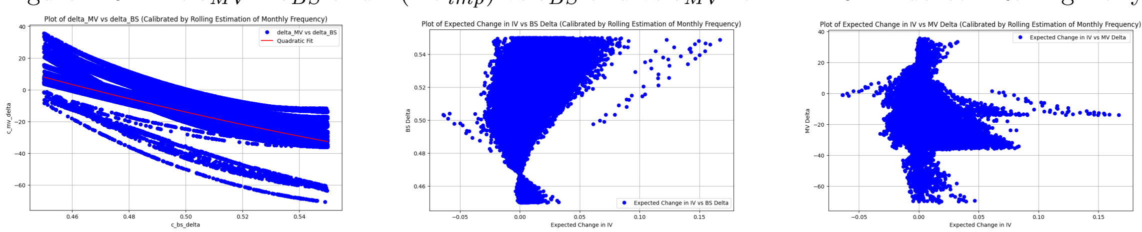

Figure 126: The $\delta_{MV} - \delta_{BS}$ and $\mathbb{E}(\Delta\sigma_{imp})$ vs δ_{BS} and vs δ_{MV} for ATM 6M Bucket - Rolling Monthly

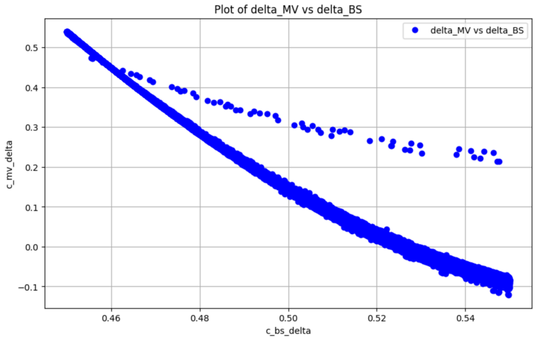

Figure 127: δ_{MV} vs δ_{BS}

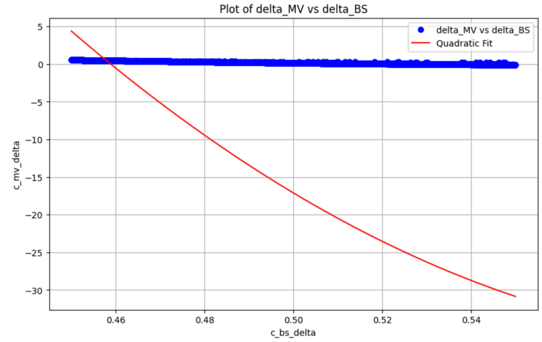

Figure 128: δ_{MV} vs δ_{BS} and the Fitting Line

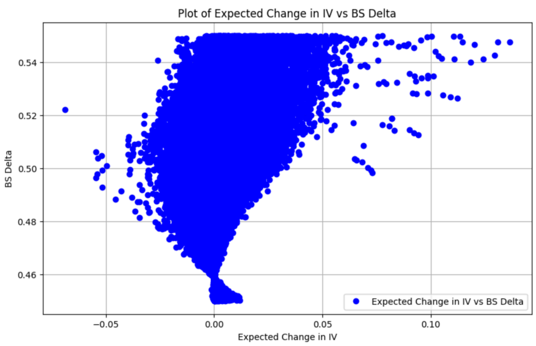

Figure 129: $\mathbb{E}(\Delta\sigma_{imp})$ vs δ_{BS}

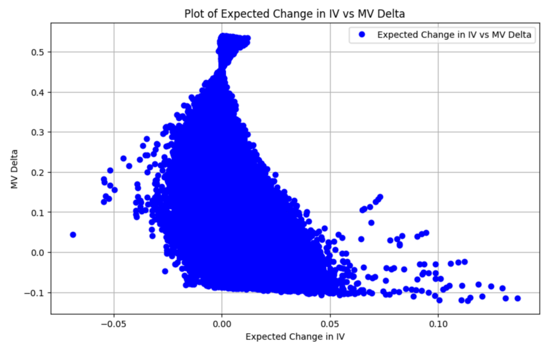

Figure 130: $\mathbb{E}(\Delta\sigma_{imp})$ vs δ_{MV}

Figure 131: The $\delta_{MV} - \delta_{BS}$ and $\mathbb{E}(\Delta\sigma_{imp})$ vs δ_{BS} and vs δ_{MV} for ATM 12M Bucket

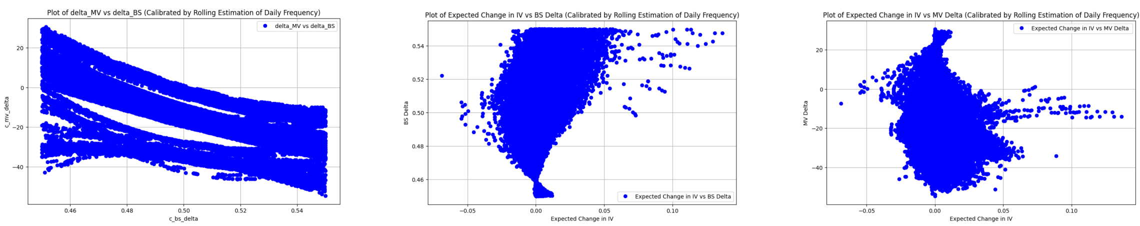

Figure 132: The $\delta_{MV} - \delta_{BS}$ and $\mathbb{E}(\Delta\sigma_{imp})$ vs δ_{BS} and vs δ_{MV} for ATM 12M Bucket - Rolling Daily

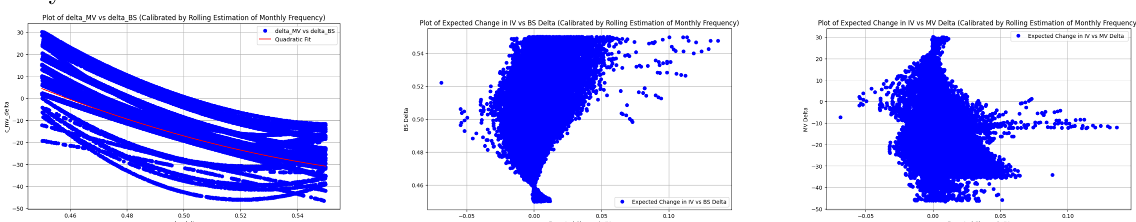

Figure 133: The $\delta_{MV} - \delta_{BS}$ and $\mathbb{E}(\Delta\sigma_{imp})$ vs δ_{BS} and vs δ_{MV} for ATM 12M Bucket - Rolling Monthly

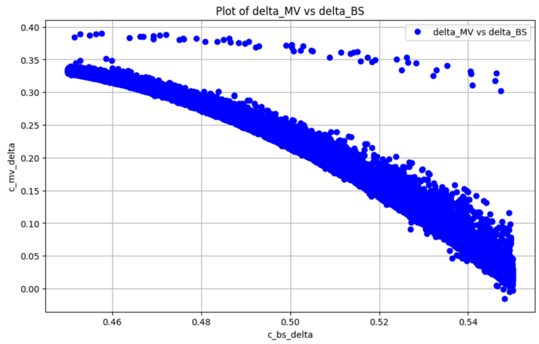

Figure 134: δ_{MV} vs δ_{BS}

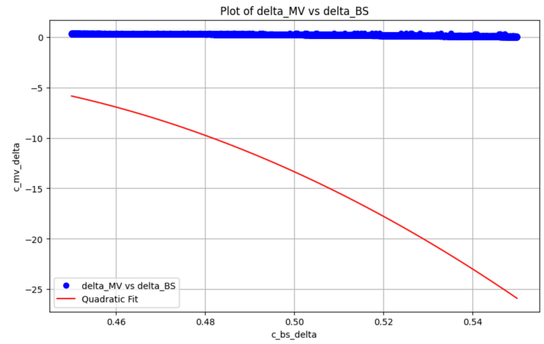

Figure 135: δ_{MV} vs δ_{BS} and the Fitting Line

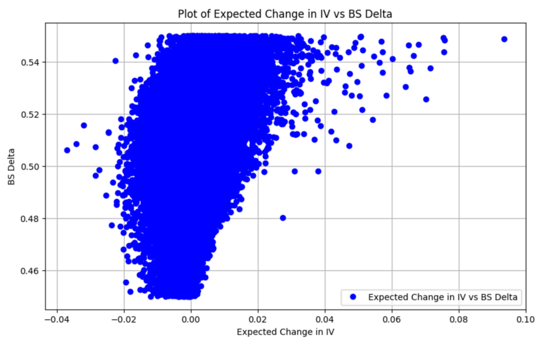

Figure 136: $\mathbb{E}(\Delta\sigma_{imp})$ vs δ_{BS}

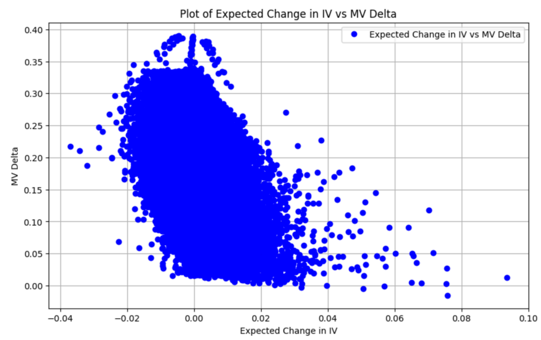

Figure 137: $\mathbb{E}(\Delta\sigma_{imp})$ vs δ_{MV}

Figure 138: The $\delta_{MV} - \delta_{BS}$ and $\mathbb{E}(\Delta\sigma_{imp})$ vs δ_{BS} and vs δ_{MV} for ATM 12MM Bucket

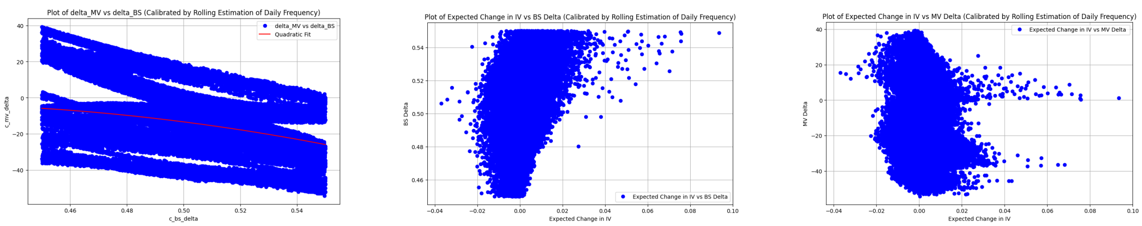

Figure 139: The $\delta_{MV} - \delta_{BS}$ and $\mathbb{E}(\Delta\sigma_{imp})$ vs δ_{BS} and vs δ_{MV} for ATM 12MM Bucket - Rolling Daily

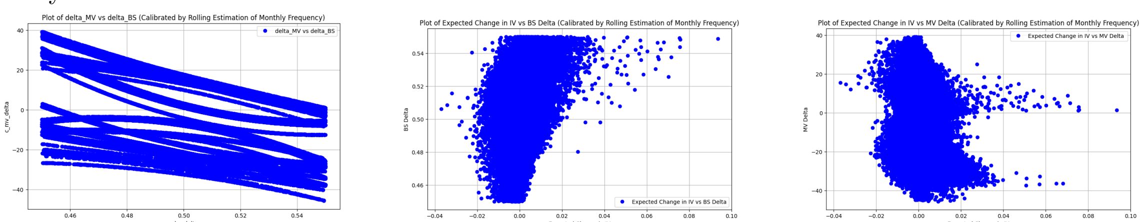

Figure 140: The $\delta_{MV} - \delta_{BS}$ and $\mathbb{E}(\Delta\sigma_{imp})$ vs δ_{BS} and vs δ_{MV} for ATM 12MM Bucket - Rolling Monthly

6.2 OTM Buckets

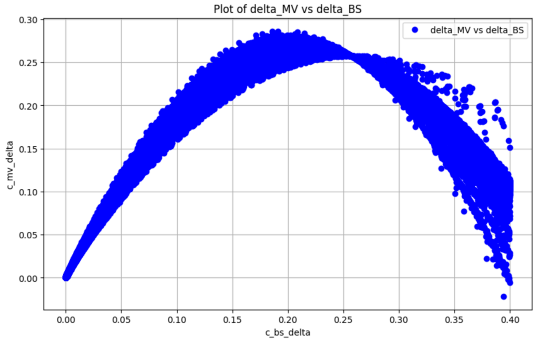

Figure 141: δ_{MV} vs δ_{BS}

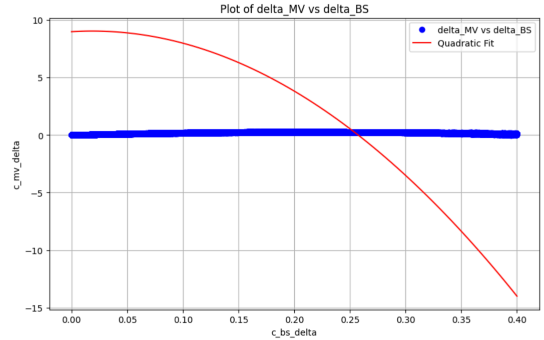

Figure 142: δ_{MV} vs δ_{BS} and the Fitting Line

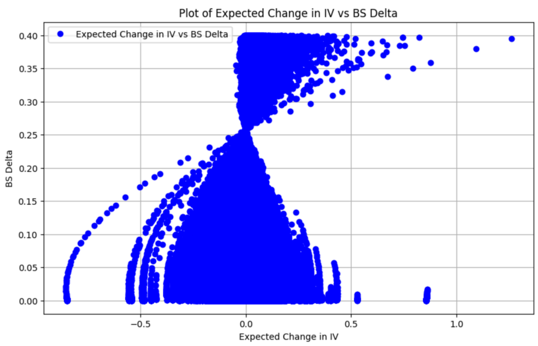

Figure 143: $\mathbb{E}(\Delta\sigma_{imp})$ vs δ_{BS}

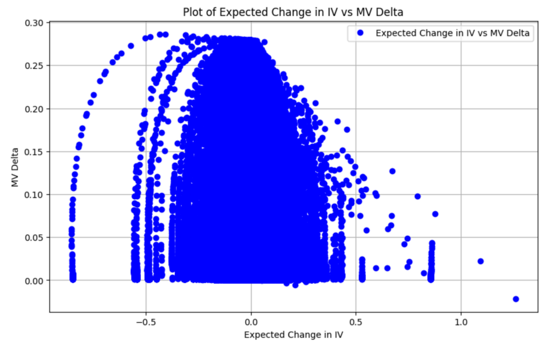

Figure 144: $\mathbb{E}(\Delta\sigma_{imp})$ vs δ_{MV}

Figure 145: The $\delta_{MV} - \delta_{BS}$ and $\mathbb{E}(\Delta\sigma_{imp})$ vs δ_{BS} and vs δ_{MV} for OTM 1M Bucket

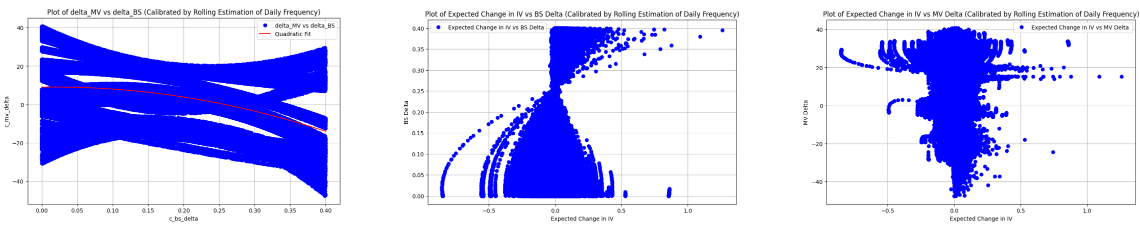

Figure 146: The $\delta_{MV} - \delta_{BS}$ and $\mathbb{E}(\Delta\sigma_{imp})$ vs δ_{BS} and vs δ_{MV} for OTM 1M Bucket - Rolling Daily

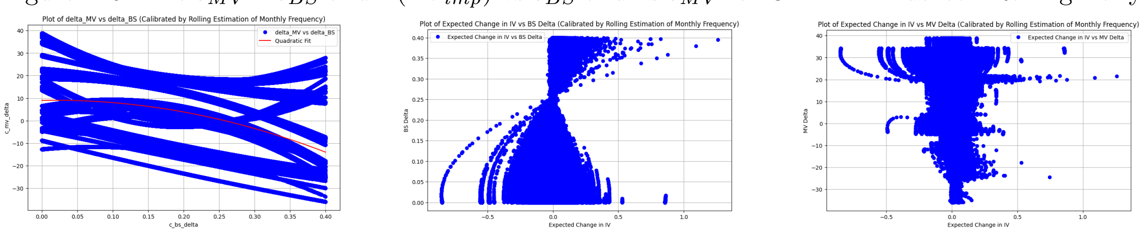

Figure 147: The $\delta_{MV} - \delta_{BS}$ and $\mathbb{E}(\Delta\sigma_{imp})$ vs δ_{BS} and vs δ_{MV} for OTM 1M Bucket - Rolling Monthly

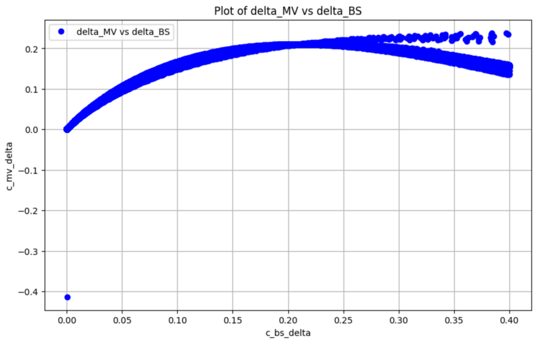

Figure 148: δ_{MV} vs δ_{BS}

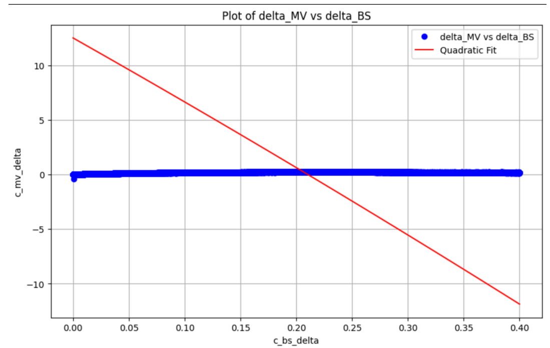

Figure 149: δ_{MV} vs δ_{BS} and the Fitting Line

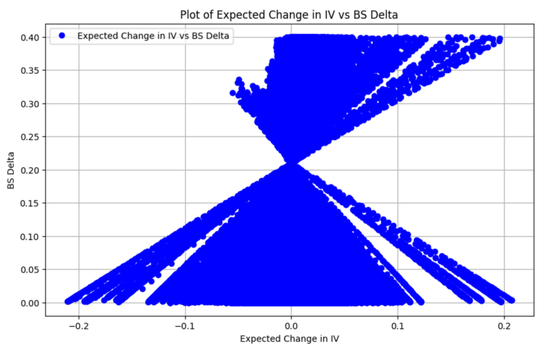

Figure 150: $\mathbb{E}(\Delta\sigma_{imp})$ vs δ_{BS}

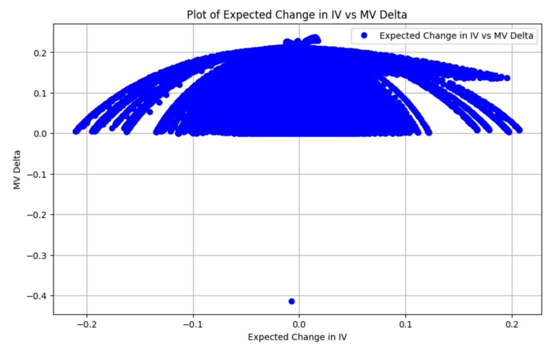

Figure 151: $\mathbb{E}(\Delta\sigma_{imp})$ vs δ_{MV}

Figure 152: The $\delta_{MV} - \delta_{BS}$ and $\mathbb{E}(\Delta\sigma_{imp})$ vs δ_{BS} and vs δ_{MV} for OTM 2M Bucket

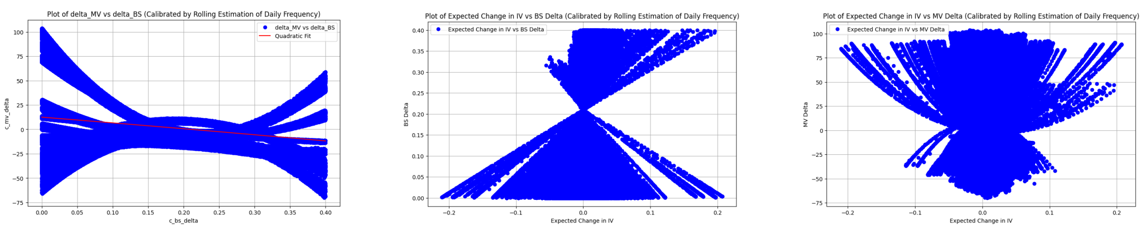

Figure 153: The $\delta_{MV} - \delta_{BS}$ and $\mathbb{E}(\Delta\sigma_{imp})$ vs δ_{BS} and vs δ_{MV} for OTM 2M Bucket - Rolling Daily

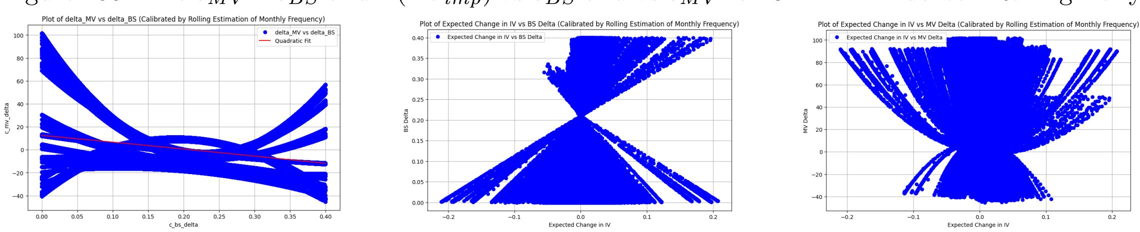

Figure 154: The $\delta_{MV} - \delta_{BS}$ and $\mathbb{E}(\Delta\sigma_{imp})$ vs δ_{BS} and vs δ_{MV} for OTM 2M Bucket - Rolling Monthly

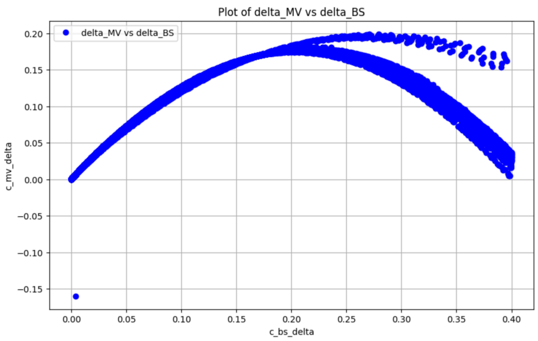

Figure 155: δ_{MV} vs δ_{BS}

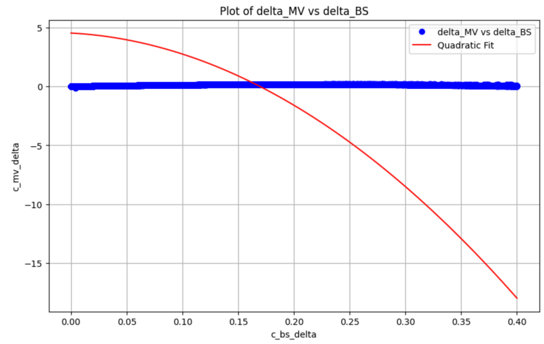

Figure 156: δ_{MV} vs δ_{BS} and the Fitting Line

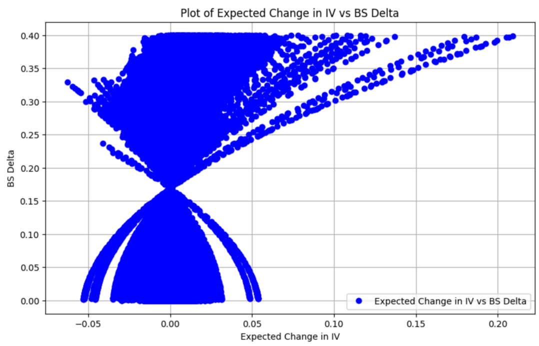

Figure 157: $\mathbb{E}(\Delta\sigma_{imp})$ vs δ_{BS}

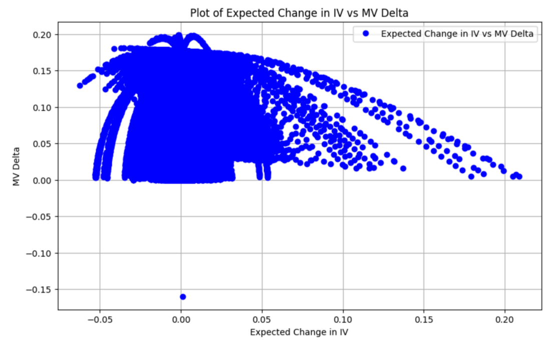

Figure 158: $\mathbb{E}(\Delta\sigma_{imp})$ vs δ_{MV}

Figure 159: The $\delta_{MV} - \delta_{BS}$ and $\mathbb{E}(\Delta\sigma_{imp})$ vs δ_{BS} and vs δ_{MV} for OTM 3M Bucket

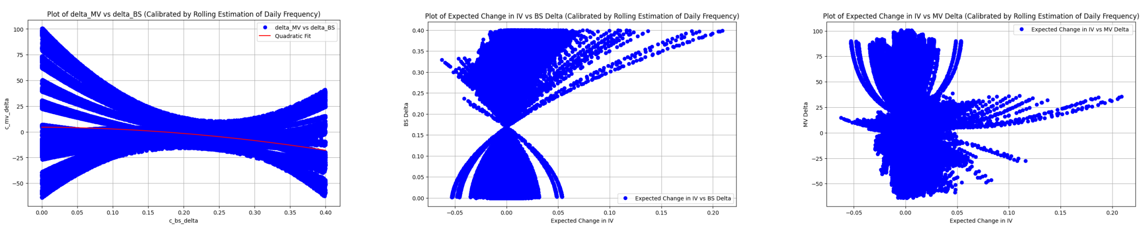

Figure 160: The $\delta_{MV} - \delta_{BS}$ and $\mathbb{E}(\Delta\sigma_{imp})$ vs δ_{BS} and vs δ_{MV} for OTM 3M Bucket - Rolling Daily

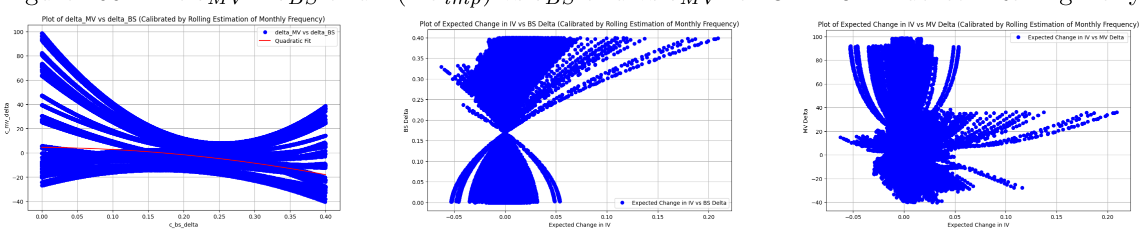

Figure 161: The $\delta_{MV} - \delta_{BS}$ and $\mathbb{E}(\Delta\sigma_{imp})$ vs δ_{BS} and vs δ_{MV} for OTM 3M Bucket - Rolling Monthly

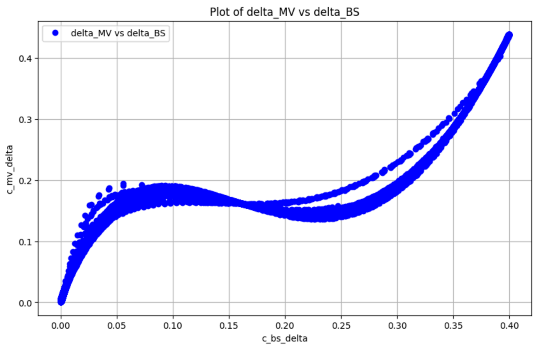

Figure 162: δ_{MV} vs δ_{BS}

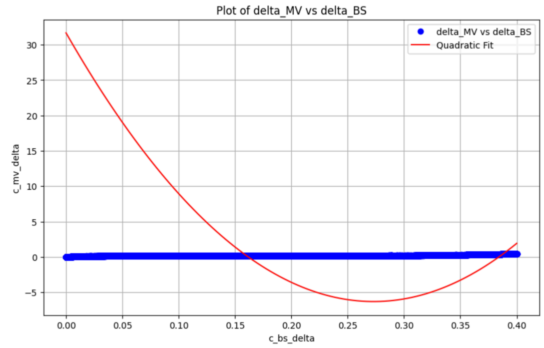

Figure 163: δ_{MV} vs δ_{BS} and the Fitting Line

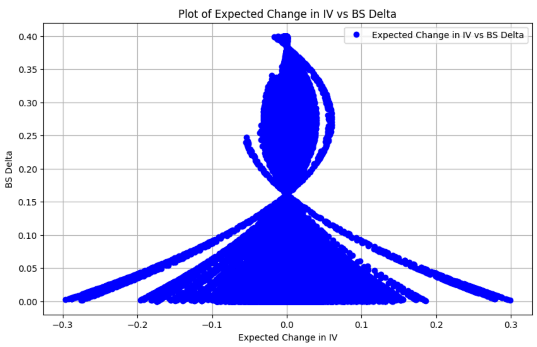

Figure 164: $\mathbb{E}(\Delta\sigma_{imp})$ vs δ_{BS}

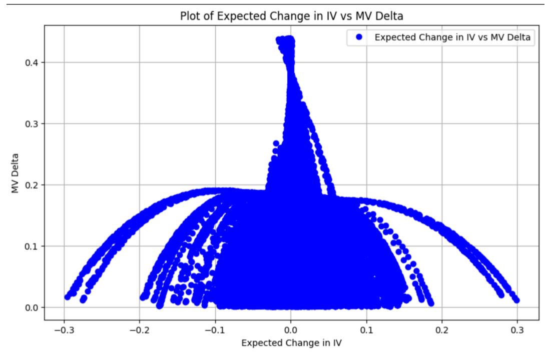

Figure 165: $\mathbb{E}(\Delta\sigma_{imp})$ vs δ_{MV}

Figure 166: The $\delta_{MV} - \delta_{BS}$ and $\mathbb{E}(\Delta\sigma_{imp})$ vs δ_{BS} and vs δ_{MV} for OTM 4M Bucket

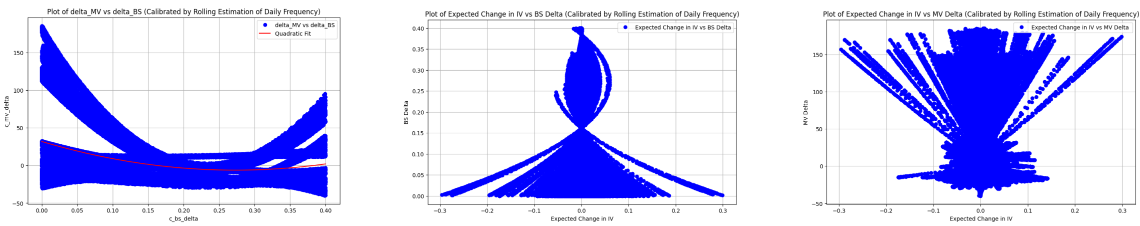

Figure 167: The $\delta_{MV} - \delta_{BS}$ and $\mathbb{E}(\Delta\sigma_{imp})$ vs δ_{BS} and vs δ_{MV} for OTM 4M Bucket - Rolling Daily

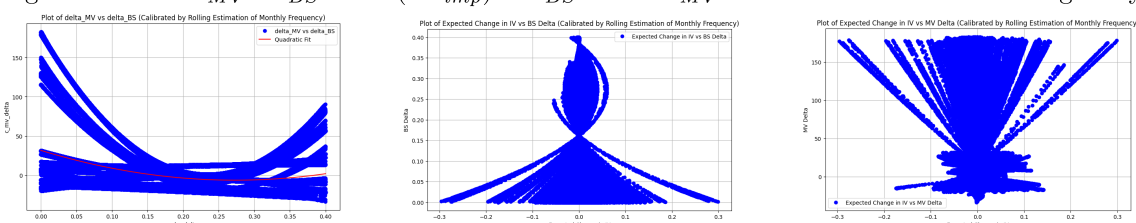

Figure 168: The $\delta_{MV} - \delta_{BS}$ and $\mathbb{E}(\Delta\sigma_{imp})$ vs δ_{BS} and vs δ_{MV} for OTM 4M Bucket - Rolling Monthly

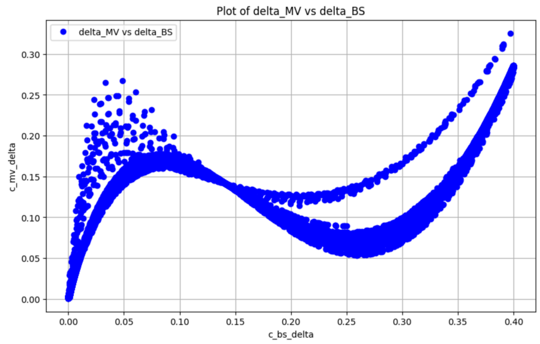

Figure 169: δ_{MV} vs δ_{BS}

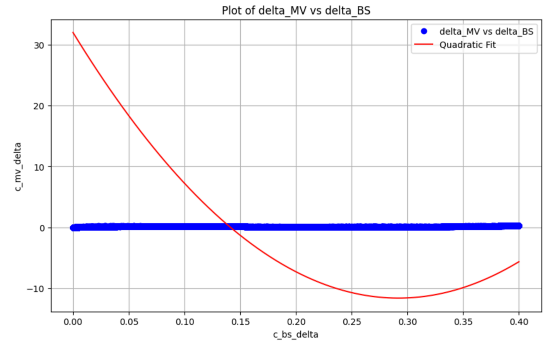

Figure 170: δ_{MV} vs δ_{BS} and the Fitting Line

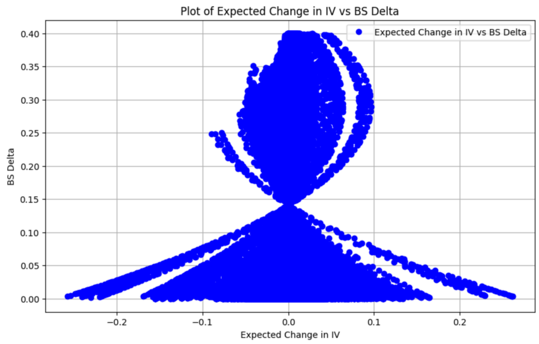

Figure 171: $\mathbb{E}(\Delta\sigma_{imp})$ vs δ_{BS}

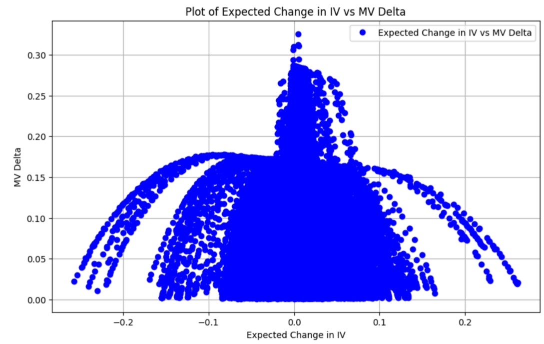

Figure 172: $\mathbb{E}(\Delta\sigma_{imp})$ vs δ_{MV}

Figure 173: The $\delta_{MV} - \delta_{BS}$ and $\mathbb{E}(\Delta\sigma_{imp})$ vs δ_{BS} and vs δ_{MV} for OTM 6M Bucket

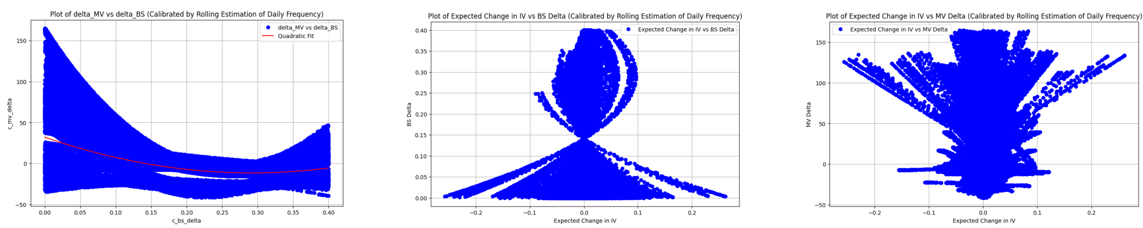

Figure 174: The $\delta_{MV} - \delta_{BS}$ and $\mathbb{E}(\Delta\sigma_{imp})$ vs δ_{BS} and vs δ_{MV} for OTM 6M Bucket - Rolling Daily

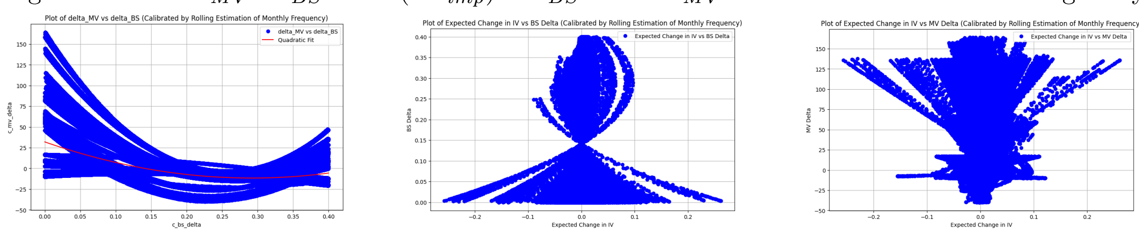

Figure 175: The $\delta_{MV} - \delta_{BS}$ and $\mathbb{E}(\Delta\sigma_{imp})$ vs δ_{BS} and vs δ_{MV} for OTM 6M Bucket - Rolling Monthly

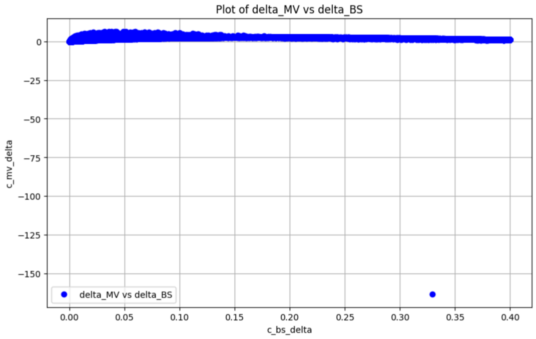

Figure 176: δ_{MV} vs δ_{BS}

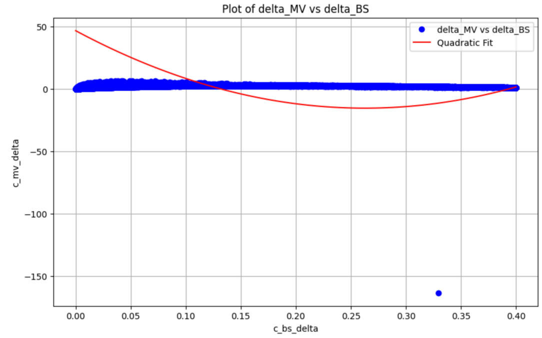

Figure 177: δ_{MV} vs δ_{BS} and the Fitting Line

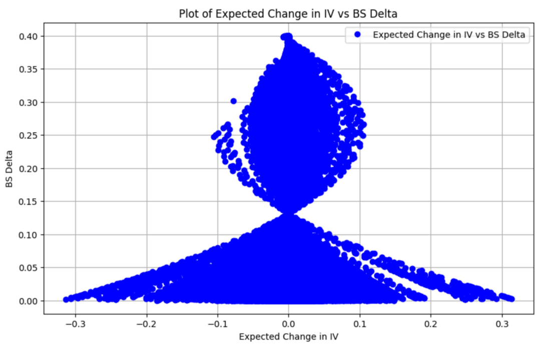

Figure 178: $\mathbb{E}(\Delta\sigma_{imp})$ vs δ_{BS}

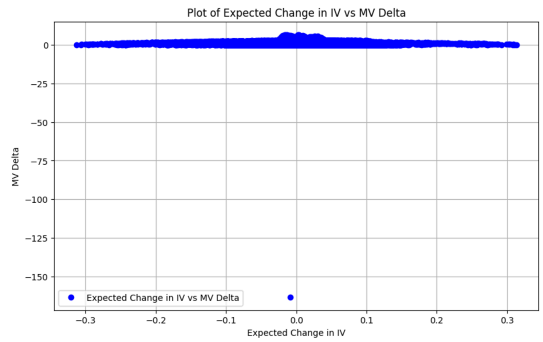

Figure 179: $\mathbb{E}(\Delta\sigma_{imp})$ vs δ_{MV}

Figure 180: The $\delta_{MV} - \delta_{BS}$ and $\mathbb{E}(\Delta\sigma_{imp})$ vs δ_{BS} and vs δ_{MV} for OTM 12M Bucket

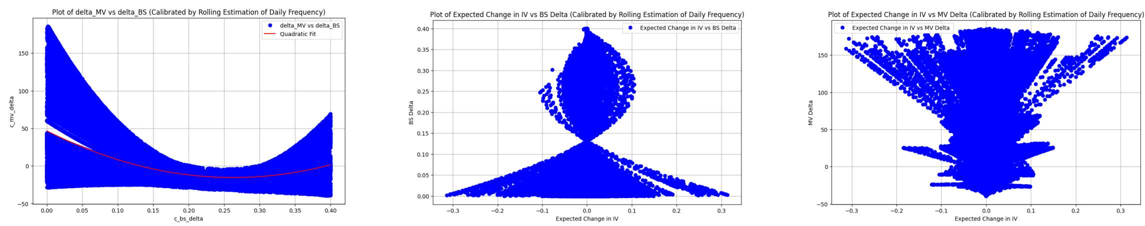

Figure 181: The $\delta_{MV} - \delta_{BS}$ and $\mathbb{E}(\Delta\sigma_{imp})$ vs δ_{BS} and vs δ_{MV} for OTM 12M Bucket - Rolling Daily

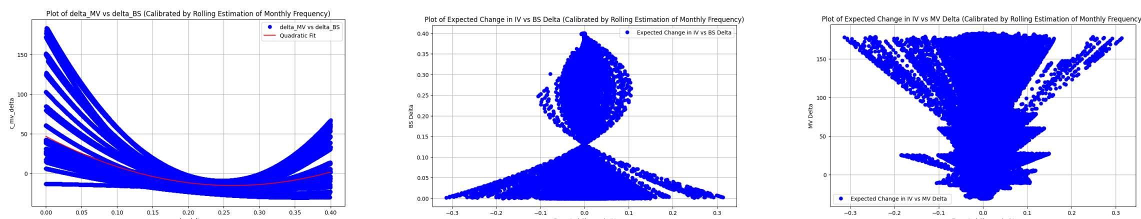

Figure 182: The $\delta_{MV} - \delta_{BS}$ and $\mathbb{E}(\Delta\sigma_{imp})$ vs δ_{BS} and vs δ_{MV} for OTM 12M Bucket - Rolling Monthly

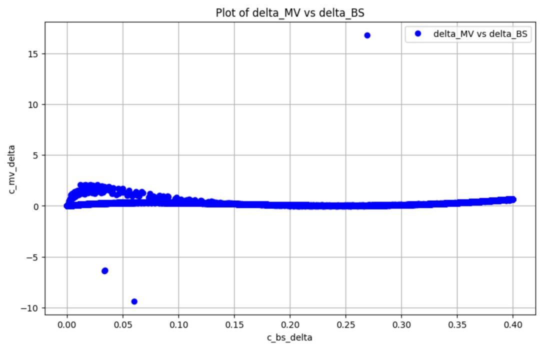

Figure 183: δ_{MV} vs δ_{BS}

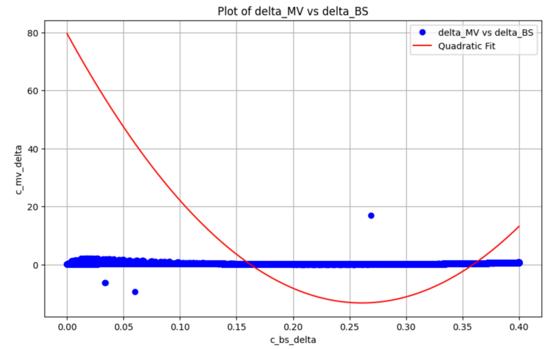

Figure 184: δ_{MV} vs δ_{BS} and the Fitting Line

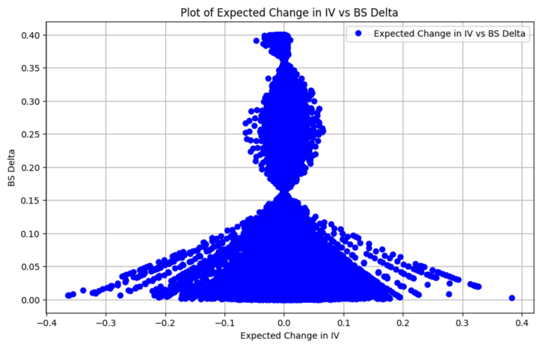

Figure 185: $\mathbb{E}(\Delta\sigma_{imp})$ vs δ_{BS}

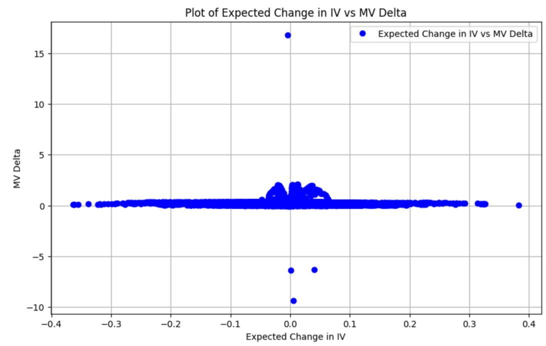

Figure 186: $\mathbb{E}(\Delta\sigma_{imp})$ vs δ_{MV}

Figure 187: The $\delta_{MV} - \delta_{BS}$ and $\mathbb{E}(\Delta\sigma_{imp})$ vs δ_{BS} and vs δ_{MV} for OTM 12MM Bucket

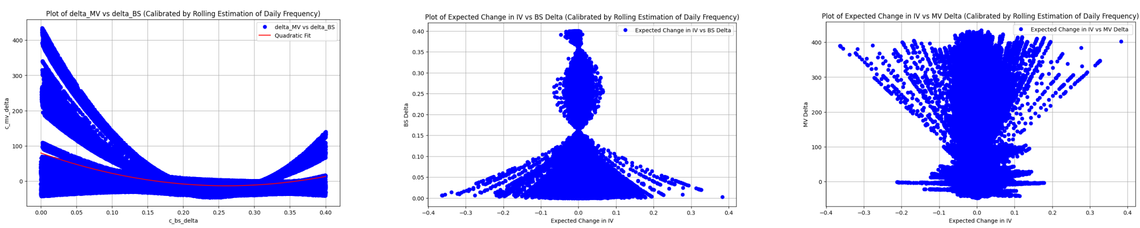

Figure 188: The $\delta_{MV} - \delta_{BS}$ and $\mathbb{E}(\Delta\sigma_{imp})$ vs δ_{BS} and vs δ_{MV} for OTM 12MM Bucket - Rolling Daily

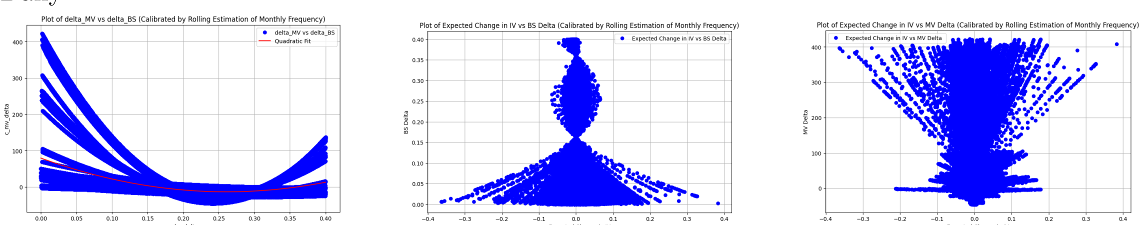

Figure 189: The $\delta_{MV} - \delta_{BS}$ and $\mathbb{E}(\Delta\sigma_{imp})$ vs δ_{BS} and vs δ_{MV} for OTM 12MM Bucket - Rolling Monthly

6.3 ITM Buckets

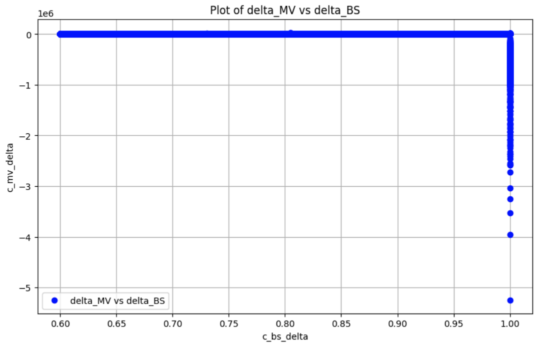

Figure 190: δ_{MV} vs δ_{BS}

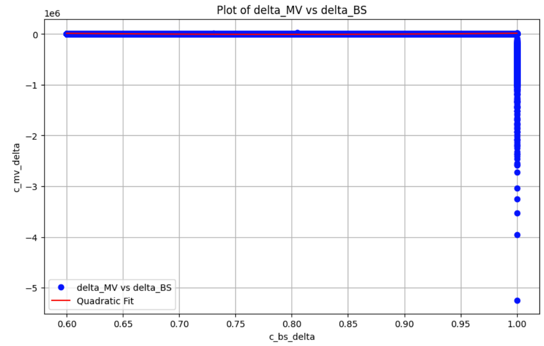

Figure 191: δ_{MV} vs δ_{BS} and the Fitting Line

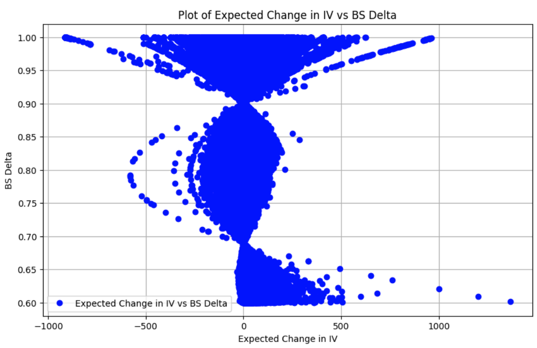

Figure 192: $\mathbb{E}(\Delta\sigma_{imp})$ vs δ_{BS}

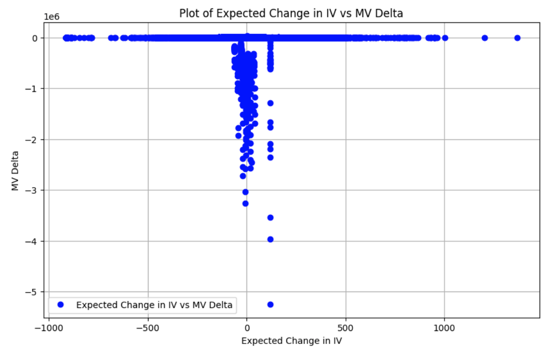

Figure 193: $\mathbb{E}(\Delta\sigma_{imp})$ vs δ_{MV}

Figure 194: The $\delta_{MV} - \delta_{BS}$ and $\mathbb{E}(\Delta\sigma_{imp})$ vs δ_{BS} and vs δ_{MV} for ITM 1M Bucket

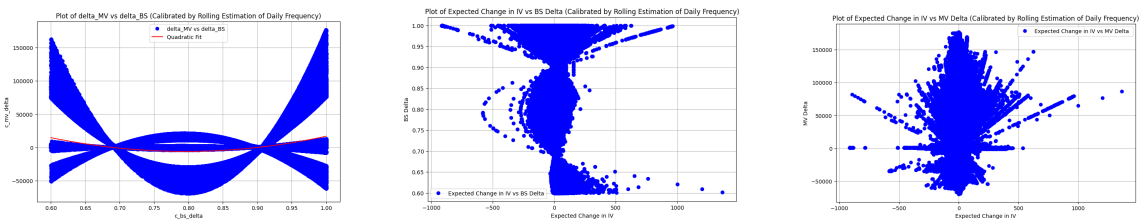

Figure 195: The $\delta_{MV} - \delta_{BS}$ and $\mathbb{E}(\Delta\sigma_{imp})$ vs δ_{BS} and vs δ_{MV} for ITM 1M Bucket - Rolling Daily

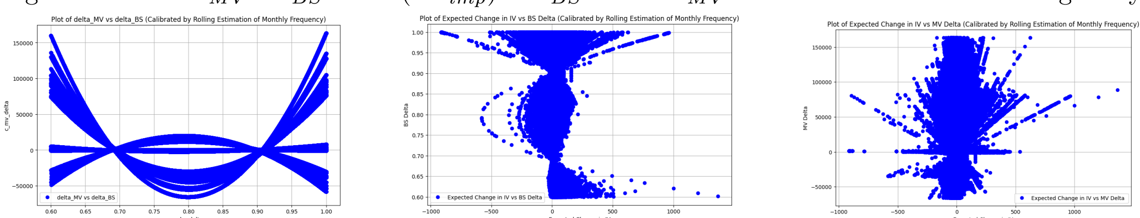

Figure 196: The $\delta_{MV} - \delta_{BS}$ and $\mathbb{E}(\Delta\sigma_{imp})$ vs δ_{BS} and vs δ_{MV} for ITM 1M Bucket - Rolling Monthly

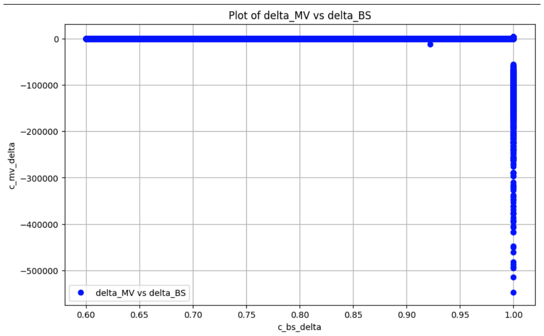

Figure 197: δ_{MV} vs δ_{BS}

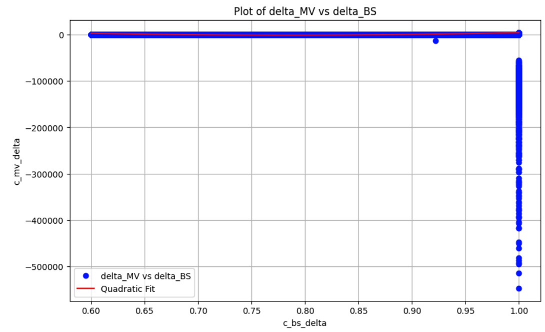

Figure 198: δ_{MV} vs δ_{BS} and the Fitting Line

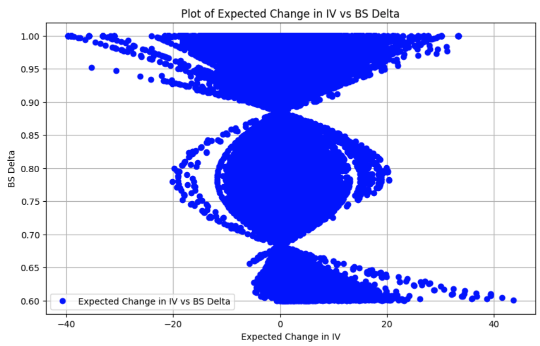

Figure 199: $\mathbb{E}(\Delta\sigma_{imp})$ vs δ_{BS}

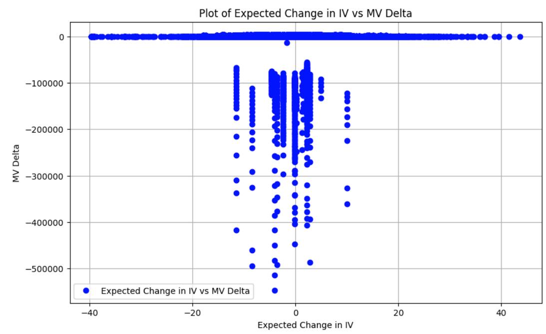

Figure 200: $\mathbb{E}(\Delta\sigma_{imp})$ vs δ_{MV}

Figure 201: The $\delta_{MV} - \delta_{BS}$ and $\mathbb{E}(\Delta\sigma_{imp})$ vs δ_{BS} and vs δ_{MV} for ITM 2M Bucket

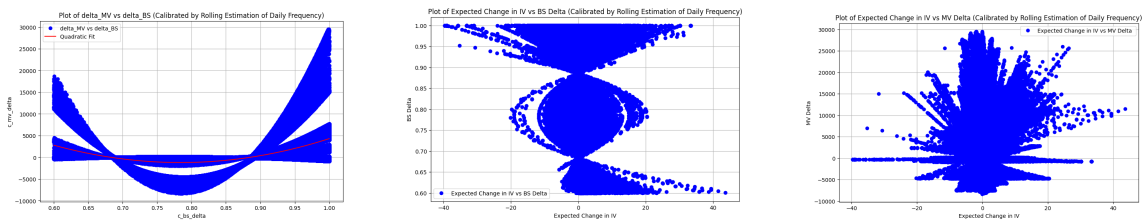

Figure 202: The $\delta_{MV} - \delta_{BS}$ and $\mathbb{E}(\Delta\sigma_{imp})$ vs δ_{BS} and vs δ_{MV} for ITM 2M Bucket - Rolling Daily

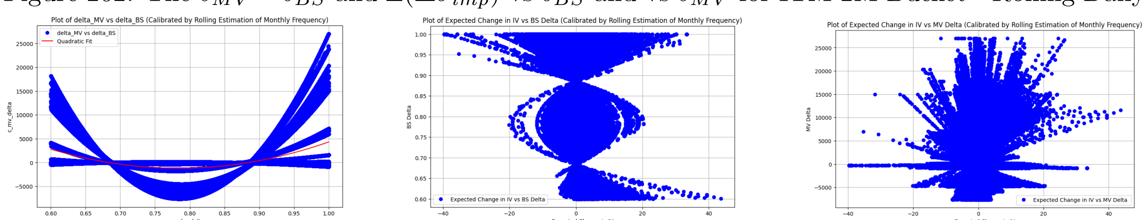

Figure 203: The $\delta_{MV} - \delta_{BS}$ and $\mathbb{E}(\Delta\sigma_{imp})$ vs δ_{BS} and vs δ_{MV} for ITM 2M Bucket - Rolling Monthly

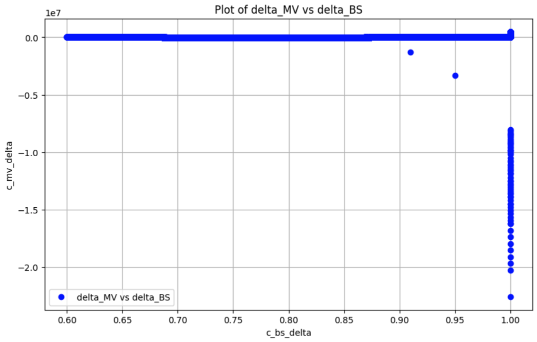

Figure 204: δ_{MV} vs δ_{BS}

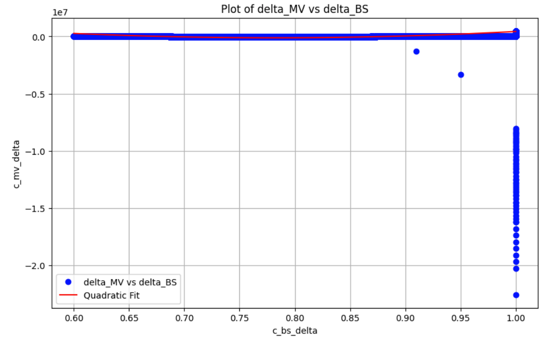

Figure 205: δ_{MV} vs δ_{BS} and the Fitting Line

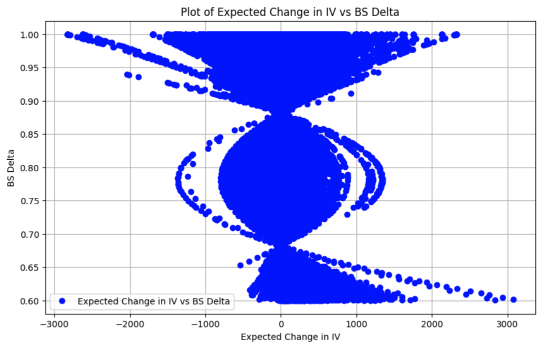

Figure 206: $\mathbb{E}(\Delta\sigma_{imp})$ vs δ_{BS}

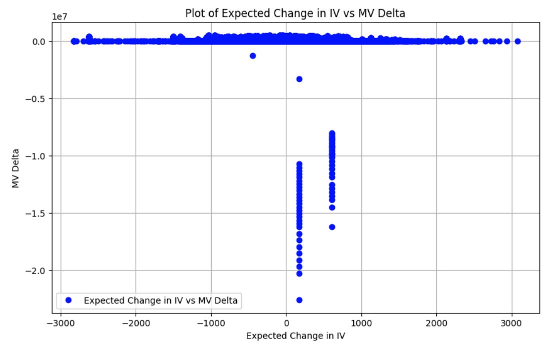

Figure 207: $\mathbb{E}(\Delta\sigma_{imp})$ vs δ_{MV}

Figure 208: The $\delta_{MV} - \delta_{BS}$ and $\mathbb{E}(\Delta\sigma_{imp})$ vs δ_{BS} and vs δ_{MV} for ITM 3M Bucket

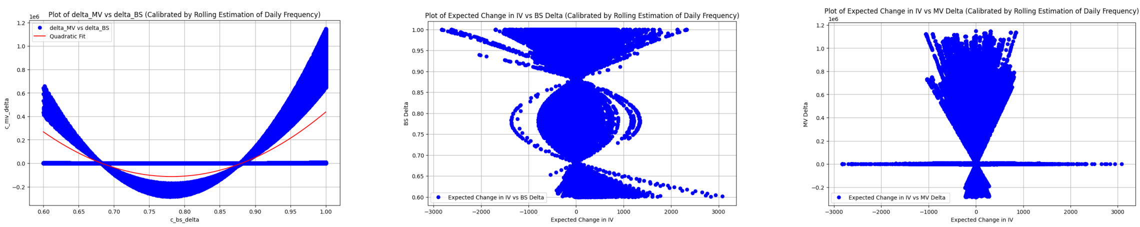

Figure 209: The $\delta_{MV} - \delta_{BS}$ and $\mathbb{E}(\Delta\sigma_{imp})$ vs δ_{BS} and vs δ_{MV} for ITM 3M Bucket - Rolling Daily

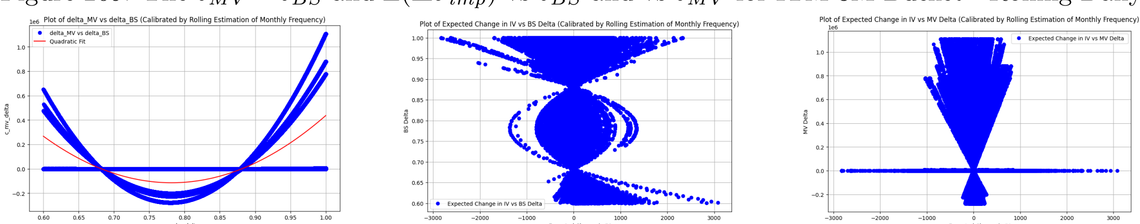

Figure 210: The $\delta_{MV} - \delta_{BS}$ and $\mathbb{E}(\Delta\sigma_{imp})$ vs δ_{BS} and vs δ_{MV} for ITM 3M Bucket - Rolling Monthly

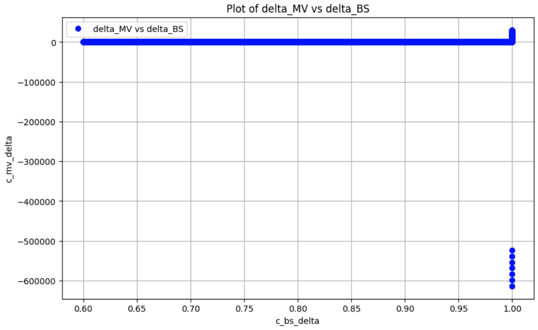

Figure 211: δ_{MV} vs δ_{BS}

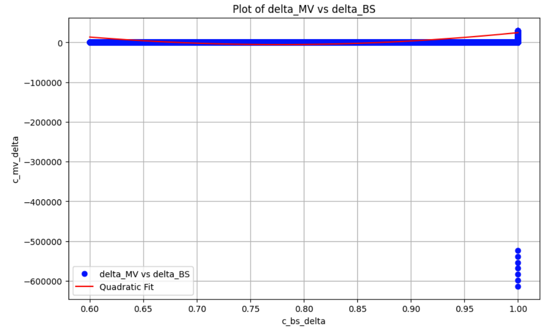

Figure 212: δ_{MV} vs δ_{BS} and the Fitting Line

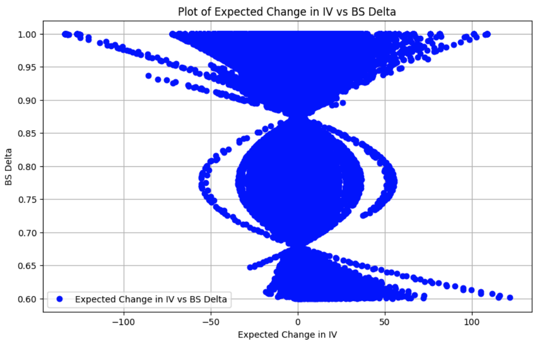

Figure 213: $\mathbb{E}(\Delta\sigma_{imp})$ vs δ_{BS}

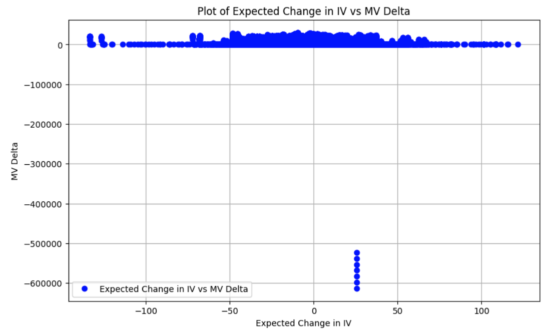

Figure 214: $\mathbb{E}(\Delta\sigma_{imp})$ vs δ_{MV}

Figure 215: The $\delta_{MV} - \delta_{BS}$ and $\mathbb{E}(\Delta\sigma_{imp})$ vs δ_{BS} and vs δ_{MV} for ITM 4M Bucket

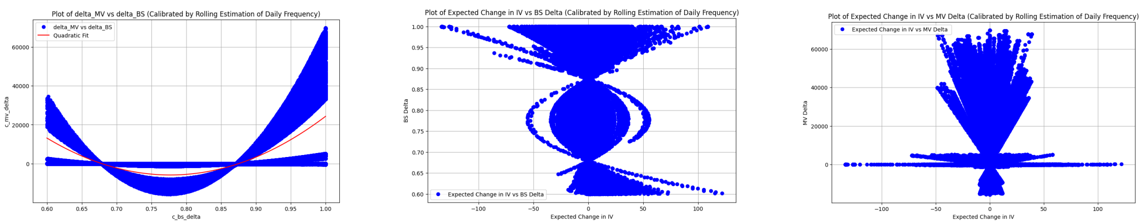

Figure 216: The $\delta_{MV} - \delta_{BS}$ and $\mathbb{E}(\Delta\sigma_{imp})$ vs δ_{BS} and vs δ_{MV} for ITM 4M Bucket - Rolling Daily

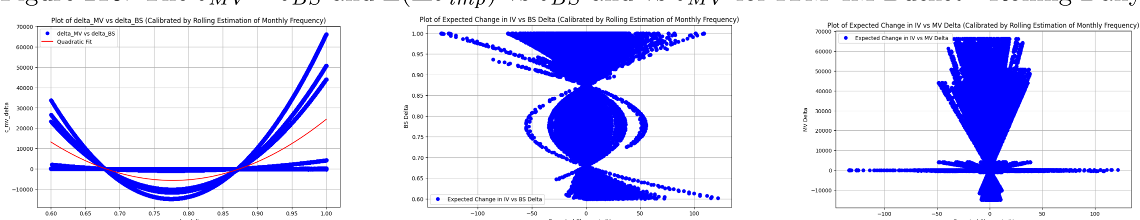

Figure 217: The $\delta_{MV} - \delta_{BS}$ and $\mathbb{E}(\Delta\sigma_{imp})$ vs δ_{BS} and vs δ_{MV} for ITM 4M Bucket - Rolling Monthly

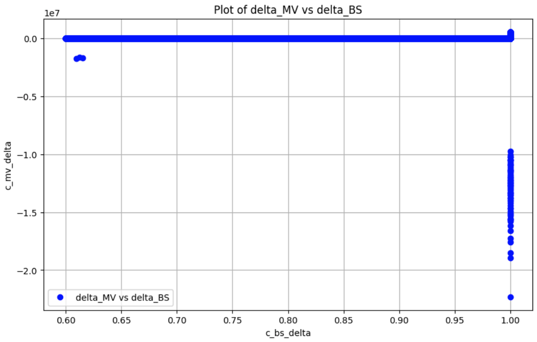

Figure 218: δ_{MV} vs δ_{BS}

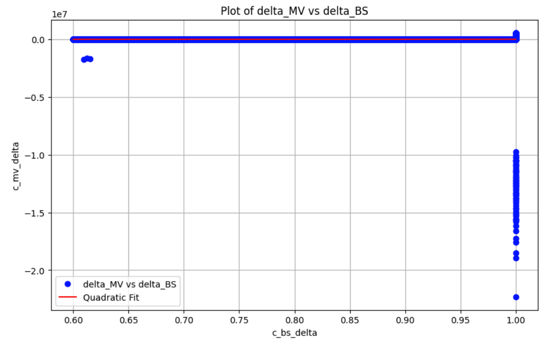

Figure 219: δ_{MV} vs δ_{BS} and the Fitting Line

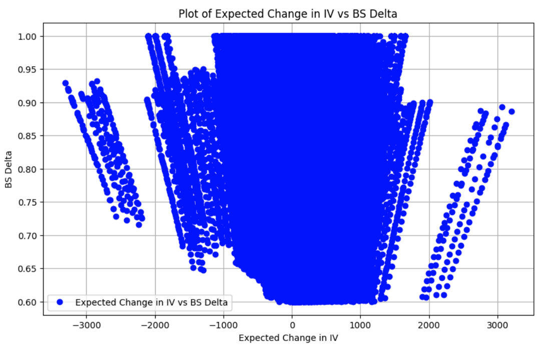

Figure 220: $\mathbb{E}(\Delta\sigma_{imp})$ vs δ_{BS}

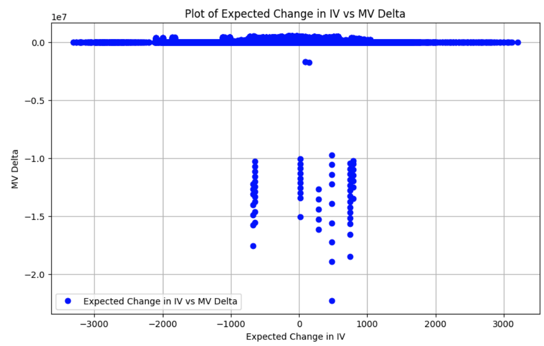

Figure 221: $\mathbb{E}(\Delta\sigma_{imp})$ vs δ_{MV}

Figure 222: The $\delta_{MV} - \delta_{BS}$ and $\mathbb{E}(\Delta\sigma_{imp})$ vs δ_{BS} and vs δ_{MV} for ITM 6M Bucket

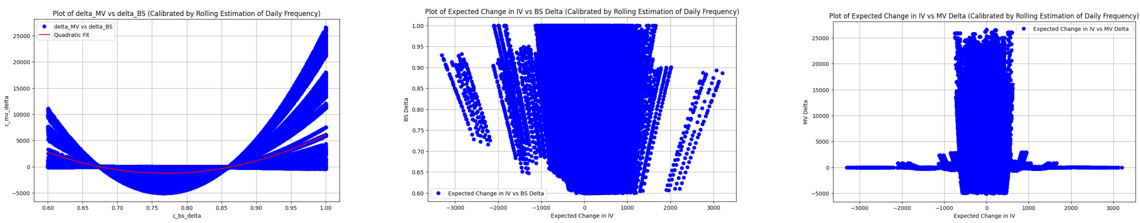

Figure 223: The $\delta_{MV} - \delta_{BS}$ and $\mathbb{E}(\Delta\sigma_{imp})$ vs δ_{BS} and vs δ_{MV} for ITM 6M Bucket - Rolling Daily

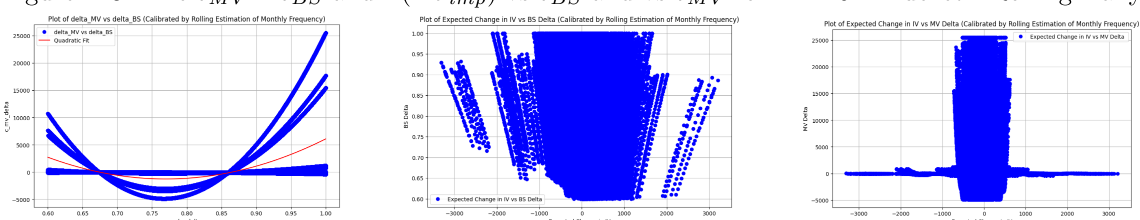

Figure 224: The $\delta_{MV} - \delta_{BS}$ and $\mathbb{E}(\Delta\sigma_{imp})$ vs δ_{BS} and vs δ_{MV} for ITM 6M Bucket - Rolling Monthly

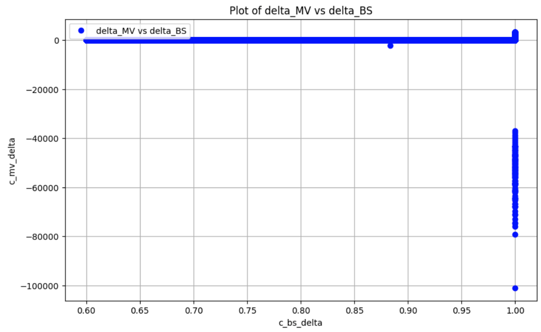

Figure 225: δ_{MV} vs δ_{BS}

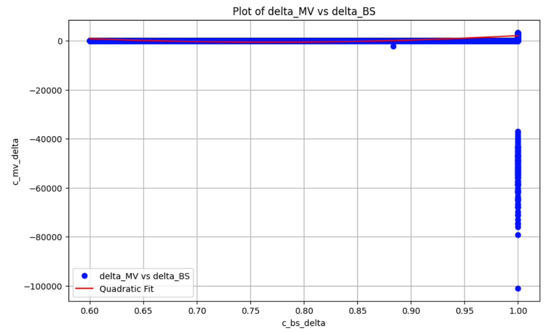

Figure 226: δ_{MV} vs δ_{BS} and the Fitting Line

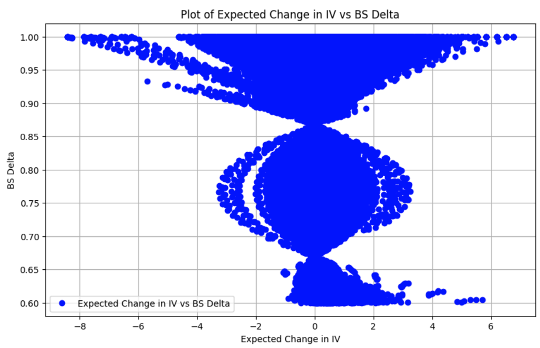

Figure 227: $\mathbb{E}(\Delta\sigma_{imp})$ vs δ_{BS}

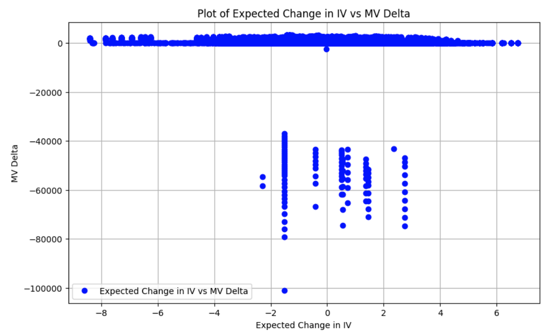

Figure 228: $\mathbb{E}(\Delta\sigma_{imp})$ vs δ_{MV}

Figure 229: The $\delta_{MV} - \delta_{BS}$ and $\mathbb{E}(\Delta\sigma_{imp})$ vs δ_{BS} and vs δ_{MV} for ITM 12M Bucket

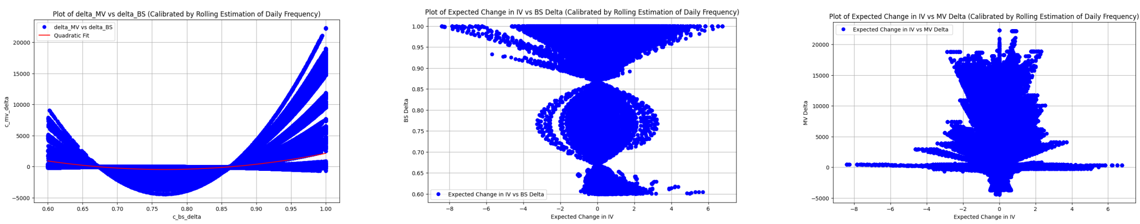

Figure 230: The $\delta_{MV} - \delta_{BS}$ and $\mathbb{E}(\Delta\sigma_{imp})$ vs δ_{BS} and vs δ_{MV} for ITM 12M Bucket - Rolling Daily

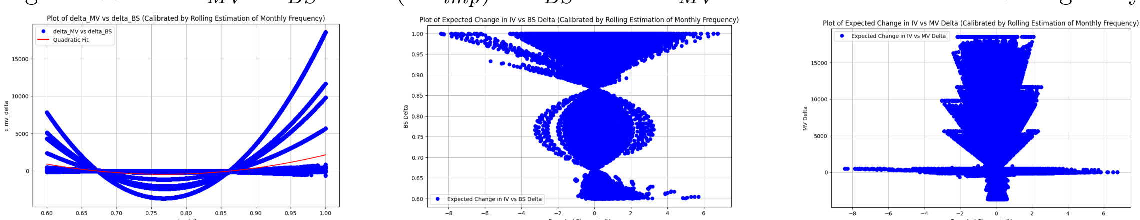

Figure 231: The $\delta_{MV} - \delta_{BS}$ and $\mathbb{E}(\Delta\sigma_{imp})$ vs δ_{BS} and vs δ_{MV} for ITM 12M Bucket - Rolling Monthly

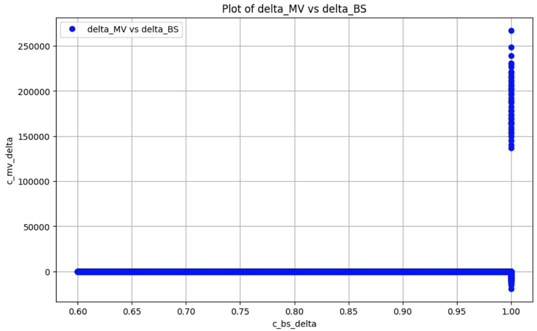

Figure 232: δ_{MV} vs δ_{BS}

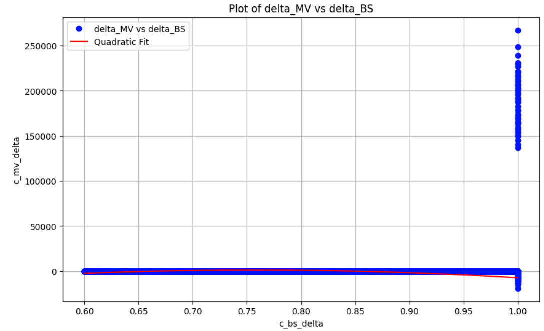

Figure 233: δ_{MV} vs δ_{BS} and the Fitting Line

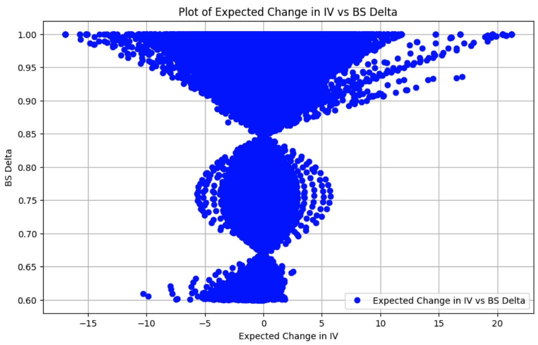

Figure 234: $\mathbb{E}(\Delta\sigma_{imp})$ vs δ_{BS}

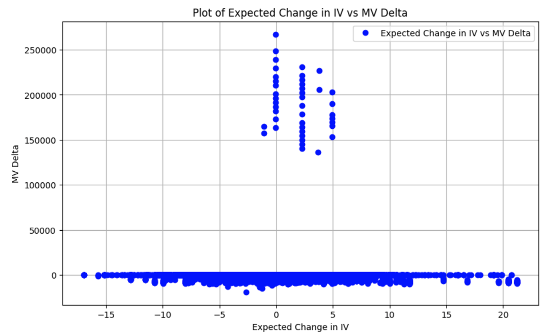

Figure 235: $\mathbb{E}(\Delta\sigma_{imp})$ vs δ_{MV}

Figure 236: The $\delta_{MV} - \delta_{BS}$ and $\mathbb{E}(\Delta\sigma_{imp})$ vs δ_{BS} and vs δ_{MV} for ITM 12MM Bucket

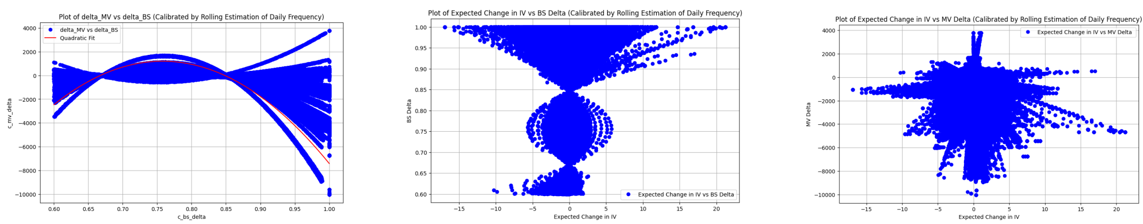

Figure 237: The $\delta_{MV} - \delta_{BS}$ and $\mathbb{E}(\Delta\sigma_{imp})$ vs δ_{BS} and vs δ_{MV} for ITM 12MM Bucket - Rolling Daily

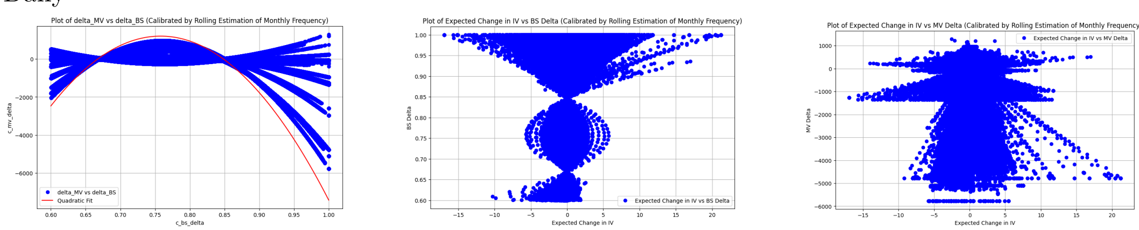

Figure 238: The $\delta_{MV} - \delta_{BS}$ and $\mathbb{E}(\Delta\sigma_{imp})$ vs δ_{BS} and vs δ_{MV} for ITM 12MM Bucket - Rolling Monthly

References

[Jae02] Peter Jaeckel. *Monte Carlo Methods in Finance*. Wiley, 2002.

[Gur11] Sebastien Gurrieri. “An Analysis of Sobol Sequence and the Brownian Bridge”. In: *SSRN* (2011). DOI: http://dx.doi.org/10.2139/ssrn.1951886. URL: https://ssrn.com/abstract=1951886.

[HW17] John Hull and Alan White. “Optimal delta hedging for options”. In: *Journal of Banking & Finance* 82 (2017), pp. 180–190. ISSN: 0378-4266. DOI: https://doi.org/10.1016/j.jbankfin.2017.05.006. URL: https://www.sciencedirect.com/science/article/pii/S0378426617301085.